ADDIS ABABA UNIVERSITY

COLLEGE OF TECHNOLOGY AND BUILT ENVIRONMENT

SCHOOL OF CIVIL AND ENVIRONMENTAL ENGINEERING

PROBABILISTIC IMPACT ASSESSMENT OF TRAFFIC OVERLOAD ON BRIDGE STRUCTURAL CAPACITY: A CASE STUDY APPROACH

A Thesis in Structural Engineering

By Gebyaw Amare

December 2025

Addis Ababa

A Thesis

Submitted in Partial Fulfillment of the Requirements for the Degree of Master of Science

The undersigned have examined the thesis entitled '**Probabilistic Impact Assessment of Traffic Overload on Bridge Structural Capacity: A Case Study Approach**' presented by **Gebyaw Amare**, a candidate for the degree of **Master of Science** and hereby certify that it is worthy of acceptance.

Dr.Abrham Gebre		March 9/2026
Advisor	Signature	Date
Dr. Edom Adane		March 10, 2026
Internal Examiner	Signature	Date
Dr. Berhanemeskel Engliz		10/03/2026
External Examiner	Signature	Date
Dr. Yenesew Mengiste		10 Mar, 2026
Chair person	Signature	Date

ABSTRACT

This study investigates the effects caused by traffic overload on bridge superstructures, especially with regards to heavy vehicles. The critical thresholds with regards to heavy traffic are discussed, taking into consideration parameters such as traffic flow and characteristics and types and patterns of overload. The work also considers design standards and bridge materials.

The methodology would commence with identification of some bridges in Ethiopia that are faced with varying degrees of traffic overload. And to get this study off the ground, data was collected from 38,188 truckloads of traffic at weigh stations managed by the Ethiopian Roads Administration in those regions that record high traffic flow of heavy vehicles.

Using the R statistical software, a probabilistic loading process was generated. This involved the examination of the material properties of key components as well as the design parameters of a chosen bridge. Probabilistic axle loads were analyzed to assess the impact on the existing bridge's capacity.

A simulation program was developed to determine static overload influence on a particular type of three-span simply-supported box-girder bridge (Mille. 3 bridge). The extreme values of the load effects for various return-period values were computed with statistical extrapolation methods.

By using the First Order Reliability Method (FORM), reliability indices (β) can be determined in order to calculate the probability of failure regarding flexural and shear modes.

The findings contribute to performance-based management in bridges, considering the impact of real-life overloaded traffic on structural reliability in relation to the life cycle maintenance approach in accordance with AASHTO LRFD/ERA.

KEYWORDS: *Probabilistic approach, Traffic overload, Extreme Value, Box-girder Bridge, Static Weighing, Assessment, Creep.*

ACKNOWLEDGMENTS

I would also take the opportunity to thank my almighty God for enabling me to complete this research. Further, I would also like to thank my supervisor, Dr. Abrham Gebre, for their immense contributions towards the completion of this project helped us to produce higher-quality work. The suggestions and guidance that come from others are considered the primary channels towards completing a project.

I cannot forget to express my sincere gratitude to Binyam Wesenseged for his contribution to making me complete this project successfully.

Next, I would like to thank Eng. Yoseph Tamiru and his colleagues for providing me with the necessary data from the Ethiopian Roads Administration.

Finally, I would like to thank my family for the endless support and help they have provided me throughout this project.

ACRONYMS AND ABBREVIATIONS

ERA	Ethiopian Rods Administration/Authority
EN	The European Standard
AASHTO:	American Association of State Highway and Transportation Officials
ACI	American Concrete Institute
AACRA	Addis Ababa City Roads Authority
WIM	Weight-in-motion
GVW	Gross Vehicle Weight
FEM	Finite Element Method
LRFD	Load and Resistance Factor Design
RTMS	Road Transport Management System
LSWIM	Low Speed Weigh-in-Motion
MSWIM	Medium Speed Weigh-in-Motion
L	Bridge span
MoU	Memorandum of Understanding
ECOWAS	Economic Community of West African States
CEMAC	Central African Economic and Monetary Community
AA	Addis Ababa
EU	European Union
GoE	Government of Ethiopia
Km/h	kilometer per hour
EVT	Extreme Value Theory.
Cm	Centimeter
CDF	Cumulative Distribution Function
FOR	First Order Reliability
POT	Peaks Over Threshold
LHS	Latin Hypercubes Sampling
LLDF	Live Load Distribution Factors
Std.dev	Standard Deviation

TABLE OF CONTENTS

LIST OF TABLES

LIST OF FIGURES

CHAPTER 1 INTRODUCTION

1.1 General

Infrastructures in transportation, particularly bridges, have been an important contributor to economic development for any country by providing connectivity between different locations. A failure in the bridge can lead to consequences in traffic flow, economy, and the safety of the people. Road integrity is fundamental to the development of urban and rural areas, depending on the state of the roads that affect the flow of commodities and human traffic. Key factors that have a significant impact on roads are design, material used and timely maintenance. To prevent bridge failure, designed to withstand traffic load and other environmental loads and undergo regular assessment [1].

This study investigates the probabilistic effect of traffic overload on the superstructural strength of a bridge along one of the country's busiest roads for heavy traffic, which passes through Addis Ababa to Samara to Djibouti. This study focuses on the significance of the bridge having a high flow of heavy traffic. Besides, the research focuses on existing design criteria, the maximum permitted design loads, the current state of bridge reliability, and the type of construction material used in the bridges.

The bridge under traffic overload is considered, and reasons for choosing the bridge include its location, traffic distribution, as well as structural significance. The data considered in this study involves 38,188 traffic weights of various combinations, as well as structural health inspections. The analysis of traffic overload is carried out using analysis techniques of traffic simulation in R Statistical Programming.

1.2 Statement of the Research Problem

The rapid economic growth and enhancement in road accessibility lead to heavier traffic load than what was considered in bridge designs. This increase in traffic overload gives rise to serious challenges to the structural capacity of the existing bridges. However, typical design approaches normally adopt deterministic models that only poorly represent the randomness in traffic. This condition severely restricts effective risk management. This study will illustrate the effects of overload on existing bridge capacity through case studies and provide valuable insights on the implications of different traffic states to the bridge capacity and the critical regions of the bridge superstructure that may potentially risk structural safety.

1.3 Objective of the research

1.3.1 General objective

The general objective of the study is to assess the impact of traffic overload on the bridge's super-structural capacity by using a probabilistic approach.

1.3.2 Specific objective

The research will pursue the following specific objectives to achieve the main goal:

- Assess the effects of traffic overload on bridge super-structural capacity.
- Assess the relationship between traffic load patterns and bridge time-varying super-structural capacity.
- Determine the critical stress points in the bridge superstructure under overload conditions.
- Analyze the long-term implications of traffic overload on bridges based on probabilistic statistical distribution.

1.4 Scope and Limitations of the Study

1.4.1 Scope of the Study

The study focused on the assessment of specific bridge superstructures in Ethiopia, selected based on their traffic volumes and structural features. It studies the effects of traffic overload on the superstructural capacity of these bridges through various traffic scenarios analysis.

Using the probabilistic approach in order to account for uncertainties, this research makes an assessment of the impacts of traffic loads and their respective probabilities on the capacity of the bridge superstructure, using statistical techniques.

Also, the review is done based on the established engineering parameters, including material characteristics, design type, and a pre-existing condition. A case study approach was used to allow for a detailed study of the chosen bridge, in which the data from traffic studies and structural analyses were combined.

1.4.2 Limitations of the Study

The reliability of this study relies on the presence of static data, as well as the assessment of the superstructures of existing bridges. The probabilistic models employed in this study are based on certain assumptions related to materials and load distributions, which might not represent real-life situations.

The time constraints may limit the scope of data gathering and analysis, especially data that relates to long-term traffic flow. The viability of this study may also be dependent on the technological tools and software being used because technological advancements may offer improvements in methodologies for the future. The main aim only focused on traffic overload; other aspects that influence bridge behavior, like environmental conditions, maintenance, and deterioration, could not be investigated. Additionally, the lack of precise headway distance and truck bypass weighing station presents a challenge, and dynamic effects, lateral branch movements, and multiple-lane bridges have not been taken into account.

1.5 Research Question

The questions that will have been answered at the end of the study are listed as follows:

- How do different traffic conditions affect the structural performance and capacity of bridges' superstructure?
- What is the relationship between traffic overload and the rate of deterioration in bridge materials and structural components?
- What are the implications of traffic overload on bridge lifespan?

1.6 The significance of the research

The research investigates the impact of traffic overload on existing bridge super-structural capacity through a critical analysis which demonstrates the need to study this phenomenon increasing traffic demands require bridge designers and maintainers to understand these effects for safety and performance purposes. The research uses probabilistic modeling to evaluate traffic-related risks which bridge designers need for their decision-making process. The research enables detailed examination of particular bridges which reveals distinctive problems that exist in Ethiopia thus adding to worldwide understanding while delivering targeted solutions for the region. The process of stakeholder involvement leads to findings which remain both significant and practical for traffic management and bridge maintenance practice improvement

1.7 Methodology

The methodology for this study encompasses several steps. The research process was initiated through gathering an extensive secondary dataset comprising 38,188 traffic weight records obtained from the Ethiopian Road Administration database. These comprehensive measurements endured systematic filtration procedures to ensure data quality and relevance for the investigation.

The subsequent analytical phase involved carefully choosing trucks for each different axle configuration, while simultaneously implementing the newly established overload restrictions stipulated by the March 2022 proclamation in Negarit Gazeta. This regulatory framework provided essential parameters for identifying vehicles exceeding permissible weight limits.

Bridge inspection and hammer testing were conducted with particular attention to detail, whereby a specific bridge was identified along heavily trafficked corridors based on multiple criteria. The selection process incorporated geographical positioning, structural design parameters, and documented instances of excessive loading.

The research methodology incorporated detailed on-site assessments following the Ethiopian Roads Authority Manual procedures. These examinations yielded precise measurements of critical bridge components, encompassing the deck structure, supporting girders, span length, and roadway dimensions.

Computational analysis was performed through R programming for traffic overload assessment. The final methodological component comprised probabilistic assessment methods to evaluate the implications of traffic overloading on bridge superstructure capacity.

1.8 Structure of the study

The structure of this thesis is organized into a series of chapters, each addressing a critical component of the investigation into traffic overload effects on bridge superstructures. Chapter 2 provides a comprehensive literature review; Emphasis is placed on integrating established principles from probability theory and statistics to support the modeling and interpretation of traffic load data. In addition, national regulations concerning permissible axle loads, along with authoritative guidelines, published standards, technical reports, and academic research, are reviewed to establish a solid contextual foundation.

Chapter 3 outlines the analytical procedures adopted for assessing the effects of overloaded traffic on the superstructure of bridges. It details the methodological approach used in the computation of load effects, including the application of influence.

Chapter 4 focuses on the processing of raw traffic data obtained from a static weigh station. It describes the filtration and refinement techniques applied to ensure data integrity and presents an in-depth statistical analysis of a sample comprising 38,188 recorded vehicle entries, characterizing the distribution and nature of observed overloads.

Chapter 5, this chapter describes a case study. It presents a detailed examination of a section of the case study bridge, including inspection results, probabilistic estimation of nominal capacity/resistance, and comprehensive descriptions of the selected bridge.

Chapter 6, The results of the analysis are interpreted concerning the literature review and field inspection findings. The chapter quantifies the overloading effects imposed by the recorded traffic data and evaluates their implications on the superstructural capacity of the bridge. In addition, extrapolation methods are used to determine extreme loading states and are specifically targeted at a 75-year return period. Additionally, modal analysis and harmonic response analysis are presented in different chapters. The modal analysis applies to both fixed and free boundary conditions.

Chapter 7 summarizes various important conclusions derived from this research and indicates implications and recommendations for further research to improve overstress assessment and control caused by traffic on bridge superstructures.

CHAPTER 2 LITERATURE REVIEW

Bridge structures need to be critical and well-designed, consisting of different necessary parts. In the first category, named the superstructure, are to be included such elements as bearings, girder (or beams), decks (inclusive of sidewalks), joints, asphalt overlays of pavements, safety barriers, and drainage structures. In the second category, named the substructure, are to be included such elements as foundations (inclusive of piles and pile caps), abutments, piers, and pier caps. Bridges generally provide critical support to the transport network and function by allowing crossing over congestion points, rivers, and valleys in urban regions. The carrying capability of the bridges assumes major significance since it defines traffic flow and the volume that the transport infrastructure can handle [2, 3].

Traffic overload on bridges refers to excessive weight that exceeds the designed capacity. Evaluation of the structural capacity of bridges under heavy traffic conditions is crucial from a safety and service-life extension perspective. It has become common for vehicles load beyond their design limit, increasing the amount of load on many bridges [4]. This study reviews different methods and findings regarding probabilistic assessment of the effects of traffic overload on bridge structures, with an emphasis on case study approaches

Traffic loads acting on bridge decks also play an integral role in simulating the impact of vehicle and pedestrian traffic. Some of the traffic loads actually represent the weight of vehicles crossing the bridges, while others are selected to ensure maximum internal forces in bridge structures due to vehicles. Although the traffic patterns and placement of heavyweight vehicles have considerably changed from the conventional live loading curves used, the basic models employed in traffic loads by designers have remained relatively unchanged. This has been the case due to traffic loads being simulated by uniform and point loads [5].

A highway bridge is intended to cross an obstacle to create a smooth traffic flow [4, 6]. In order to maintain the functionality of the bridge, the bridge's carrying ability should be higher than the loads acting on it. The nature of loads that the bridge is subjected to is important in determining the bridge’s safety and viability. Therefore, the viability of the bridge may be compromised due to the weight of heavy trucks. The load effects caused may pose higher threats compared to the Gross Vehicle Weights only [6, 7, 8].

2.1 Vehicular Legal Loads

Highway vehicles are so highly variable in both their size and configuration that it is impossible for any one vehicle or load model to accurately capture the effects of all vehicles. Consequently, a legal rating truck needs to be selected that represents the axle spacing and relative axle weights of the average vehicle. Various design manuals specify a legal truckload for a range of axle configurations and weights. For example, the [3] on Performance Evaluation of Reinforced Strength Evaluation of Bridges includes Figure 2.1 showing the axle configurations and loads for three legal truckloads that are to be used in capacity Assessment.

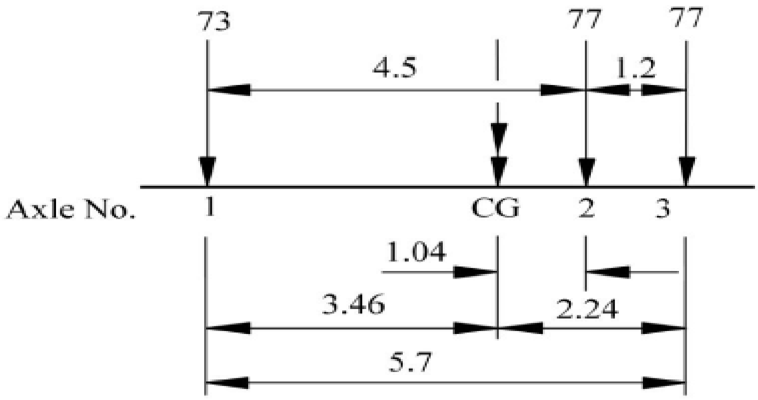

Legal Load one

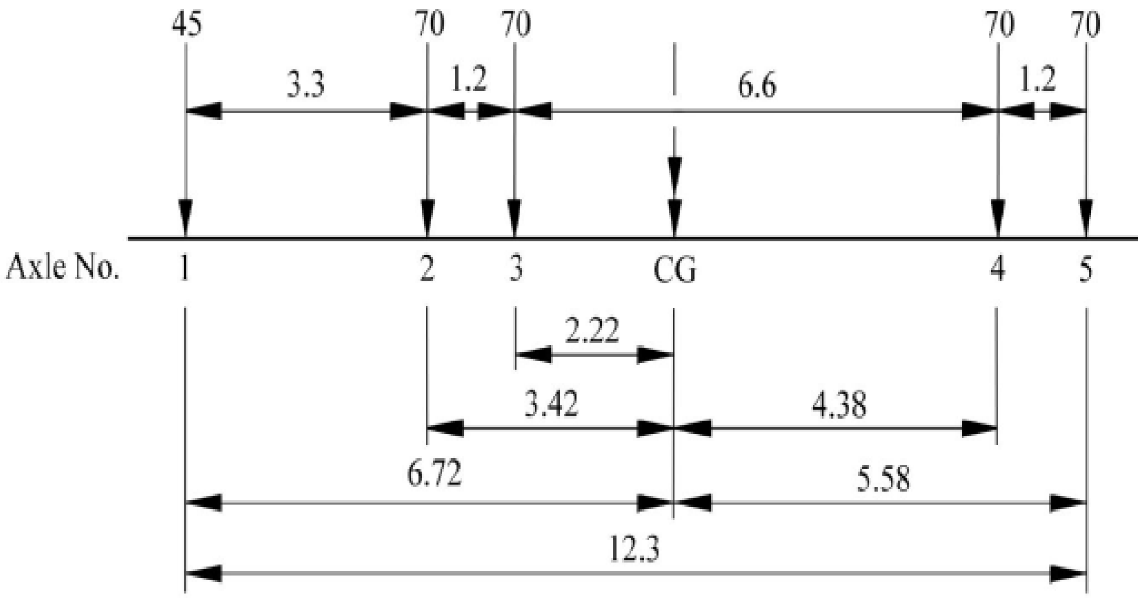

Legal Load two

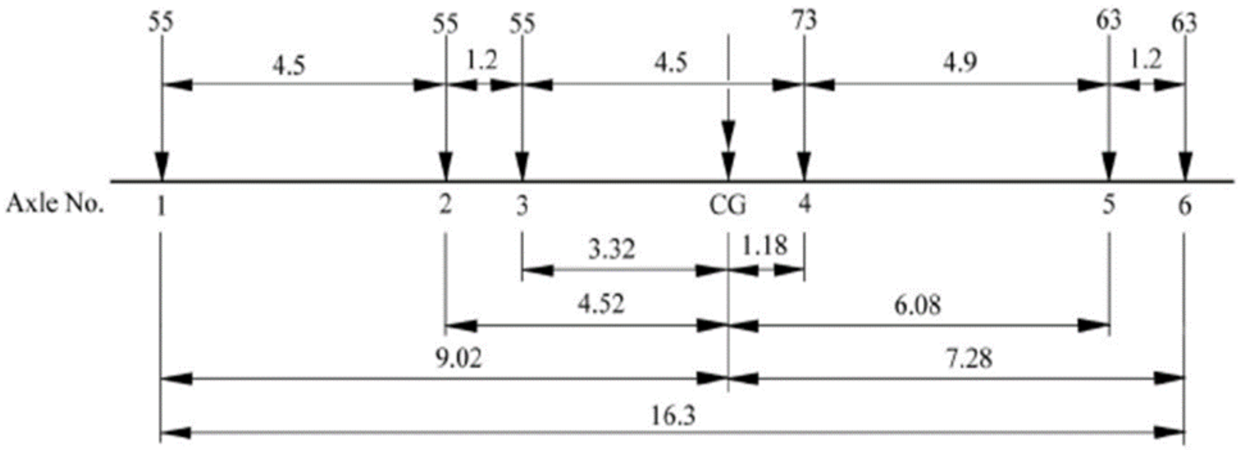

Legal Load Three

Figure 2-1 Load configuration of three of the legal loads, ERA design manual Part II

2.2 Overloading limit

The current axle load limit regulation was approved in a proclamation in March of 2022, as published in Negarit Gazeta. These restrictions have a major impact on construction, maintenance, and highway safety. The regulation of the Council of Ministers No. 491/2022 titled "Council of Ministers Regulation to Amend Vehicle Weight and Dimension Regulations" has outlined eight basic articles. A summary is given in Table 2.1.

Table 2-1 Restrictions as to the size of the vehicle

No.	Size restriction	Limits
1	Outside width of any vehicle, trailer, semitrailer, including load thereon.	≤ 2.65 meters
2	Total Height of any vehicle, including load thereon	≤ 4.6 meters
3	The total length of any vehicle	≤ 12.5 meters
4	Total length of articulated vehicle or track tractor and its trailer, including the front and rear bumpers or loads.	≤18.5 meters
5	Total length of any combination (truck-trailer or semitrailer) vehicle	≤ 22 meters
6	Combination of Motor Vehicles	≤ 2 units

Table 2-2 Restrictions as to the weight of a vehicle

No.	Weight restriction	Limits
1	The Steering Axle weight	≤ 8 tons
2	Single (Drive) Axle weight	≤ 10 tons
3	Tandem Axle weight	≤ 18 tons
4	Tridem Axle weight	≤ 24 tons

According to the Council of Ministers Proclamation 2022, published in the Negarit Gazeta, a tandem axle unit consists of two axles that are suspended side by side with a distance of 1.2 meters to 2.5 meters between them. These axles are connected in such a manner that any weight applied to them would automatically be divided between them in an axle unit. A tridem axle unit is composed of three axles that are suspended together also with a gap of 1.2 meters to 2.5 meters between them. These axles are connected in such a manner that any weight applied to them would be divided equally between them in an axle unit. A steering axle refers to an axle controlled by the driver of any vehicle for the purpose of steering.

2.3 Probability distribution function

The Probability distribution function or Cumulative Distribution Function (CDF) of a continuous random variable X is expressed using its probability density function f(x) via the process of Cumulating PDF to acquire CDF, and CDF defines probabilities that the random variable is less than or equal to the value of x. [9, 10].

2.4 Probability Distributions

Probability distributions play a critical role in the study of the behavior of random variables in the fields of engineering and scientific study. These describe the way in which the probability of the value of the variable is distributed. In this section, the definitions, equations, and graphical representations for the five most basic continuous probability distributions, Normal, Uniform, Log-Normal, Exponential, and Gamma distributions, will be defined. These are typically used owing to mathematical manipulability and applicability [9, 10].

a. Normal Distribution

The normal distribution or Gaussian distribution is actually a continuous probability distribution that follows a symmetric curve that is shaped like a bell. It can be defined using the mean and standard deviation parameters. The mean and standard deviation are used to describe the position and variation of the distribution, respectively. [9, 10, 11].

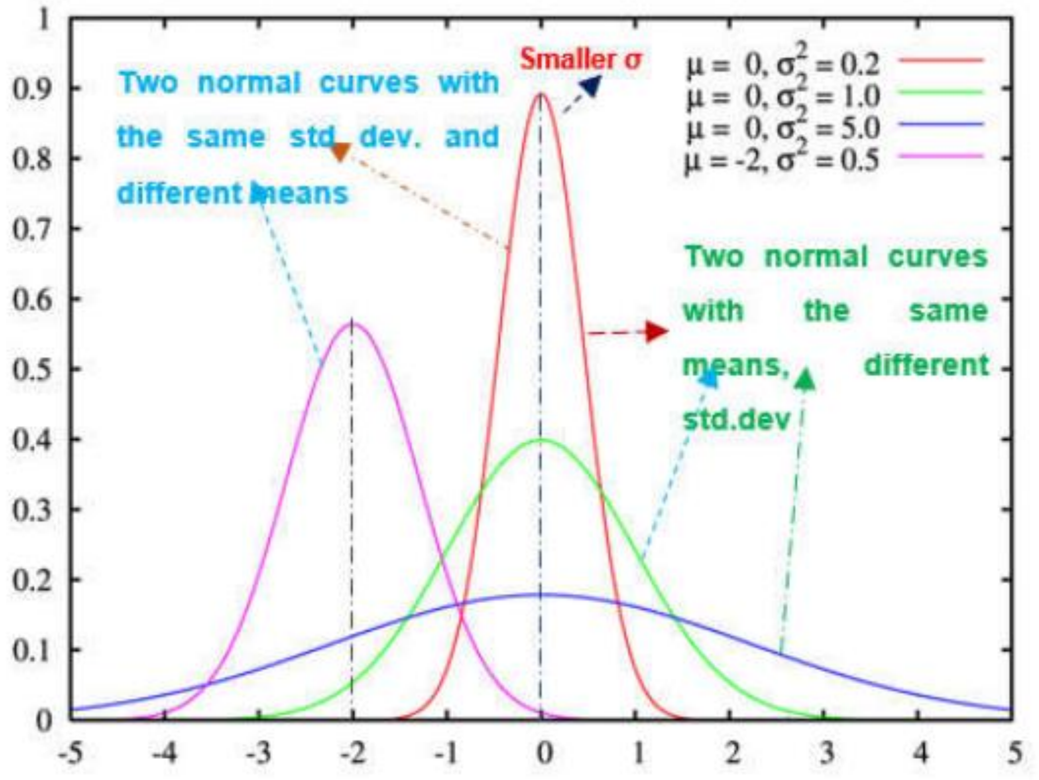

Figure 2-2 pdf of the Normal distribution for various mean values and constant standard deviation

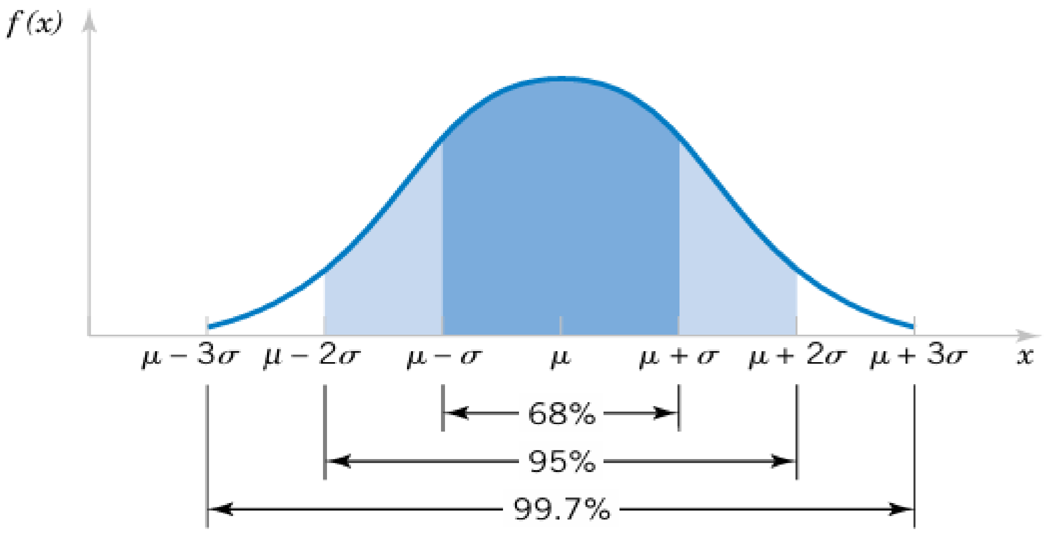

Figure 2-3 Areas of approximation in the Normal Distribution.

b. Uniform Distribution

The uniform distribution is a probability distribution where every outcome in the interval [a, b] is equally likely [9, 10, 11].. It is given by the minimum value a and the maximum value b.

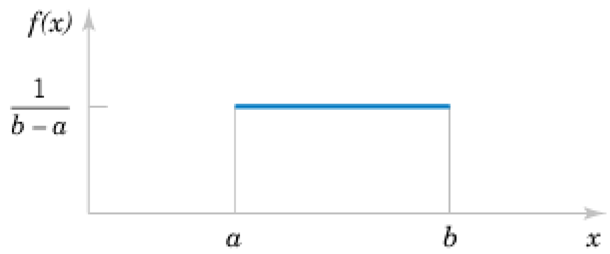

Figure 2-4 pdf of uniform distribution

c. Lognormal Distribution

A log-normal (or lognormal) distribution is a continuous probability distribution of a random variable whose logarithm has a normal distribution [9, 10].

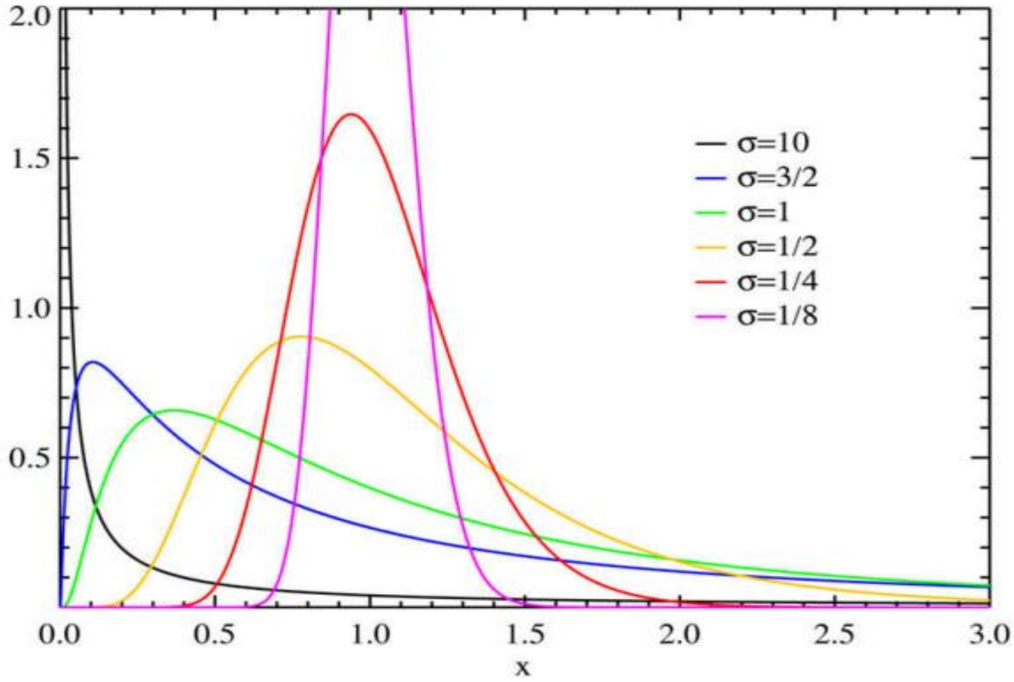

Figure 2-5 pdf of a long-normal distribution for various mean values and constant standard deviation

d. Exponential Distribution

The exponential distribution models the time between independent events that happen at a constant average rate. [9, 10]. It is one of the common distributions used in reliability analysis.

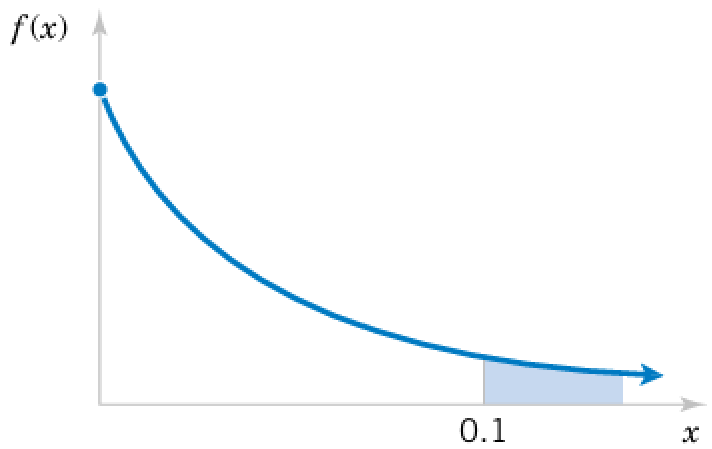

Figure 2-6 PDF of the exponential distribution

e. Gamma Distribution

The gamma distribution is a continuous probability distribution; it has some similarities with the lognormal distribution. It has the same behavior of extending infinitely in the right tail. Also, it is only defined for positive values of X. The values in the gamma distribution tend to extend infinitely in the positive direction; this makes them skewed. The gamma distribution is able to display this behavior because of the probability density function [9, 10].

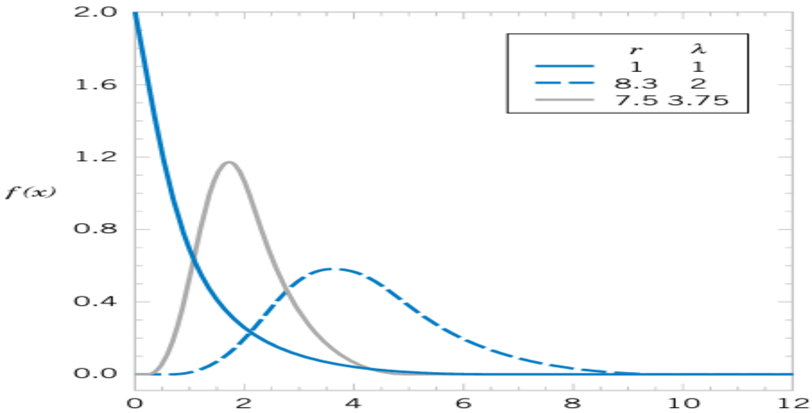

Figure 2-7 pdf of the Gamma distribution for selected λ and r values

2.5 Extreme Value Distribution

Extreme Value Theory primarily deals with extreme and significant events that occur in reality. The theory implies that in observing maxima within a group of random variables which are independent and identically distributed in terms of a specified parent distribution, said maxima would fall into one of three different distributions depending upon the shape parameter of the parent. The shape parameter of zero represents the Type-I Gumbel distribution, that which is positive represents the Type II Fréchet distribution, and that which is negative represents the Type III reversed Weibull distribution. The theorem that validates this concept is the Fisher-Tippett theorem. [9, 12].

This research focuses on extreme values to assess the likelihood of the occurrence of a random variable over a particular threshold. There are two prominent ways to model extreme value observations, namely the use of the block maxima approach and the peak over threshold (POT) method. The block maxima approach requires the division of observations into time units or blocks. The method can overlook significant observations.

On the other hand, the POT method focuses on observations that exceed a particular threshold. it demands significant attention to determine the specific threshold.

1. Extreme Value Block Maximum Distributions

The Block Maximum technique in Extreme Value Theory concentrates on the maximum recorded in predefined sizes of blocks of data. The application of this technique further triggers the notion of Extreme Value Distributions. These distributions are used in modeling the statistical behavior of the block maxima [9, 12].

The Generalized Extreme Value (GEV) distribution is a unified model comprising three extreme value distributions: the Gumbel, Fréchet, and Weibull distributions. The GEV distribution is generally useful for extreme value analysis, either maximum or minimum, for a sample of a random process. The GEV distribution is also applied in the analysis of the reliability of structures. [9, 12]. The three families of the Extreme Value Distributions are:

- Gubmbel:$F(x) = \exp\left\{- exp\left[-\frac{x-\mu}{\sigma}\right]\right\}, -\infty < x < \infty$
- Fréchet: $F(x) = \exp\left\{- exp\left[-\left(\frac{x-\mu}{\sigma}\right)^{\alpha}\right]\right\}, for\ x > \mu$
- Weibull: $F(x) = -\exp\left\{-\left(\frac{x-\mu}{\sigma}\right)^{\alpha}\right\}, for\ x < \mu$

The cumulative distribution function (CDF) of the GEV distribution is defined as:

$$F(x) = exp\{-\left[1 + \xi\left(\frac{x - \mu}{\sigma}\right)\right]^{-\frac{1}{\xi}}\}, \quad for\ 1 + \xi(\frac{x - \mu}{\sigma}) > 0$$

Where: μ is the location parameter, σ > 0 is the scale parameter, ξ is the shape parameter.

Depending on the value of the shape parameter ξ:

ξ = 0 corresponds to the Gumbel distribution

ξ > 0 corresponds to the Fréchet distribution.

ξ < 0 corresponds to the Weibull distribution.

2.6 Return Period

Let's take a random variable X, and the threshold value will be denoted as X_T. If an event x surpasses the threshold value X_T at any point where the occurrence of the event happens, this phenomenon is known as an extreme event. The time duration between two occurrences of the event $X > X_T$ is called the recurrence interval. $E(\tau)$ denotes the return period as T for the occurrence of the event $x \geq x_T$. The probability of an event occurring will be the inverse of the return period.

Hence, T-year return period event is $X \geq X_T$, which occurs, on average, once in T years.

2.7 Characteristic Load Value

Load characteristic value refers to those loads that are highly uncertain but at the same time are expected to occur at any time in the working life of the design of the structure. The characteristic values of the variables of the loads are taken to be high quantiles. Load action characteristics are defined as their representative value. Representative value of the action refers to a value used in the verification of the limit state, in which the constructions are such that they have stopped meeting their design requirements [13].

2.8 A Review of Extreme Values and Probabilistic Methods of Assessment of Load Effects in Bridges

The research by [14] provides a detailed analysis of the development of probabilistic techniques being used to determine the overload effects of bridge structures. The study discusses the limitations of conventional techniques used in determining overload effects. The authors argue that probabilistic techniques should play a crucial role in understanding uncertainties associated with traffic overload effects. The use of these techniques helps in understanding extremes that may occur.

In the course of carrying out the review, the authors discuss and categorize different probabilistic methods, which include the use of statistical models, the theory of extreme value, stochastic processes, Bayesian techniques, and transformation models. These methods are separately used to deal with different challenges posed by uncertainty when designing bridges, taking into consideration the uncertainty of the weights and spacing of the axles, in addition to the impact of the overload on the bridge structure itself.

A crucial aspect under consideration is extreme value theory, specifically by techniques such as Block Maximum and Peaks Over Threshold (POT). The Block Maximum technique takes a simpler approach by concentrating on the maximum value of the loads within a fixed time period, using extreme value distributions including Gumbel or Fréchet distributions. On the other hand, POT analysis recognizes exceedances beyond a threshold value, making it a more effective technique to represent the right tail of the loads, particularly to capture high occurrences of events related to high loads.

The assumptions of normal distribution in the Block Maximum scheme are also considered in the review. It is indicated that even though the method is simple and easy to implement, the resulting normal distribution may not be entirely representative of the traffic pattern data. Such an aspect may cause the results to be less representative of the actual load effects of the bridge. The authors propose an extension of the use of models in the evaluation of bridge safety and integrity, which would play a significant role in the future.

In studies on heavy traffic load behavior, [6] applied both the Chow approach and the live load model described by Sivakumar for Ethiopian short to medium-span bridges to examine the phenomenon of rare events in traffic loadings using the Extreme Value Theory approach. As for EVT models, the Gumbel distribution is a very beneficial one and also belongs to Type I Extreme Value. One principal requirement for the outcome of this approach is that highly unlikely events, like truckloads, should be independent. The rationale is that, in traffic flow, events are unrelated with little possibility that any event would impact another event. The Gumbel distribution is particularly useful with regard to this issue because it is capable of avoiding difficult calculations concerning parameters, enabling immediate calculations with actual data for maxima.

a. Chow method

For the graphical representation of the distribution of the effects of loading, the reduced variable "y", which is related to the exceedance probability, has been determined by the use of the equation developed by Chow. This method greatly facilitates the plotting of the probabilistic trends of the extraordinary effects of overload traffic, which lie in the tail area of the distribution of the effects of loading.

$$y = -\ln\left[\ln\left(\frac{T}{T-1}\right)\right] \qquad \text{Equation 2.1}$$

where T is the return period and given by $T = \frac{1}{p}$

The value of the frequency factor K_T associated with the Normal Distribution is given by the standard normal deviate, x. On the other hand, in the context of Gumbel or Extreme Value Type I distributions, the value of the frequency factor, K_T is calculated by a formula devised by Chow (1988).

$$\mathrm{K_T} = \frac{\sqrt{6}}{\pi}\{\mathrm{K_T} = \frac{\sqrt{6}}{\pi}\{0.5772 + \ln[\ln(\frac{\mathrm{T}}{\mathrm{T}-1})]\} \qquad \text{Equation 2.2}$$

The estimation of the return period of extreme events required the identification of the appropriate population size. This was addressed by the Block Maxima method, whereby from defined intervals, extreme values are extracted consistently for selection in one population, hence offering reliable statistical analysis.

b. Sivakumar et al. [2011]

Studied the applicability of the normal tail-fit method in estimating peak loads for different return periods. It was observed in their results that although the method works satisfactorily for short-term predictions, such as predictions made within a month, it sometimes goes wrong when similar predictions are made for longer return periods. In order to overcome such problems, S. Sivakumar presented an advanced method by applying an Extreme Value Type-I Distribution (Gumbel Distribution) due to the attraction of the probability field related to its normal distribution. Because of this transition, it becomes possible to estimate extreme loads more accurately with mean and standard deviations calculated using certain defined equations in the proposed method.

$$\mu_{max} = \mu + \sigma\sqrt{2\ln(N)} - \frac{\sigma(\ln[\ln(N)]+\ln(4\pi))}{2\sqrt{2\ln(N)}} \qquad \text{Equation 2.3}$$

$$\sigma_{max} = \frac{\sigma}{\sqrt{2\ln(N)}} \qquad \text{Equation 2.4}$$

2.9 Bridge Structure Distress

Structural bridge distress refers to the various types of damage, deterioration, or failures that can occur in bridge structures due to factors such as age, environmental conditions, design error, material quality, or heavy usage. These distresses can manifest in different forms, such as cracks, corrosion, deformation, spalling, and other structural issues that compromise the integrity and safety of the bridge [15].

2.10 Existing Bridge Assessment and Inspection

2.10.1 Existing Bridge Assessment

Proper evaluation of the health of bridge components is considered the foundation of effective bridge management. Assessment of the deterioration of bridge structures is a significant part of bridge management, as it ascertains safety as well as longevity of such structures. Knowledge about mechanisms of deterioration, along with proper evaluation, is essential in ensuring long life of bridges [16]

When evaluating an existing bridge, design standards are applied, which is not desirable. Indeed, some bridges have been rated as unsafe based on design standards, while their reliability is high enough, using probabilistic assessment [17] which leads to the conclusion that it is possible that an assessment of a structure based on design standards may cause unwanted loss of funds during repair and reinforcement work. Therefore, it is not unexpected that probabilistic assessment is increasingly being supported, especially with respect to assessments.

2.10.2 Bridge Inspection

The results of load rating in terms of accuracy and reliability are highly dependent on data. It is imperative that prior information regarding the condition of a bridge be obtained prior to load rating. In cases where specific information is not known, guidance is available on estimating such information. There may also be a need for the use of judgment in a structure's evaluation, especially in modifying factors for condition and factors of safety based on site-specific information [8].

Fundamental data required for load rating should be gathered from field inspection and from data available within the existing bridge. Whenever possible, it is recommended that all critical plan data be validated during the course of the inspection.

Geometric Data:

- Span and member lengths
- Support conditions, continuity, and overhangs
- Bridge skew at each bearing
- Spacing of girders, trusses, and floor beams
- Widths of roadway, traffic lanes, and sidewalks

Member and Condition Data:

- Types and actual sizes of members
- Material grades and specifications
- Data on reinforcing, pre-stressing, and post-tensioning
- Material deterioration and loss assessments
- Condition ratings and flagged issues

- Identification of fatigue-sensitive details
- Presence of fracture-critical members and connections

Loading and Traffic Data:

- Actual thickness of the wearing surface, if applicable
- Non-structural attachments and utilities
- Number and arrangement of traffic lanes on the bridge
- Intensity of pedestrian traffic
- Average daily truck traffic (ADTT) or traffic volume and composition
- Any posted load limits
- Any posted speed limits
- Condition of the roadway surface at both approaches and on the bridge
- Roadway conditions, including bumps at deck joints

2.11 Schmidt hammer test

The Schmidt hammer test, also known as the rebound hammer test, is an non-destructive test that determines the compressive strength of concrete or rock. In this test, the compressive strength of materials is determined by striking them with a hammer that has a steel point and measures the rebound strength of the hammer. The result is measured and related to the compressive strength of the materials [18].

The process for carrying out the Schmidt hammer test includes a number of key steps to determine the concrete strength. The first is preparation, and for testing concrete strength, one must select a suitable part of the concrete to perform this test on. This is because it is important to clean and dry this concrete surface before testing.

Then, you have to choose the best Schmidt hammer suitable for your application after checking the material. Next, you would have to position the hammer in a perpendicular position against the surface you are assessing.

When you are ready to move ahead with a test, you would press your hammer against your concrete prior to the triggering of the spring mechanism and then release it. This will enable you to make contact with the surface, and you will need to monitor the rebound that follows. Once this rebound has happened, you will be able to determine the rebound value that is shown on the hammer’s scale.

To improve the level of reliability and precision of the outcome of your tests, it’s a great practice to run a series of tests, preferably a minimum of ten different tests. This will help you determine the average value.

After the conduct of the test procedures, the outcome can be evaluated in terms of the calculated mean of the recorded readings. Using the rebound readings, one can determine the hardness and strength of the concrete in line with the correction factor.

At last, it is also crucial that all the findings be documented effectively. While documenting the findings, the information may range from the date, time, location, and environment under which the test is done to any observation the material may be under.

2.12 Probabilistic Bridge Load Rating

This method assesses the load-carrying capacity of a bridge by taking into account the uncertainties that are associated with traffic loading, material, and behavior. This technique provides a more precise estimate of the capabilities of a bridge under various loading conditions compared to the deterministic technique [14].

This assessment employs statistical models to represent variability in traffic loads, taking into consideration matters such as weight distribution and traffic flow. However, probabilistic modeling is also employed to evaluate resistance capacities against uncertainties in strength and size characteristics. The generalized formula is applied for determining the probabilistic load rating [14].

In the probabilistic load rating of bridges, the reliability index (β) is employed to determine the probability of failure of the components of the bridge. In research conducted by [19] the reliability assessment of the deflection of a reinforced concrete box girder bridge was carried out based on the principles of reliability indexes. With the First Order Reliability Method (FORM), the research found the reliability index to be roughly 6.5, which affirms the reliability of the structure under various service conditions to a great degree. In the study, the reliability degradation of the structure based on the effects of various deterioration factors such as creep, corrosion, and traffic growth was also considered. The findings of the study indicate that the reliability index intensity approaches the threshold value of 2.8 and drops to below the value after 58 years of its service.

$$P_f = P(g(x) < 0 \quad \text{Equation 2.5}$$

$$g(x) = R(x) - S(x) \quad \text{Equation 2.6}$$

where P_f is the probability of failure, g(x) is the limit state function, R(x) is the resistance, and S(x) is the load effect. Thus, the first-order reliability index is to be computed from the equation below [20].

$$\beta = \frac{\mu_R - \mu_S}{\sqrt{(\sigma_R)^2 + (\sigma_S)^2}} \quad \text{Equation 2.7}$$

Where:

β is the reliability index,

μ_R and μ_S are the mean value of resistance and load effects, respectively, and,

σ_R and σ_S are standard deviations for the resistance and load effects, respectively.

Rate of deterioration in bridge structures can be calculated from probabilistic approaches related to the variation in the passage of time and variations in the structural reliability of bridges. According to research in [21] assessing the state of bridges from both probabilistic approaches and field testing makes it possible to achieve better accuracy in rationalizing long-term behavior. The study explains that degradation in the strength and section properties of materials has played an important part in degradation and reduction in bridge reliability, mainly in old bridges. The rate of decrease in the defined index related to bridge reliability reflects how safety decreases gradually at different ages in bridges and thus forms the basis for lifetime prediction from comparisons between degradation and safety margins.

Rate of deterioration

$$= \frac{\beta_o - \beta_t}{t} \quad \text{Equation 2.8}$$

Lifetime Prediction

$$= \frac{\beta_t - 1}{-d\beta_t/dt} \quad \text{Equation 2.9}$$

Where:

β_o is starting reliability, β_t is the actual reliability index at time t, t is the number of years (or time units) between the two β measurements

CHAPTER 3 METHODOLOGY

3.1 General

The research methodology explains the process that has been adopted to analyze the effects of traffic overload on the superstructural capacity of bridges. The proposed research methodology breaks down and explains the process that has to be followed to analyze and explore different effects and consequences caused due to traffic overload on bridges. The research methodology has adopted a case study approach to explore different effects and consequences of traffic overload on bridges. The case study that has been selected fulfills all major parameters such as traffic static weigh data, location, and year of construction.

This systematic analysis assesses the state and functionality of the bridge, taking into account the long-term impact of traffic congestion resulting from overload. The major probabilistic variables are:

a) Load distribution

b) Material characteristics

c) Structural response

Secondary data has been collected from January 2023 to December 2024.

3.2 Traffic Data Collection

This research originates from the efforts of carefully gathering vehicular traffic data. This serves as the basis for the entire research process. To start this research, it was fundamental to identify an area of research where traffic flow overloading takes place. Having surveyed different options, the path connecting Addis Ababa to Djibouti was chosen. This particular path has high significance in Ethiopia's export-import activities. This serves as the main trading route for Ethiopia. This particular location was thus ideal for research because of its significance, coupled with the heavy flow of trucks.

To obtain the most representative data, the information about the weight of vehicles as well as their axle loads was collected from the existing weigh stations along this road. Specifically, this information was collected from Samara weigh stations assisted by the Ethiopian Roads Administration. Because this information had been previously collected by official systems of monitoring, this information can be identified as secondary information. The specific technical information about the structure of this axle load information will be presented in the forthcoming chapter.

In addition to the mentioned secondary data, as well as gaining an insight into truck configurations and their axels, another survey was carried out with the help of a site visit. The survey was carried out at the Samara Customs branch office at the Mile Customs Control Station, Tuluditu, and Sululta. The result of this survey gave the maximum and minimum total length. Based on site observation, an insight into truck configurations was noted with an aim of providing input during the modeling and assessment phases of this research.

3.3 Processing and Preparation of Weighing Station Data

The traffic flow information obtained from the weighing stations had to go through an intensive processing stage in order for it to be accurate and useful. The initial information was carefully arranged in a manner that underwent a rigorous filtration process with a view to eliminate any information that had any flaws. The processed information was then appropriately grouped in terms of axle combinations. As a way of supplementing and complimenting classifications, a field study was carried out in order to witness axle combinations.

Thus, with this authentic data in hand, this study aimed to examine the influence of critical loading effects, specifically the bending moments and shear forces created by heavy vehicles on the chosen case study bridge. Some of the major calculations carried out in this study involved influence line calculations, which required accurate data inputs of axle loads and spacings.

3.4 Development of an Analytical Program Using R

For running the very extensive and cumbersome calculations involved in the analysis of traffic overload effects, a program was developed in the R programming language. This program was specifically customized for the simulation of traffic movements and computation of the corresponding structural responses, especially the calculation of maximum load effects at a bridge induced by vehicles passing over it using the influence line. The R script developed here became very instrumental in managing the process with ease, where a total of 23698 vehicle overload cases were analyzed in order to determine the critical overloading effects at the key location of the selected bridge.

3.5 Statistical Characterization of Traffic Data

The data obtained from Samara weighing stations was for 38,188 heavy trucks. In a bid to understand better the flow of traffic on this transport corridor, various statistical values have been calculated. These values include centrality, dispersion, and distribution. It was essential in determining a model and extrapolation of rare load events. The choice of data was informed by its relation to heavy trucks on transport corridors in Samara. The relevance of heavy trucks on transport corridors made them ideal for this study.

3.6 Database Development and Data Refinement

As part of the process of data processing, all the data gathered from the Ethiopian Roads Administration and field surveys underwent rigorous screening. This was done using techniques that filter out data that showed irrational or incomplete information. Pre-screening of all gathered data was fundamental in ensuring that no misleading conclusions emerged from less- accurate data. After screening, all data was systematically organized and grouped to provide an appropriate foundation for assessing traffic overload on the capacity of the superstructure of the bridge.

3.7 Load Effect Simulation on Bridge Structure

Using the processed and cleansed traffic database, simulations of truck movements across the bridge were conducted to determine the structural effects. Applying the influence line technique, the mid-span bending moments and shear forces due to trucks of various combinations were determined. Considering the magnitude and intricacies involved in the computations, the developed R program was critical in automating the computations. The program ensured an accurate estimation of the load effects with a focus on determining the critical overload situations. A detailed description of the simulation model is provided in the next chapter.

3.8 Predicting Extreme Loading Events

Even if the analysis represented real cases of overloading, an important aim was to approximate how likely extreme cases of load might be that could happen over very long periods of time. As it is highly impractical to simulate data covering several decades directly in the traffic load case, it has been decided to use the method of statistical extrapolations. By matching the results of the load effects to an applicable probability distribution function, it has been possible to approximate typical values for the return period of 75 years, thereby giving a realistic estimate of the maximum load conditions that may be expected to act on the bridge throughout its life.

3.9 Case study: Bridge selection and Existing Condition Assessment

After the independence of Eritrea in 1993 and a break in relations in 1998, Ethiopia lost access to its former ports and re-oriented all maritime trade through Djibouti. The Addis Ababa–Djibouti corridor became elevated as the country's most vital trade artery, carrying upwards of the bulk of seaborne imports and exports.

[22] Zeroes in on the fact that today, more than 90% of the country's sea trade depends on it. In underlining its economic lifeline, the country's steady supply of fuel, building materials, foodstuffs, and manufactured goods makes this transport route one of the busiest freight corridors in this part of the world.

According to [22], This heavy concentration of cargo traffic places enormous strain on transport infrastructure, and particularly bridges that endure frequent and overloaded axle weights. The corridor provides an appropriate and practical basis for examining how recurrent traffic overloads influence the structural reliability of bridges in a probabilistic framework.

The paper targets the route that connects Addis Ababa and Djibouti because the route is increasingly important for the country's trading and transport sector. The principal links between Addis Ababa and Djibutu are the Addis Ababa-Samara-Djibutu highway line and the Addis Ababa-Dire Dawa-Dewale-Djibutu highway line. This study represents the probabilistic effects of overloaded traffic on bridges that were initially designed with conventional deterministic methods but according to modern design standard upon construction.

For Addis Ababa to Djibouti corridors, three weigh stations are at Mojo, Awash, and Samara along this corridor. However, Awash weigh station at the time of study was hampered by defective Automatic Recording System equipment such that it lacks capacity to analyze traffic congestion. Similarly, the Mojo station is less reliable because trucks can use two alternative routes from Addis Ababa, and this introduces bias in the selection of bridges for study. In contrast, the Samara weigh station has given dependable and comprehensive records and, therefore, represents the best source for assessing overload effects on bridges.

This weigh station is governed by the Ethiopian Roads Administration and is estimated to be approximately 3.7 km from Samara City. It weighs the trucks that carry heavy loads destined for the Addis Ababa-Samara-Djibouti railway line.Its positioning is of great significance in that it weighs the trucks that pass through inland cities of Mekelle, Kombolcha, and Addis Ababa. It is also significant in that it enables an evaluation of the effects of the overloads on the performance of the bridge Mile-1 to Galafi.

In this study, a systematic set of selection criteria was prepared and used to identify an appropriate case study bridge from the above-described stretch of bridges. The selection was focused on those bridges that are not only the common structural types present in the area but also possess those specific requirements which can realistically and accurately provide the impact assessment of overload. The Key Criteria for Case Study Bridge Selection:

1. Traffic Static Weigh Data Availability:

Availability of traffic data is integral to any data-driven bridge load assessment. The bridge of investigation ought to be located close to a permanent or temporary weigh station along routes that have been subjected to static weight or WIM traffic surveys. Otherwise, it would not be possible to capture the variability of axle weights and vehicle flows required in probabilistic analysis based on measured traffic data.

As pointed out in [23], WIM data give the most accurate basis for modeling traffic load and are therefore an essential part of reliability analysis of bridge performance.

2. Geographical Setting

The bridge should be part of a critical transportation corridor with proven high-density flow: the Addis Ababa–Samara–Djibouti corridor.

3. Year of Construction

The construction year was also an important variable in the analysis since it was an indicator of the design lifespan of each bridge and its ability to handle the rising traffic load. The consideration of bridges that are still within their expected service life avoids the uncertainties associated with older structures which may already show significant deterioration. Therefore, by considering such bridges, it would be possible to clearly isolate the direct influence of the present-day traffic overloads on structural behavior without the confounding effects of advanced aging. By excluding the relatively aged bridges, the assessment also offers a more reliable basis for understanding how current loading patterns influence the long-term performance of existing bridges. [24].

4. Structural Type and Design Standard:

A structural response of a concrete girder bridge is quite different from that of a steel truss or masonry arch under applied loads [25]. In the assessment, consideration was taken of the bridge types commonly used in the routes, like reinforced concrete girders and slab bridges, and concrete I-girders. The basis of determining the conventional overload effect evaluation in these structures has to be referred to established design codes [2, 3, 26].

5. Span Length and Configuration

The length of the span within the bridge significantly influences the susceptibility of the bridge to traffic loads, as well as the type of behavior associated with it. A shorter span is especially susceptible to the shear action caused by heavy single wheel loads, while a medium span with lengths measured between 15-35 meters can be susceptible to the action of bending moments and shear forces generated by heavy truck loads. Long spans measured above 35 meters are usually susceptible to various combines loads from vehicles, thus experiencing more complex behavior compared to shorter spans, medium spans, as well as other spans in relation to their supportive structures, which may be simply supported or continuous structures within the system [27].

6. Damage Rate

The damage rate of a bridge refers to the rate at which its structural elements deteriorate over the years; hence, this becomes an important factor for choosing a bridge for detailed study. [28] underline that performance-based ranking relies on inspection results for grading individual components, and the grades are combined to reflect the overall condition as it varies with age, allowing fair comparisons with time and underlining the bridges that have increased deterioration rates in later years as priority cases for more detailed evaluation.

7. Document Availability

The design and construction records of the bridge should be accessible for accurate modeling and comparison with actual performing data.

With the appropriate bridge identified according to the aforementioned parameters, there was an in-depth knowledge attainment regarding the state of the bridge conducted by data collection, involving both site visitation techniques and Schmidt Hammer testing.

These inspections in the field were conducted in accordance with the inspection manual as described in the Ethiopian Roads Authority Manual. These ensured a standardized inspection of the structural parts of the bridge. The measurements taken included the girder dimensions, abutment dimensions, spans of the bridge, and the widths of the road bridge and the whole bridge. Apart from these measurements, the structural integrity of the bridge was required in relation to the capacity of the analysis.

3.10 Bridge Super Structural Capacity Assessment

Finally, incorporating the results of the traffic overload analysis and the assessment of the bridge superstructure, there has been a focus on the impact of traffic overload and the capacity of critical points. The significance of incorporating the assessment results is that there is a better understanding of the impact of overload on the structure of the bridge while giving insights into the present state of the bridge structure based on the actual working conditions.

CHAPTER 4 TRAFFIC WEIGHT DATA COLLECTION AND ANALYSIS

4.1 General

Ethiopia has also established statistical weigh stations for traffic surveys and axle load enforcement since 1990, as required by the Council of Ministers. This paper uses secondary information from the Ethiopian Roads Administration in its research on the complexities and uncertainty of traffic flow on heavy trafficked roads in Ethiopia. The paper presents a case study of a particular bridge on one of these roads that are heavily trafficked. The case study is a method of establishing the effect of traffic overload on structural capacity.

The data includes information about 38,188.00 truck passages, as the axle count is largely measured from the Semera weigh station, positioned along the country's vital import-export route.

Within this section, it is important to evaluate the reliability of the car data gathered from a set of measurements. The method involves a data filtration process that gets rid of inaccuracies. The pre- and post-filtered data are evaluated using the approaches mentioned. Finally, the assessment of 37833 truck loading data offers an insight into the level of 23698 overloading.

4.2 Measurements of Traffic Loading

Traffic counters are mostly employed to obtain traffic information. The determination of axle loads and their gross vehicle weights requires weighing, which can be carried out in various ways [6].

1. Static weighing
2. Low-speed weigh-in-motion
3. High-speed WIM systems

The most accurate and common technique used is static weighing, primarily used for direct action.

The low-speed weigh-in-motion system functions in a controlled manner and mostly at a speed of below 10 km/h. The low-speed WIM system has been set up and is in operation at the toll gates of the Addis Ababa – Adama Expressway.

The high-speed WIM is intended for measurement of dynamic axle weights in a free-flowing traffic stream. The type of data that is provided is real-time information concerning several factors: individual axle weights and total axle weights, axle spacings, speeds, headways between trucks, gross weights, and classification.

4.3 Analysis of Axle Load Data

Data gathered from the Samara weigh station to aid in the completion of this thesis from the Ethiopian Roads Administration, and the time frame involved was from January 2023 to December 2024. Even though there were several factors recorded, the research was carried out only on the recorded axle weight.

The number of heavy vehicles registered was 38,188. The data given by the Samara weigh station came in Excel form and was presented as shown below: Classification of vehicles was done depending on the total number of axles.

Table 4-1 Sample of collected axle load data

Axle load Data									
			Weight of axles (in tons)						
No.	Date	A_1	A_2	A_3	A_4	A_5	A_6	A_7	GVW (in ton)
1	1/1/2023	6.52	8.46	10	-	-	-	-	24.98
2	1/1/2023	5.56	12.62	6.68	9.9	-	-	-	34.76
3	1/1/2023	5.3	7.86	8.26	10.68	11.4	-	-	43.5
4	1/1/2023	5.62	7.16	6.24	6.8	5.74	10.2	-	36.02
-									
-									
-									
-									
38,188	12/31/2024	6.34	10.38	10.4	7.7	9.3	8.6	9.34	45.74

A normal way of distinguishing between trucks is based on the axle number. Knowing the weight on each of the axles is very critical in distinguishing various types of vehicles found at the sites [4, 6, 7, 29].

The earlier classification of vehicle data stressed that weight information was an essential data in determining the load effect produced by the actual vehicles crossing the bridge superstructure.

4.3.1 Cleaning (Filtering) Out Unreliable Weight Data

In the course of traffic flow data organization and cleaning, unclassified vehicles failing to meet known classification requirements were not taken into account. These vehicles include those that fail to meet the general categories of vehicles described in [2, 30]. These kinds of vehicles are well known for their irregular characteristics, such as non-standard axle arrangement. Although they don't appear as frequently as normal vehicles, the extreme weights and sizes may cause an unusual burden on the bridge structure in question. In this regard, they form the most challenging group in the determination of structural strength, taking into consideration the extreme bridge weights they are capable of producing. According to the guidelines described in [2] accurate classification is fundamental in obtaining reliable results in modeling loads; however, these vehicles form an exception in this regard, owing to their extreme characteristics that challenge normal standards.

However, in using static weighing machines to obtain data, the objective of this thesis is to formulate the best practices and methodologies developed by various authors in various countries to achieve this objective. The major part of this literature has been related to WIM technology, which has been adapted to provide the requirements of this study related to the data-cleaning process of this research. Some researchers have tackled the problems caused by misleading information provided by WIM systems. It is important to analyze WIM information to remove misleading information to focus on making high-quality information used in traffic load models [29].

The data cleaning approaches suggested by [29, 30] highlight the importance of the characteristics of traffic data and the systems used in the WIM based on national regulation constraints. For the research conducted within the thesis, several methods will be used, taking into consideration the groundbreaking efforts of various significant authors [6, 7, 13, 29, 30].

On the basis of globally applicable standards of traffic data processing, this research follows a filter screening of raw data to exclude unconvincing and meaningless values for analysis. This is basically done to eliminate values that are not capable of representing bridge loading realistically and are presumably accountable to classification and measurement inaccuracies. Vehicle entry values with less than three axles and more than seven are thus filtered out since they normally represent misclassified and extraordinary cases with limited usage to normally assess bridge load values. Similarly, values with gross weights of less than 3.5 tons are also filtered out since they normally offer insignificant values to represent extreme load effects with limited accuracy of measurements. Values representing individual axle weights of more than 40 tons are also filtered out since they are normally values of defective sensor measurements based on extraordinary data points with least usages to represent actual traffic conditions [6, 7, 13, 29, 30].

3-Axle Vehicles

On the basis of secondary data collected from the Ethiopian Roads Administration in Samara Station, it is observed that there are 405 vehicles with three axles, constituting 1.06% of all vehicles. These vehicles have Gross Vehicle Weights (GVW) varying from 12.94 tons up to 43.6 tons. Observations made during visits made to the Samara customs branch office at the Mile customs control station revealed that cars with trailers, dump trucks, and Isuzu FSR were part of the 3-axle vehicles in Ethiopia. Dump trucks were crucial in the evaluation of the maximum weight.

4-Axle Vehicles

The category included a total of 1,306 vehicles, constituting 3.42% of all, designated as four axle vehicles with Gross Vehicle Weights ranging from 16.40 tons to 61.94 tons. Such a category of data was of great importance and was selected for further scrutiny, as explained for the relevance of appreciating the characteristics and potential of the aforementioned category of vehicles.

5 or More Axle Vehicles

On the basis of secondary data, it has been calculated that the vehicles with five or more axles account for approximately 95.16% of the total vehicles. The Gross Vehicle Weights (GVW) of the vehicles having five to seven axles are given in Table 4.2, which will provide useful information in the coming analysis of the heavy vehicles.

Table 4-2 The data includes trucks with three to seven axles, their maximum and minimum weights, and the total number of registered vehicles.

Number of Axles	Number of Trucks	Min. GVW (in tons)	Max. GVW (in tons)	% of the total
3	405.00	12.94	43.6	1.06
4	1,306.	16.4	61.94	3.42
5	1,399.00	18.24	67.88	3.66
6	34,080.00	34.12	70.18	89.24
7	862.00	44.68	70.28	2.26

From the gathered secondary information, it has been identified that vehicles possessing five or more axles make up 95.16% of all vehicles. The Gross Vehicle Weights (GVWs) of vehicles in which five to seven axles are included are shown in Table 4.2. This information serves to be appropriately insightful for further study on heavy vehicles.

4.3.2 Outcome of the Filtered Unreasonable Data

The aim of the filtration process was to eliminate the unreasonable data in the collected series between January 2023 and December 2024. Almost 99.7% of the truck data was taken for the next analysis. Such an impressive result shows the quality of the data generated and makes the next analysis even more reliable.

In this extensive filtering process, it was ensured that the upper limits of the specifications of the vehicles being filtered were well noted. The negative records were recognized, and the subsequent removal of the vehicles with realistic weights from the filtering process was carried out. This particular process was done using Excel templates.

Table 4-3 Outcome of Filtration of Vehicle Data

No. axles	No. of Vehicles Before Filtration	No. of Vehicles after Filtration	Percentage of unreasonable vehicle data, [%]
3.00	405.00	402.00	0.74
4.00	1,306.00	1,299.00	0.54
5.00	1,399.00	1,390.00	0.64
6.00	34,080.00	33,895.00	0.54
7.00	862.00	847.00	1.74
Total	38,052.00	37,833.00	0.93

4.4 Statistical Methodology

4.4.1 Accuracy of Data

There are numerous sources of potential errors in weighing systems. First and foremost, these may be categorized according to the scale itself and related matters such as installation and leveling. Other sources are external and include approaches to the scale on truck systems, oscillation while weighing, friction involved in truck and scale interaction, and suspension and braking systems of trucks [6].

Although the static scale is known for the accuracy it provides in the readings it gives, it is prone to some errors too. To address these errors associated with the scale readings, a scale tolerance has been set. The tolerance shows the expected scale error based on the type of scale used as well as the effects of the various external variables [6]..

4.4.2 General Statistical Properties of the Data

This topic presents information on statistics that are calculated based on trucks that move along the route towards Semera. The statistics include all heavy trucks that have 3-7 axles, ranging from January 2023 to December 2024. A total number of 37,833 truck data entries were considered in obtaining useful findings from the data. The calculations done for the mass of the axles, shown in Table 4-5, show that many trucks have axle masses higher than the regulations, set at 8 tons and 10 tons for the first and subsequent axles, respectively. Notably, these findings show that there may be errors associated with the estimated mass values for the static axles. Additionally, it is observed that both Axle 2 and Axle 3 have alarming trends that deserve further inquiries.

The statistical properties of the front and rear axles in relation to their load distribution are provided in Table 4.4 below. These loads are measured in tons and taking into consideration the number of vehicles that fall into each load range of the axles. These statistics are fundamental in understanding the traffic load patterns based on axle loads.

Table 4-4 General statistical properties of each axle from the weighing station data.

	A_1	A_2	A_3	A_4	A_5	A_6	A_7
Min.	3.02	3.48	0.81	0.30	0.02	0.04	0.10
Max.	20.80	21.54	22.02	34.58	28.86	33.18	15.82
Mean	6.85	11.87	11.44	9.91	9.00	9.84	7.40
Standard Deviation	0.94	1.75	2.01	1.78	1.42	1.81	3.00

	A_1	A_2	A_3	A_4	A_5	A_6	A_7
Tons							
1.0-2	-	-	1	13	5	45	8
2.1-3	1	-	4	24	22	35	29
3.1-4	1	20	30	26	3	39	59
4.1-5	143	49	202	161	107	135	177
5.1-6	8,274	166	447	614	1,250	633	105
6.1-7	15,332	401	658	1,148	2,091	831	58
7.1-8	11,437	914	1,273	2,020	4,287	2,029	33
8.1-9	2,148	1,455	2,324	6,770	9,447	6,805	41
9.1-10	306	2,363	4,337	11,782	12,577	11,334	129
10.1-11	84	4,971	4,559	6,996	5,031	6,488	119
11.1-12	29	6,839	5,536	3,585	857	2,598	47
12.1-13	16	11,706	11,382	2,476	249	1,938	26
13.1-14	13	6,960	5,487	1,248	97	1,177	11
14.1-15	10	1,750	1,452	410	43	399	4
15.1-16	11	201	120	115	13	155	1
16.1-17	5	26	12	22	16	58	-
17.1-18	7	9	7	8	14	16	-
18.1-19	4	-	1	6	7	7	-
19.1-20	7	1	-	1	5	5	-
20.1-21	5	-	-	-	5	5	-
21.1-22	-	1	1	-	2	1	-
22.1-23	-	-	-	-	-	1	-
23.1-24	-	-	-	-	-	2	-
24.1-25	-	-	-	-	-	2	-
25.1-26	-	-	-	1	2	2	-
26.1-27	-	-	-	1	-	1	-
27.1-28	-	-	-	-	1	-	-
28.1-29	-	-	-	1	1	-	-
29.1-30	-	-	-	-	-	-	-
30.1-31	-	-	-	-	-	-	-
31.1-32	-	-	-	2	-	-	-
32.1-33	-	-	-	-	-	-	-
33.1-34	-	-	-	-	-	1	-
34.1-35	-	-	-	1	-	-	-
35.1-36	-	-	-	-	-	-	-
Total	37,833	37,833	37,833	37,431	36,132	34,742	847

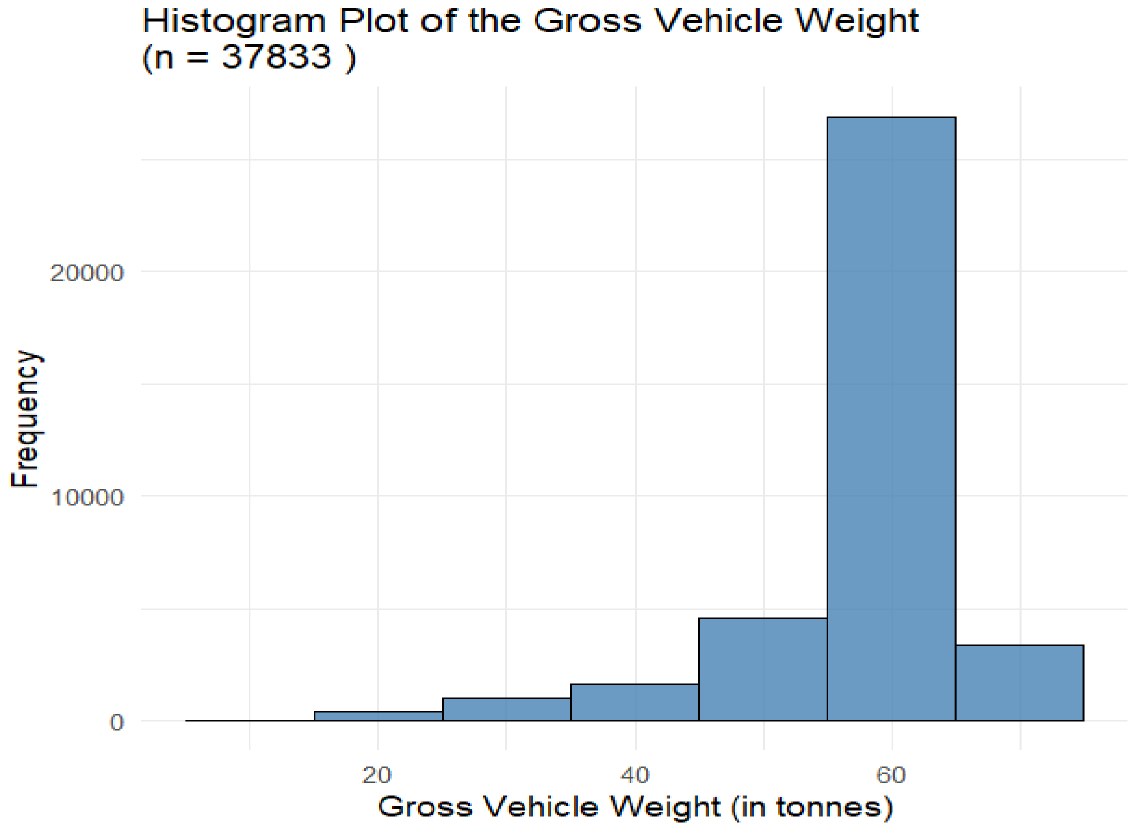

Figure 4-1 Histogram Plot of the Gross Vehicle Weight

4.4.3 Statistical characteristics related to axle arrangements

Statistical characteristics and theoretical distributions of secondary data from Ethiopian Roads Administration are shown in the following table.

Table 4-5 Statistical properties corresponding to axle configuration

Vehicle Type	Statistical Properties	Weight of axles (in Tons) A_1	A_2	A_3	A_4	A_5	A_6	A_7
3-Axle Vehicle	**Mean**	7.34	10.40	10.77	-	-	-	-
	Mode	6.16	7.22	12.46	-	-	-	-
	Standard Deviation	1.94	3.28	2.94	-	-	-	-
	Skewness	1.36	0.12	-0.14	-	-	-	-
4-Axle Vehicle	**Mean**	6.26	9.20	7.26	7.68	-	-	-
	Mode	6.18	9.32	5.12	5.94	-	-	-
	Standard Deviation	1.05	2.45	2.29	2.92	-	-	-

Vehicle Type	Statistical Properties	Weight of axles (in Tons) A_1	A_2	A_3	A_4	A_5	A_6	A_7
	Skewness	4.77	0.29	0.95	2.40	-	-	-
5-Axle Vehicle	**Mean**	6.53	9.72	9.32	8.95	10.03	-	-
	Mode	5.70	11.66	8.66	9.04	10.72	-	-
	Standard Deviation	2.09	2.26	2.22	2.12	3.28	-	-
	Skewness	4.54	0.33	0.32	0.28	0.48	-	-
6-Axle Vehicle	**Mean**	6.88	12.09	11.71	10.01	8.96	9.91	-
	Mode	7.10	12.72	12.98	9.68	9.46	9.50	-
	Standard Deviation	0.83	1.49	1.72	1.61	1.27	1.76	-
	Skewness	0.20	-0.81	-0.07	0.31	0.46	0.55	-
7-Axle Vehicle	**Mean**	6.76	11.65	11.02	10.76	9.03	6.93	7.40
	Mode	6.36	11.36	10.02	10.02	9.78	5.02	4.78
	Standard Deviation	0.82	1.86	2.04	2.06	1.39	1.64	3.00
	Skewness	0.57	-0.66	0.03	-0.03	-0.35	0.94	0.15

Considering the theoretical patterns for various vehicle axle configurations, the gross weight of vehicles-an overall measure of vehicle weight-seems to follow a Weibull probability distribution. This is evident for three-axle to seven-axle trucks, where the shape of the distribution closely resembles a Weibull probability distribution, as depicted in Figures 4-2 and 4.6.

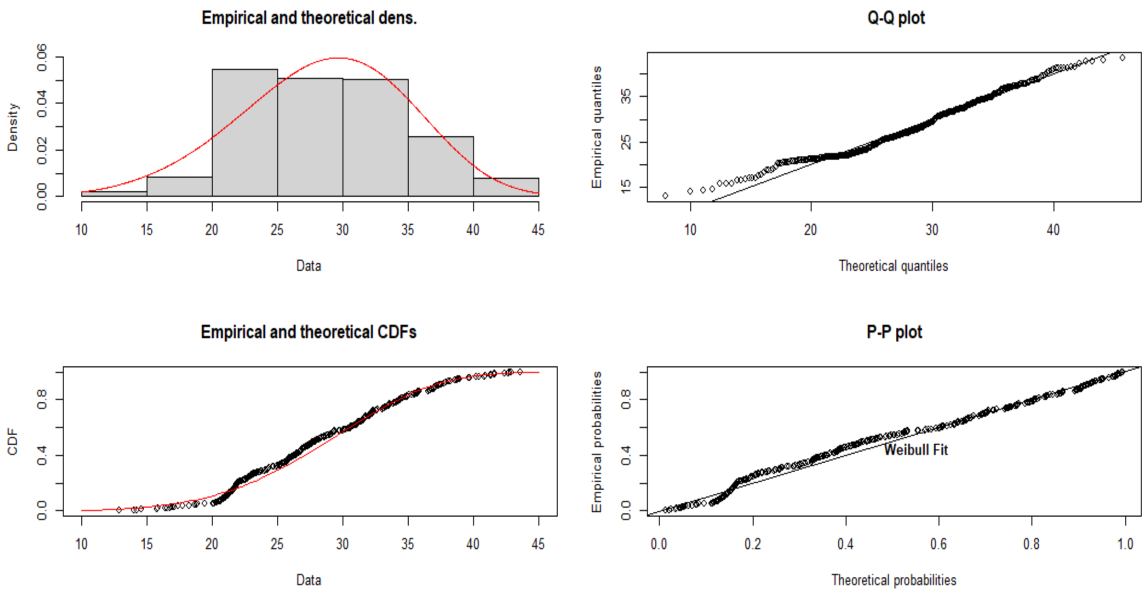

Figure 4-2 Histogram plot and Weibull Distribution plot of GVW 3-axle trucks.

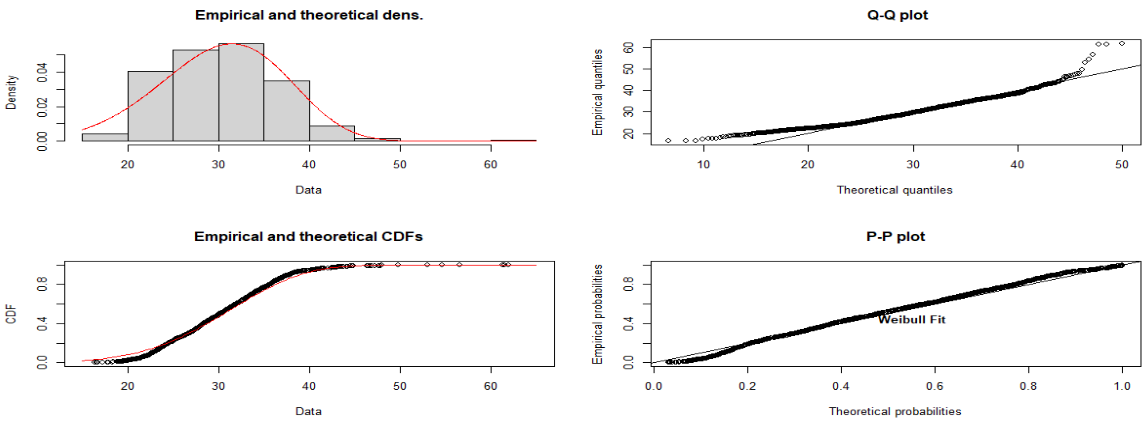

Figure 4-3 Histogram plot and Weibull Distribution plot of GVW 4-axle trucks

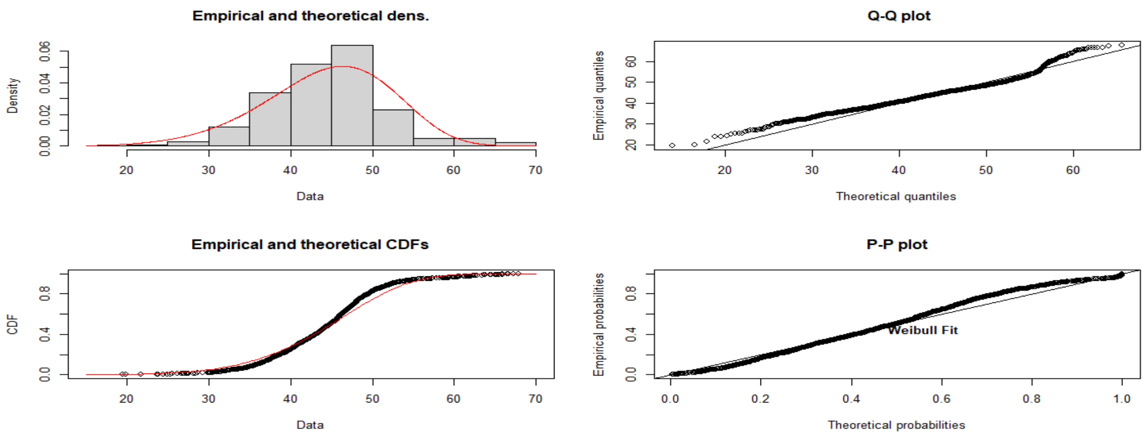

Figure 4-4 Histogram plot and Weibull distribution plot of GVW 5-axle trucks.

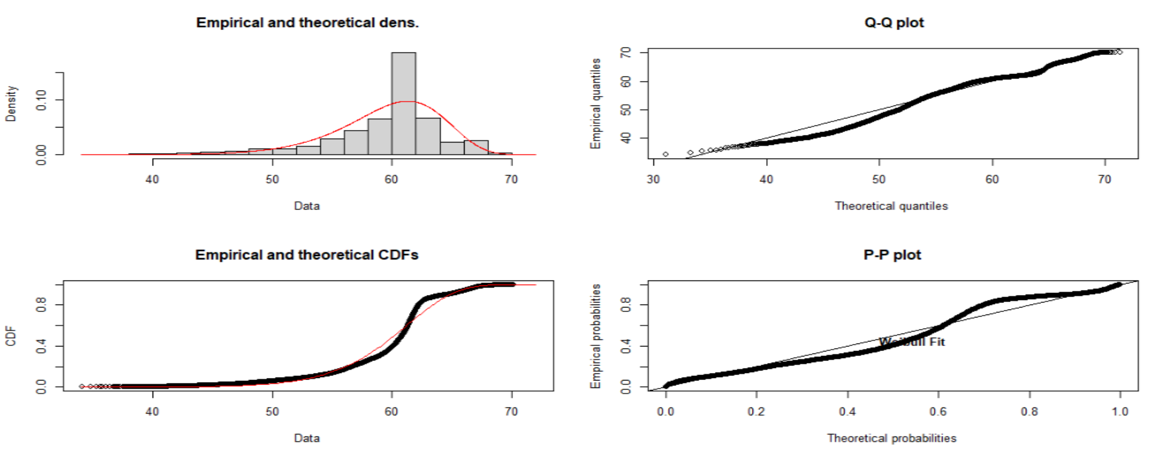

Figure 4-5 Histogram plot and Weibull distribution plot of GVW of 6-Axle trucks

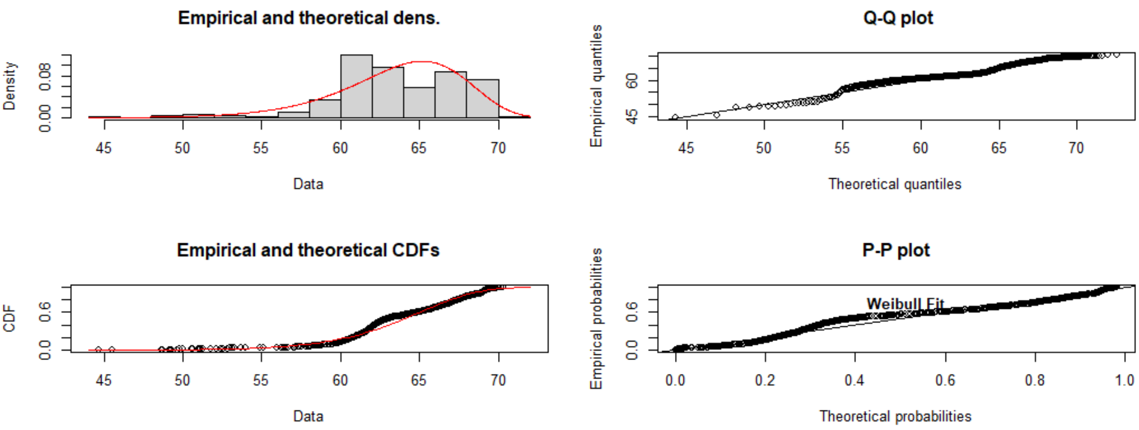

Figure 4-6 Histogram plot and Weibull distribution plot of GVW 7-Axle trucks

As shown in Figures 4-2 to 4-6, the gross vehicle weight of the trucks follows one dominant type of Weibull probabilistic distribution. The data measured from the weigh station in Samara will then be used as the key basis for the Probabilistic Impact Assessment of Traffic Overload on the existing bridge. This analysis gives insight into the superstructure capacity of the existing bridge under different conditions of traffic overload.

4.5 Field Measurements of Axle Spacing

One of the parameters that can significantly influence traffic characteristics is the spacing of the axles of successive trucks. The measurement of axle spacings is also an important factor in this regard. In this research, it has been found that the data gathered from the static weigh station did not include truck axle spacings.

It was observed that in the case of Ethiopian WIM data [31] inter-axle distances in trucks follow a lognormal distribution; this was consistent with international research on heavy trucks. The values of inter-axle distances are positively skewed; they are never negative. However, in some truck groups, double peaks are observed in their distributions. These can be accounted for by using a mixture of lognormal distributions.

To find the types of heavy trucks that frequently move through bridges in Ethiopian, a field study was carried out. Axle spacing measurements for the truck axles were also carried out at the Samara Customs Branch Office, located at the Mile Customs Control Station, Tuluditu, and Sululta stations. During the same exercise, the authors managed to accrue information regarding the total truck length, which had a minimum and maximum value, along with the corresponding means and standard deviations, which are shown in Tables 4-6 and 4-7, respectively. These findings will significantly contribute to determining the overload impact on bridge structures.

Table 4-6 Measured the Maximum and Minimum length

Number of Axles	Minimum	Maximum
Three	4.5	6.15
Four	5.85	14.2
Five	12.35	15.67
Six	12.62	16.33
Seven	13.7	16.23

Figure 4-7 Inter-axles spacing sample measurement at Mile Customs Control Station.

Table 4-7 The Statistical Properties of Vehicle Axle Spacing

No. Axle	Statistical Properties	Axle Spacing					
		S1	S2	S3	S4	S5	S6
Axle - 3	Mean	3.897	1.724	-	-	-	-
	Standard Deviation	0.344	0.364	-	-	-	-
Axle - 4	Mean	3.597	5.812	2.078	-	-	-
	Standard Deviation	1.040	1.278	0.255	-	-	-
Axle - 5	Mean	3.540	1.380	6.853	1.413	-	-
	Standard Deviation	0.247	0.059	0.271	0.019	-	-
Axle - 6	Mean	3.672	1.426	5.286	2.364	1.388	-
	Standard Deviation	0.508	0.022	0.426	1.206	0.047	-
Axle-7	Mean	2.853	1.950	2.730	3.205	2.850	1.325
	Standard Deviation	1.153	0.658	1.429	1.964	1.550	0.083

4.6 Overloading

Some studies have also focused on the important aspect of overloading of vehicles that is common on the major transport routes in Ethiopia. Research undertaken using data from weigh station points like Holeta Weigh Station, Modjo Weigh Station, Awash Weigh Station, Sululta Weigh Station, Semera Weigh Station, Sendafa Weigh Station, and Alemgena Weigh Station showed that the major percentages of the trucks that transport goods in Ethiopia were overloading in terms of the weight of the axle and the weight of the gross vehicle weight of the trucks [6, 32, 33, 34].

The most disturbing values were found in Sendafa, Sululta, and Awash, where overload rates were measured to be 97%, 90%, and 92%, respectively, for periods of two to three weeks [33]. Even in areas where monitoring is common, like Holeta and Modjo, overload rates varied from 28% to 67% depending on the interval measured [33, 34]. In a study where Modjo, Sululta, and Semera stations were observed for a period of two years, about 53.3% of total trucks were found to be overloaded [6].

The incidence of over-loaded vehicles is a major concern affecting the durability and safety of roads and bridges. This is especially the case in short to medium spans of bridges which are not meant to be loaded this much. There has been a call for strict enforcement of the laws in relation to weigh bridges staff as well as improvement in infrastructure planning [6, 33, 34].

In Sendafa, Sululta, and Awash, the highest percentages of overloaded vehicles were recorded to be 97%, 90%, and 92%, respectively, within very short observation periods [33]. The two busiest routes, Modjo and Holeta, recorded considerable percentages of overloading, between 28% and 67%, depending on the recording interval [33, 34]. In a different study, carried out over two years on Modjo, Sululta, and Semera, 53.3% of truck vehicles were found to be overloading, pointing to a serious problem [6].

The existing regulation on axle load standards is stipulated in a proclamation that was decreed in March 2022, and this is according to Negarit Gazeta. The standards play an essential role in construction and road safety. Council of Ministers Regulation No. 491/2022 has eight major articles and is named "Council of Ministers Regulation to Amend Vehicle Weight and Dimension Regulations." A summary of this regulation is presented in section 2.3 in Table 2.1.

Vehicular standards beyond these limitations require the collection of a special permit. However, axle spacing in weighing stations does not actually get considered. An easier approach provides for up to 8 tons on the steering axle, up to 10 tons on the single(drive) axle, up to 18 tons on the tandem axle, and up to 24 tons on the tridem axle, irrespective of axle spacings. Therefore, the level of overload on the roads can be assessed for the given data for the evaluation of overload occurrence. Results are presented in Tables 4, 5, and 6. The violation of an overloaded truck or vehicle is 62.74%, which violates the axle weight limit regulation rules (2022) on Gross Vehicle Weight (GVW). Moreover, it has been recognized that 24.39% of the heavy vehicle has exceeded the limitation regarding Gross Vehicle Mass, ensuring the attention required by abnormal vehicles for law enforcement agencies.

Table 4-8 Number of observed illegal vehicles

Number of axles	**Number of vehicles**	**% of overloaded vehicles**	
		% In terms of axles	**% In terms of GVWs**
3	402.00	73.6%	61.4%
4	1,299.00	49.7%	17.8%
5	1,390.00	59.9%	33.5%
6	33,895.00	63.7%	24.1%
7	847.00	44.4%	15.0%

4.7 Discussion

Traffic data from the Samara weighing station provides a good and illustrative hint at the nature of heavy vehicle operations across Ethiopia. There is a vast variation in gross vehicle weights and axle arrangements; truck types also reflect considerable variability. Notably, 3 and 6-axle trucks dominated, which might reflect a correlation between structural configuration and total weight for the vehicle.

In general, the data integrity from Samara was sound throughout this study. However, certain data records were regarded as having erroneous weight values. These noisy variations, which must have been due to malfunctioning equipment or data recording problems, were screened out with due care to ensure analytical accuracy. After data advancement, a statistical axle load and total vehicle weight analysis was conducted in detail. It became evident that although the overall vehicles tended to follow Weibull probabilistic distributions, the vehicles with six or seven axles followed patterns better approximated by Weibull probability distributions, since such vehicles can carry heavier and more variable loads.

CHAPTER 5 CASE STUDY

5.1 General

To analyze the impact of traffic overload on the existing bridge superstructure under real traffic. This chapter describes the case study bridge through a detailed investigation of a specific bridge that meets the key selection criteria outlined in Section 3.9.

This bridge has been subjected to increasing traffic over the years. This makes it a selective candidate for investigation. Its importance as an essential transport route further emphasizes its importance since any disruption of its service will have widespread effects on connectivity in the region. The bridge was chosen not only for its geographical location but its susceptibility to continuous overloading, which reflects a tendency seen on other bridges of its kind on the national level [27].

This study aims to analyze the structural response of the selected bridge under traffic loads beyond expected legal limits. The research employs the actual weight of trucks and influence line theory to assess the structure's response based on the provided parameters.

It then gives a general overview of the case study bridge, selected based on pre-set criteria, its structural profile, including geometric dimensions and material composition. While describing these elements, the study also entails an on-site inspection to verify assumptions made about its structural condition and detect any signs of distress or fatigue.

The key parameters for the selected case study bridge, such as structural type, abutment dimensions, span lengths, and the widths of the roadway and the entire bridge condition, were recorded and used as inputs for the assessment of the overload effect process.

5.2 Specific Case Study: Bridge Selection and Condition of Bridge Inspection

5.2.1 Specific Case Study Bridge Selection

According to the criteria set under Section 3.9, the routes considered were the Addis Ababa - Samara -Djibouti route. The Ethiopian Roads Administration Samara Weight Station is located about 3.7 km from the city of Samara. Due to its proximity to the said place, truckers coming from the port of Djibouti via Mile-1 head to some of the destinations along the way, such as Mekelle, Kombolcha, Addis Ababa, and others.

This routing allows for an effective assessment of the impact of overloaded trucks in relation to the infrastructure in the region between Mile 1 and Galafi. In this section, 170 bridges are identified using the Bridge Management System of the Ethiopian Roads Administration.

For conducting this study, bridges on the Mile-1 to Galafi course were identified. The information was obtained from the Bridge Management System of the Ethiopian Road Administration. It was necessary to conduct a case study of appropriate bridges. The basic information required for each bridge was noted, such as its name, type, construction year, and composition.

Such information has been indicated in Annex B. The information compiled above has been utilized in the creation of a set of data that ensures the bridge selected has relevant structural as well as historic features.

These bridges are varied in nature and size and consist of reinforced concrete slab bridges, masonry arch bridges, deck girders, box culverts, and some box girder bridges. Most of the bridges are shorter in span and are dominated by 78.24% bridges that are less than 10 meters in size.

According to the criteria for the choice of the bridges as described in section 3.9, criterion three eliminates 59 bridges. The bridges that are eliminated are those that were constructed before 1950 and have served beyond their expected lifespan, as described in [2], The reason for such elimination is that it is only appropriate to investigate the effect of traffic overloading on bridges that are still within their expected service life.

In section 4.5, the maximum length of the track is given as 16.33 meters. The criteria given in criteria 4 and 5 eliminated 106 bridges, including smaller structures with spans of less than 16.33 meters, slab, and box culverts, and the sixth criterion eliminated girder bridges with low levels of damage constructed in 2017: Gudiaytu-1, Eraso, Robe, and Seraytu bridges.

In this category, there are only two box girder bridges left. These are the Gelaba Bridge, which is registered A1-13030 and has an entire structural design of 111.9 meters and was completed in 2001 and has spans of 37.3, 37.3, and 37.7 meters. The second box girder bridge is marked as Mille No. 3 and is registered as A1-11-009. Its structural composition is 90 meters, taking up 29.5, 31, and 29.5 meters for the spans, and is established in 2004. It stands along the Mille-Samara Road Segment.

By taking into account the important criteria, Mille No. 3 Bridge was selected for this research in terms of having greater availability of structural records, span size, and easy site visitability compared to the Gelaba Bridge. The design of the Mille No. 3 Bridge embodies the typical characteristics of medium span, multicell concrete box-girder bridges. The bridge has simply supported spans and multiple lanes, making it highly susceptible to overloaded traffic. The location of this structure on one of the busiest routes increases the possibility of exposure to traffic overload effects.

The bridge has spans that are sensitive to the overloading condition. It is of high significance in linking the towns of Addis Ababa, Samara, and Djibouti. It is located in the Dichoto section of the Mille-Samara Road. Also located in the Combolcha district. The high flow of trucks makes it requires a structural evaluation.

Figure 5-1 Mile Bridge Elevation

5.2.2 Condition of Bridge Inspection and Testing

Assessing the superstructural strength of the bridge by the actual truck weight, it is crucial to have an up-to-date, comprehensive inspection of the bridge before anything is done.

In regard to the Mille Bridge, which is along the chosen route, this review was done with the help of the Ethiopian Roads Administration (ERA), according to their guidelines presented in the inspection manual. The bridge, named ERA Structure Mile No. 3, is a box girder type along the Mile-Samara Road section. It was constructed in 2004 by ERA at an investment of approximately 350 million Birr. In comparison with other bridgeworks in the region, it is fairly new. Connecting the only way from Ethiopia over the Mille River Gorge to Djibouti, this bridge work facilitates all trade traffic across the route.

It has three spans with lengths of 29.5m, 31m, and another 29.5m. It has two concrete piers and five columns with masonry abutments. The bridge is found at a distance of 515 kilometers from Addis Ababa and is at an altitude of 499 meters above sea level.. In its structure, it has Mat set in settled alluvial materials with an alignment following the curved road layout. To finish it off, it has an asphalt overlay layer of 50mm thickness for longer durability and smoother movement.

Table 5-1 General overview of the Mille Bridge based on the field investigation and data collected from the ERA BMS.

Bridge Location	Combolcha District, Dichoto section of the Mille-Samara Road Segment, 515.23 km from Addis Ababa.
Bridge Type	Reinforced Concrete Box Girder
Year of Construction	2004
AADT	2,265
Width (m)	23
River Width (m)	105
Topography	Flat
Superstructures Description	
No. of Span	3
Span Length Composition(m)	29.5+31+29.5
Carriage Way Width (m)	14
Sidewalk Width, both sides (m)	2
Slab Thickness (cm)	22
Girder Depth (m)	1.5
Distance from the center of bearing to end of the beam	350
No. of Lanes	4

Piers and Foundations	
Pier	Ten piers, each standing 9 meters tall and 1 meter wide, are topped with a pier cap.
Foundations	The foundation is an RC direct or mat foundation, measuring 25.6 meters in length and 4 meters in width.
Abutments and Foundations	
Abutment Type	Masonry
Height A1 (m)	9
Width	23
Wing Wall Length	8
Foundation	The foundation is an RC direct or mat foundation, measuring 25.6 meters in length and 8.2 meters in width.
Ancillaries	
Bearing Type	Rubber
Expansion Joint Type	Steel Sheet
Guard Railing Type	RC and Steel

The field inspection was conducted between March 27th to March 29th, 2025, to examine the superstructure capacity of the bridge with relevant parameters being girder size, abutment, span size, road breadth, and bridge width. Locations for bearings were carefully taken. The idea was to get a good picture of the condition of the bridge at present. Being a box girder structure, no major flexural or shear cracks were observed. That means the structural damage has been minimal and slightly degraded under long loading. There was some sign of wear and misalignment at the expansion joints, which caused some irregularities on the surface of the road.

This condition likely results from repeated loading over time. Based on general observation, the major structural elements such as piers, bearings, deck, and abutments were in good condition. However, there were scours around one pier and at the abutment on the Addis Ababa side. While such erosion should be kept under observation, it is not considered to affect the current capacity of the bridge.

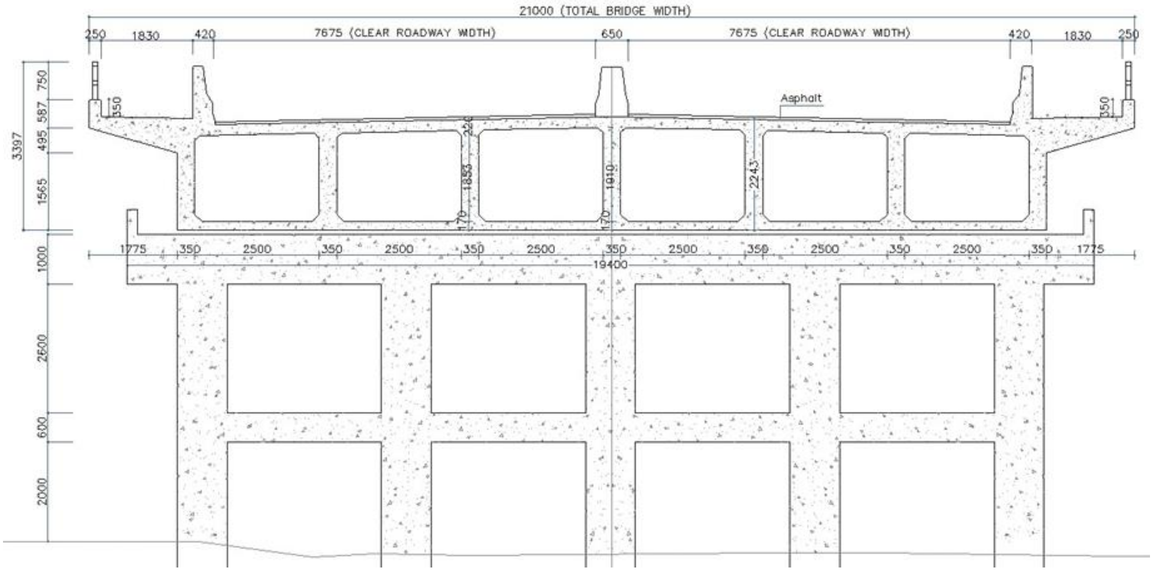

Figure 5-2 Typical Section of Mille Bridge

Figure 5-3 Existing Surface feature of Mille Bridge

The Schmidt hammer test was conducted to assess the concrete compressive strength of the bridge. This evaluation occurred across three spans, with testing taking place at five distinct locations for inspecting the interior girder. The Schmidt hammer used for this purpose is owned by Gie Engineering Private Limited Company and has been calibrated by the Ethiopian Metrology Institute (EMI) laboratory to ensure accuracy.

For each testing location, a total of fifty rebound tests were carried out, and the average of these rebound values was recorded at each test location. The recorder reflecting the rebounded value of the bridge concrete can be found in Table 5.2.

Figure 5-4 Sample of Conducting a Schmidt hammer sample on the Bottom Flange of the interior girder.

Table 5-2 Schmidt hammer rebounded value on the interior girder

Rebound value (R)										
Test-1			**Test-2**		**Test-3**		**Test-4**		**Test-5**	
No.	**Top Flange**	**Bottom Flange**	**Top Flange**	**Bottom Flange**	**Top Flange**	**Bottom Flange**	**Top Flange**	**Bottom Flange**	**Top Flange**	**Bottom Flange**
1	40	45	39	50	40	48	39	50	37	45
2	38	42	40	40	35	38	40	40	34	42
3	38	39	35	32	35	33	35	32	35	38
4	36	37	30	43	32	44	30	43	34	37
5	36	39	35	48	35	48	35	48	34	38
6	29	30	34	45	31	45	34	45	36	30
7	39	39	37	40	36	40	37	40	36	37
8	31	40	38	43	39	43	38	43	25	40
9	36	37	37	43	42	43	37	43	37	32
10	35	42	40	50	43	52	40	50	33	41
Average	35.8	39	36.5	43.4	36.8	43.4	36.5	43.4	34.1	38
Direction • ↑(Held Vertical)										

The mean compressive strength for the interior girder was approximately 40 MPa for this rebound hammer test. Although this appears to be comparatively high, this is certainly not a thorough measure of concrete strength. The rebound hammer can only determine concrete surface strength, which can vary highly from concrete strength depth. Moisture content, carbonation, concrete surface quality, and testing orientation can create errors to some degree. As such, this is entirely unreliable for concrete strength evaluation. The ACI 228.1R report strongly states that this and other non-destructive tests are actually better for comparison rather than detailed assessment. To better provide insight for this evaluation, new secondary test data for 2023 was collected from the Ethiopian Roads Administration to help fill this gap where actual sampling on the bridge structure is impossible to gather and provide more accurate data.

To assess the superstructural capacity, material strength properties were acquired for secondary materials from the material properties used during construction from the Ethiopian Roads Administration through its bridge management database. These data were necessary in performing accurate sectional analyses across different components of the bridge. In that regard, the entire bridge was assumed to be constructed using Class A concrete, grade 30. Cylindrical compressive strength of the concrete was found to be 24 MPa and was assumed to act uniformly on critical structural components of the bridge, including the top slab, girder web, and bottom slab. Besides acquiring information on concrete mix design, details on reinforcement bars used within the structure were also obtained from the same source. Accordingly, deformed reinforcing bars of diameter 200 mm and over were assigned a yield strength of 460 MPa, while for other diameters less than 200 mm, a lower yield strength of 300 MPa was considered.

Building on this, outlined by [3] the assessment of the superstructural performance of aging bridges, especially those that have been in service for a long time, should be made with due consideration to present physical conditions and deterioration developed over a certain period of time. This allows for a more practical and cautiously realistic assessment of the structure's load-carrying capacity under present-day usage.

The bridge was designed and constructed, when initially built, with a steel yield strength of 460 MPa, along with a concrete compressive strength of 24 MPa. In addition, the resistance factor to be used in design calculations was taken as 0.90 for both bending and shear, assuming ideal construction and material conditions. However, certain adjustments were made for probabilistic reassessment of the structural capacity of this bridge after 21 years of service (from its completion in 2004), reflecting issues of aging and uncertainty.

In the absence of direct testing, the yield strength of the steel and the resistance factor were conservatively revised to 400 MPa and 0.75, respectively, to account for any possible long-term effects such as corrosion and fatigue. This was done following [3] in order to account for the actual properties of the material during service in the evaluation of the safety of the structure. The compressive strength of the concrete was kept constant 24 MPa.

ERA's evaluation framework places emphasis on the fact that assumptions and parameters adopted at the time of initial design may not reflect the current condition of a structure accurately. Where direct inspection or testing cannot be carried out, conservative values should be used to ensure the reliability and safety of the structure for the future.

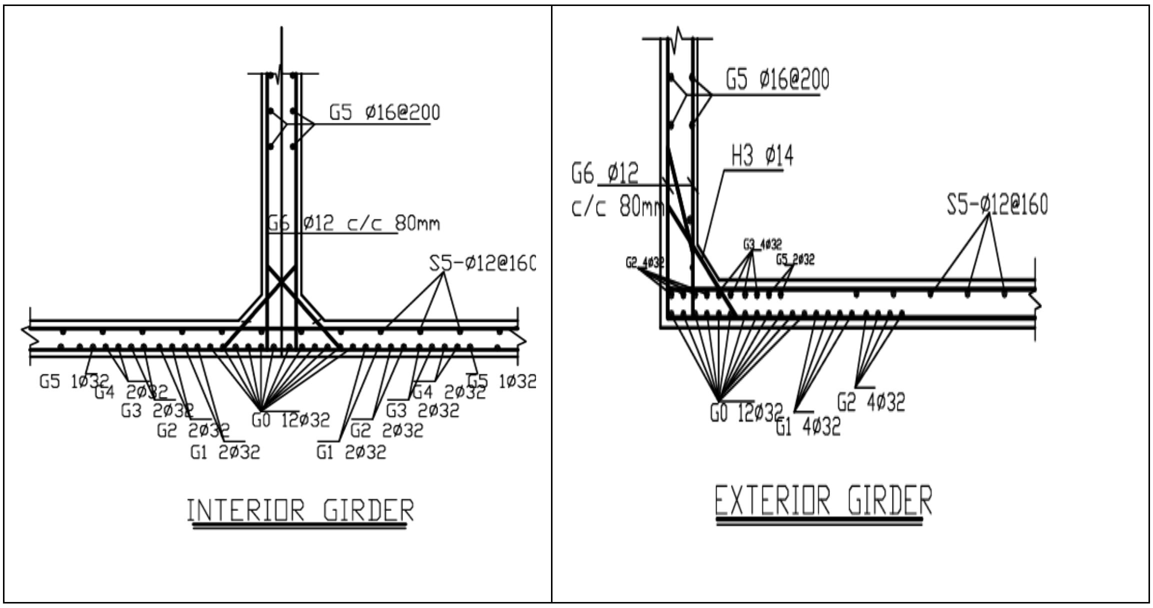

Figure 5-5 Interior and Exterior girder reinforcement detailing

5.3 Probabilistic Flexural and Shear Capacity Estimation

5.3.1 Current Probabilistic Flexural and Shear Capacity

Flexural stiffness of reinforced concrete sections of box girder bridges is considered to be of primary importance in assessing the performance of bridges concerning the ultimate limit states. Unlike the conventional models [2, 26, 35], which use specific values of characteristics, in reality, the behavior of the bridge is affected by uncertainties of material properties, long-term behavior, and simplifications used in the calculations.

As a result, deterministic analysis cannot be an ideal way to represent true safety margins of the structure. In contrast, probabilistic analysis is more realistic and can represent safety margins more precisely, taking into account that flexural strength can be a random variable affected by many parameters. In this way, it is possible to determine statistical measures of the strength of the beam [36].

Shear capacity of reinforced concrete box-girder bridge beams is another important factor in the determination of structural safety under the action of traffic overload and long-term decay. The traditional design procedures in a deterministic way determine the shear capacity by employing fixed values of material and geometric properties to define a nominal resistance, and they normally cannot capture the characteristic variability of concrete strength, steel yield stress, effective depth, and contribution of stirrups and aggregate interlock. In fact, these variables all have natural fluctuations due to material inconsistency, variations in workmanship, and other environmental conditions.

In general, according to the probabilistic view provided in [36], by considering the shear capacity as a random variable, its behavior can be described by statistical properties. With this approach, it becomes possible to predict that the actual shear resistance may be lower than the applied demand

The nominal bending moment represents the theoretical capacity of the beam to resist bending stresses before applying any safety or resistance factors. It can be modeled as [2]:

$$M_n = A_s f_y \left(d - \frac{a}{2}\right) = A_s f_y \left(d - \frac{1}{2} x \frac{(A_s f_y)}{0.85 f_c' b}\right) \qquad \text{Equation 5.1}$$

Where:

A_s is the reinforcement area, f_y is the steel yield strength stress, f'_c is the concrete compressive strength, d is the effective height of the beam, b is the width of the girder flange and, a Stress block depth.

$$M_R = \Phi * M_n \qquad \text{Equation 5.2}$$

The nominal shear resistance represents the theoretical capacity of the beam to resist shear stresses before applying any safety or resistance factors. The shear nominal resistance (V_n) of a beam can be modeled by summing the contributions from concrete (Vc) and shear reinforcement (V_s) [26]:

$$V_n = V_c + V_s \qquad \text{Equation 5.3}$$

The concrete contribution V_c is calculated using the following formula [26] :

$$V_c = \alpha \cdot f_{cd} \cdot b_w . d \qquad \text{Equation 5.4}$$

Where:

α is a coefficient depending on the type of concrete 0.035, f_{cd} is the design compressive strength of concrete, b_w is the width of the web, and d is the effective depth of the beam.

The shear reinforcement contribution, V_s, is given by [26]:

$$V_s = \frac{A_s \cdot f_{yd} \cdot d}{s} \qquad \text{Equation 5.5}$$

where:

A_s is the area of shear reinforcement, f_{yd} is the design yield strength of the reinforcement, d is the effective depth, and s is the spacing of the shear reinforcement.

$$V_R = \Phi * V_n \qquad \text{Equation 5.6}$$

Table 5-3 Statistical distribution of random variables

Random Variables	Mean Values	CoV (%)	Std.dev	Distribution	Reference
Compressive strength of concrete (f'_c) (MPa)	24	10.0	2.4	Longnormal	[19]
Yield strength of flexural reinforcement(f_y) (MPa)	400	5.0	20.0	Longnormal	[19]
Area of Longitudinal reinforcement A_{s1} (mm^2)	24,127.4	5.0	913.36	Normal	[19]
Resistance factor (Φ)	0.75	10.0	0.075	Normal	[19]
Bridge span composition (m)	29.5 +31.0 +29.5	0.05	1.48 +1.55 +1.48	Normal	[19]
Deck thickness(mm)	220	0.5	1.1	Normal	[19]
Web width(mm)	350	0.5	1.75	Normal	[19]

Random Variables	Mean Values	CoV (%)	Std.dev	Distribution	Reference
Web depth(mm)	2223.91	0.5	10.4	Normal	[19]
Girder spacing(mm)	2850	1.0	14.25	Normal	[19]
Bottom Flange slab thickness(mm)	170	0.5	0.85	Normal	[19]
Area of shear A_{sv} (mm^2)	226.2	5.0	11.31	Normal	[19]
Shear rebar spacing(mm)	80	5.0	4.0	Normal	[19]
Asphalt Wearing surface (t_A) (mm)	50	5.0	2.5	Normal	[19]
Live Load Model	1.0	18	0.18	Extreme Type-I	[37, 38]
Dead Load Model	1.0	5	0.05	Longnormal	[19]

Based on the above statistical data, analysis of probabilistic resistance of the identified bridge was carried out using R programming. In flexural resistance, a total of five variables were considered, resulting in 243 combinations. In shear resistance, a total of seven variables were considered, resulting in 2187 combinations. The output of this analysis is presented in Table 5.4.

Table 5-4 Statistical Properties of Bridge Resistance

Resistance	Mean Values	CoV (%)	Std.dev
Shear (V_R)	1,970.91	4.94	97.36
Moment (M_R)	11,732.78	5.71	670.06

5.3.2 Probabilistic Time-Variant Flexural and Shear Capacity

As the live loads applied to a bridge evolve through time and the structure itself gradually deteriorates, the bending moment and shear capacity of the bridge are evaluated over its entire service life. When assessing how these effects change with time, the analysis accounts for the time-dependent nature of both the applied loads and the structural resistance [19].

The time-variant nominal bending moment and shear force are the primary references used to determine the flexural and shear strength of a reinforced concrete beam section throughout its service life. They represent the beam's calculated capacity to resist bending and shear stresses before applying any safety or reduction factors. These are estimated using equations 5.3 and 5.5. For time-variant analysis, the following are considered [19]:

5.3.2.1 Corrosion type

For carbonation-related corrosion under semi-arid exposure conditions, an i_{corr} value of 0.10 μA/cm² is adopted [39, 19]. The onset of corrosion is taken to occur after 30 years of service [19]. After this point, the gradual loss in reinforcement diameter, based on uniform corrosion, is evaluated using Equation (5.9) [19].

$$\emptyset(t) = \emptyset_o - \alpha P_x(t), P_x(t) = 0.0116 I_{corr}(t - t_o), t > t_o \qquad \text{Equation 5.7}$$

In this expression, $\phi(t)$ represents the remaining bar diameter at time t, while ϕ_0 is the original diameter. The parameter α takes a value of 2 for carbonated concrete [19]. The term $P_x(t)$ denotes the average depth of corrosion penetration, or the reduction in bar radius, at time t. The parameter t_0 is the starting time of corrosion, t is the elapsed time from the beginning to now and I_{corr} means corrosion current density. The analysis should take into consideration reduction of bar area and loss in bond strength caused by decrease in concrete cracks and degradation of loading stiffness due to reinforcement corrosion. Together, those effects model the gradual reduction in the stiffness of the bridge due to corrosion. The variable t_0 is the time at which corrosion starts, and t is the time elapsed since that time, while Icorr stands for the corrosion current density. That reinforcement corrosion causes concrete cracking [19].

5.3.2.2 Creep Coefficient

To estimate the creep coefficient over time, the creep expression in Equation 5.10 is applied, and the corresponding reduction in the concrete's compressive strength is calculated based on that relationship [19, 40].

$$\varphi(t, t_o) = \frac{(t-t_o)^{0.6}}{(10+(t-t_o)^{0.6})} \varphi(t_0)\gamma_c \qquad \text{Equation 5.8}$$

In this context, $\varphi(t, t_0)$ represents the creep coefficient at time t resulting from a load applied at time t_0, while $\varphi(t_0)$ is the ultimate creep coefficient, equal to 2.35 [19]. The variable t denotes the age of the concrete in days, t_0 is the day the load is first applied, and γc is a correction factor for non-standard conditions, as reported in [41].

The effective compressive strength, accounting for probabilistic time-dependent variations, is determined using the formulation presented in equation 5.11 [42, 43, 44].

$$E'_{c,\mathrm{eff}}(t) = \frac{E'_c}{1+\varphi(t,t_0)} \qquad \text{Equation 5.9}$$

Where, $f'_{c,\mathrm{eff}}(t)$ is Time-variant effective concrete compressive strength, f'_c Nominal compressive strength of concrete, and $\varphi(t, t_0)$ is the Creep coefficient at time t.

In the time-dependent traffic overload impact assessment, factors such as corrosion rate, applied loads, and creep coefficients are considered. The statistical characteristics and probability distributions of these time-varying variables are presented in Table 5.5. Using these variations, different combinations were generated through an R program employing the Latin Hypercube Sampling (LHS) method. The reliability indices for shear and bending moments were then determined over the remaining service life of the bridge, evaluated at five-year intervals [19, 39]. The resulting values are summarized in Table 5.6.

Table 5-5 Statistical distribution of time-variant random variables

Random Variables	Mean Values	CoV (%)	Std.dev	Distribution	Reference
Corrosion Rate ($\mu A/cm^2$)	0.1	0.3	0.0003	Longnormal	[19, 39]
Attache Penetration, $P_x(t)$	Equ. 5.7	0.02	20.0	Longnormal	[19]
Time of Corrosion initiation (years)	30	0.2	913.36	Normal	[19, 39]
Creep Coefficient $\varphi(t_0)$	2.35	10.0	0.235	Normal	[19]

According to the Statistical distribution of time-variant random variables data above, R programming was used to analyze the time-varying probabilistic resistance of the predetermined bridge by equally dividing each variable into intervals. The results from this simulation are comprised in Table 5.6.

Table 5-6 Statistical Properties of Time-Variant Bridge Resistance

Remaining Bridge Service Life (year)	Resistance					
	Moment (M_R) (kNm)			Shear (V_R) (kNm)		
	Mean Values	Std.dev	CoV (%)	Mean Values	Std.dev	CoV (%)
5	11731.78	539.708	4.60	1970.51	97.34	4.94
10	11731.61	539.654	4.60	1969.68	97.30	4.94
15	11725.76	539.385	4.60	1967.322	97.19	4.94
20	11719.91	539.116	4.60	1965.032	97.07	4.94
25	11714.06	538.847	4.60	1962.789	96.96	4.94
30	11708.21	538.578	4.60	1960.583	96.85	4.94
35	11702.36	538.309	4.60	1958.404	96.75	4.94
40	11696.5	538.039	4.60	1956.248	96.64	4.94
45	11690.64	537.769	4.60	1954.11	96.53	4.94
50	11684.79	537.500	4.60	1951.986	96.43	4.94
55	11678.93	537.231	4.60	1949.875	96.32	4.94

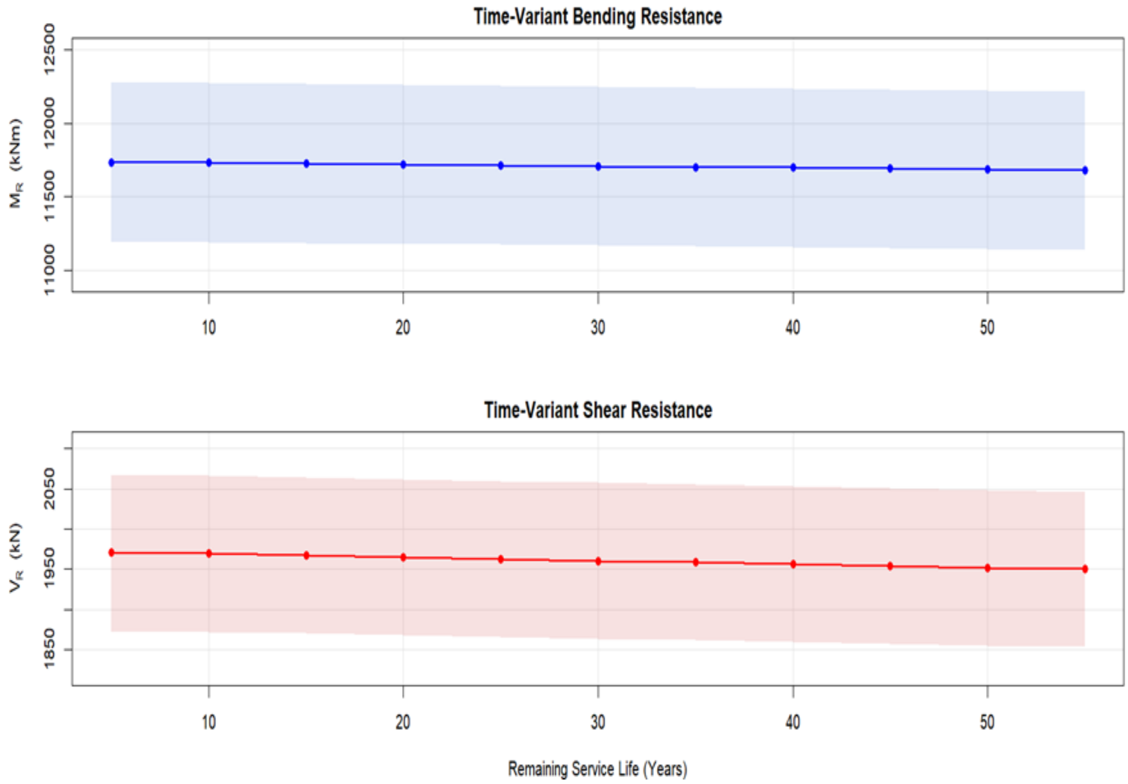

Figure 5-6 Time-Variant Resistance Profile of a Reinforced Concrete Bridge over its Remaining Service Life

CHAPTER 6 ANALYSIS AND DISCUSSION OF RESULTS

6.1 General

The previous chapter discussed how the data were collected, organized, and filtered, as well as the theoretical distributions of axle masses and the selection of bridges affected by traffic overload. This chapter explores the impact of traffic overload on selected existing bridge superstructures using the available data. This section offers a detailed overview of a program developed by the author to generate and simulate traffic combinations. The program was created in the R programming language, and the simulation results are summarized and presented.

6.2 Data organization for simulation traffic overload

The data collected from the static weighing station in Samara was organized into spreadsheets according to the number of axles on each vehicle. During the site survey, the recorded axle spacings were then randomly matched with their corresponding axle configurations, as outlined in Table 6-1 below. This process ensured a systematic approach to analyzing the traffic simulation.

Table 6-1 Sample Vehicle classifications along with their associated inter-axle spacings

Axle Number	A_1	S_1	A_2	S_2	A_3	S_3	A_4	S_4	A_5	S_5	A_6	S_6	A_7
Three	150.49	4.31	194.04	1.4	83.19	-	-	-	-	-	-	-	-
Four	134.40	3.58	85.54	5.88	82.40	2.11	305.29	-	-	-	-	-	-
Five	73.38	3.86	146.17	1.4	141.07	7.16	123.41	1.4	181.88	-	-	-	-
Six	60.23	3.3	108.30	1.4	113.6	5.65	79.26	1.4	81.238	1.4	932.93	-	-
Seven	65.92	3.31	133.81	1.4	92.80	4.8	49.64	1.4	93.39	1.4	83.19	1.4	213.07

- Axle Numbers – types vehicle per axle numbers.
- A_1-A_7 -Weight of Axles given in kN with their corresponding locations.
- S_1-S_6 – Inter axle spacings in meters.

6.3 Recorded Vehicle Configuration and Classification Sample

Configuration and loading of 3-Axle Truck Sample.

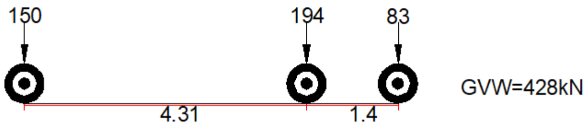

Configuration and loading of 4-Axle Truck Sample.

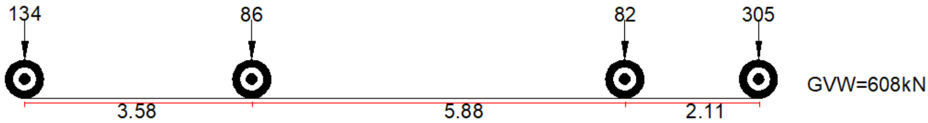

Configuration and loading of 5-Axle Truck Sample.

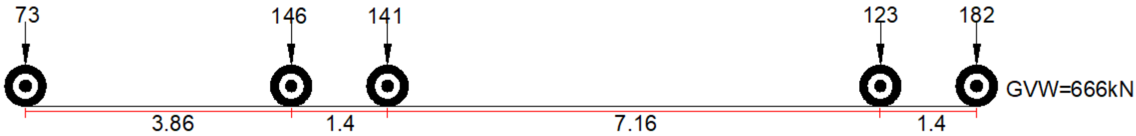

Configuration and loading of 6-Axle Truck Sample.

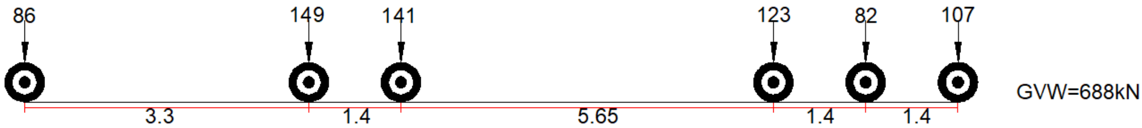

Configuration and loading of 7-Axle Truck Sample.

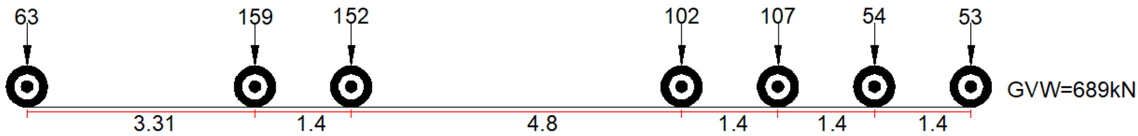

Figure 6-1 Sample Actual Truck Axle Configuration and Loading

6.4 Headway Distributions

Headway distributions are referred to as the time intervals that vehicles take to cross a bridge. The knowledge of headways is important in determining the capability of the bridge to carry loads, as headways influence the loads on the bridge.

Headway distributions are critical in bridge analysis for simulating dynamic loads due to traffic flow. The need for precise load representation cannot be overemphasized in identifying just how much load a bridge can support. Furthermore, the rate and spread of traffic loads, dependent on headways, are also useful in fatigue evaluations. A bridge is subjected to repeated loading by traffic flow; understanding headways can provide a better estimate of different lifespans within a bridge. [2].

Moreover, headway distributions offer insights into traffic flow characteristics, which are key for assessing how different traffic conditions impact a bridge's performance. Variations in these time intervals can lead to diverse load patterns, affecting how the bridge responds to dynamic forces [6].

Due to the absence of direct measurements of vehicle headway spacing, the assessment of traffic overload was based on critical loading scenarios generated by individual heavy vehicles. For bridges with short to medium spans, such single-truck events are widely recognized as the primary contributors to peak structural responses [13, 27, 45]. This methodology is adopted for this study, in agreement with established probabilistic and simulation-based assessments of traffic overload, which are calibrated to reflect the probability of simultaneous heavy vehicles governing extreme load effects.

6.5 Live Load Distribution Factor (LDF)

Live Load Distribution Factor (LLDF) is a critical parameter in designing or assessing bridges, as it approximates the distribution of traffic loads on the girders of a bridge without having to depend on finite element analysis [46, 47, 48]. The LLDF formulae, given in the AASHTO LRFD bridges design specifications, have been used extensively for designing as well as rating girder bridges. Investigations have confirmed the conservative nature of these LLDF distribution factors, both in designing as well as in the process of load rating [46, 47, 48] . For the current study, a live load distribution factor of 0.78 for moment and 0.92 for shear was assumed [49].

6.6 Influence lines

The curve or the graph showing the position of the load for maximum effect and the value of the various bending moments, shears, reactions, etc., at the section of a member or the joint of a structural frame due to a moving load departing from one position to another on the curve or graph, is called the influence line for that section. Influence lines have been widely used in the analysis phase to compute the load effects due to truck traffic on bridges with various spans. The bridge is 90 meter long consisting of three simply supported spans. The spans measure 29.5, 31 and 29.5 meters respectively. The bridge is simply supported, and seven load effects are considered [6]:

1. Bending moment at mid-span of each of the three spans of the simply supported bridge.
2. Shear force at two interior supports of a simply supported bridge.
3. Shear at the left-end support of a simply supported bridge.
4. Shear at the right-end support of a simply supported bridge.

The theoretical influence lines used in this thesis are shown below: bending moment at mid-span of each of the three simply supported bridges, shear at the left-end support of a simply supported bridge, shear force at the two interior supports of a simply supported bridge, and shear at the right-end support of a simply supported bridge.

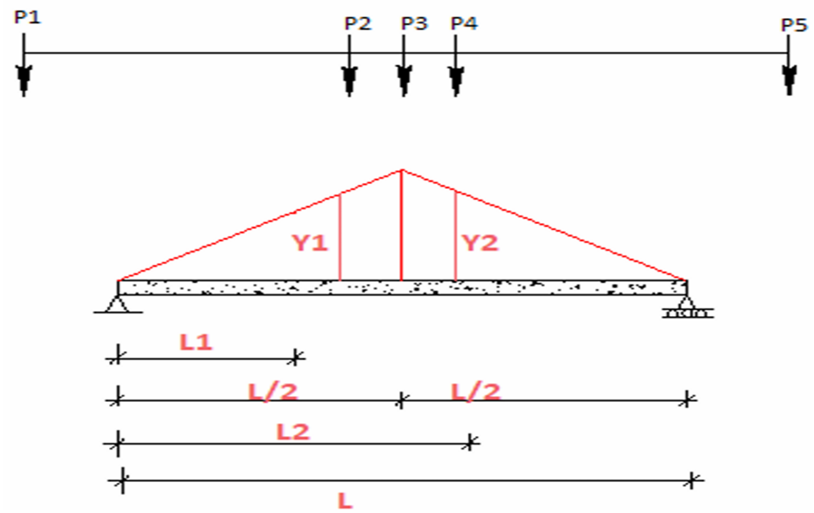

Figure 6-2 Mid Span Moment Influence Line

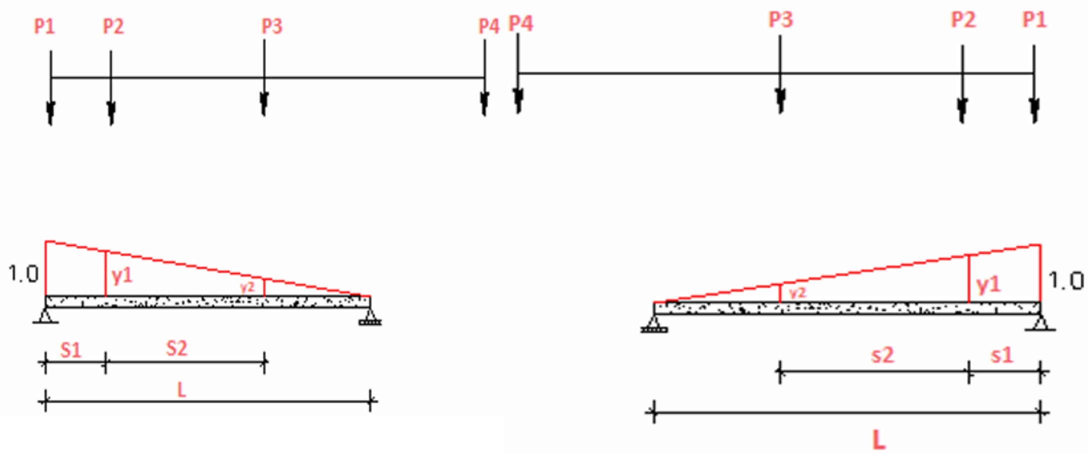

Figure 6-3 Shear Influence Line

6.7 Development of the Load Effects Calculation

The vehicle data collected over two years was organized based on the data gathered. Instances of overload were extracted and placed into a separate Excel worksheet. To examine the effects of vehicle overloading, a custom program was developed using R. Initially, the axle-related data was filtered through various techniques as specified in section 4.3.1, allowing for the transformation of the static axle loads into six distinct configurations that represent typical axle load scenarios concerning GVW.

Subsequently, a probabilistic load distribution for these configurations was prepared, using R to analyze the load distributions on the chosen concrete box-girder bridge. This analysis included assessing the influence of the probabilistic load distribution on the bridge's superstructure capacity.

In addition, the extracted traffic overload data, formatted in Excel, was imported into the R program, which then computed the traffic loads' effect across the bridge spans and determined the maximum load effects for each scenario using the influence lines method detailed in section 6.5.

This R program effectively calculates the effects of traffic overload based on data obtained from the Samara weighing station. A flowchart in Figure 6-2, illustrated below, was developed by [6] and is used for the development of the R program.

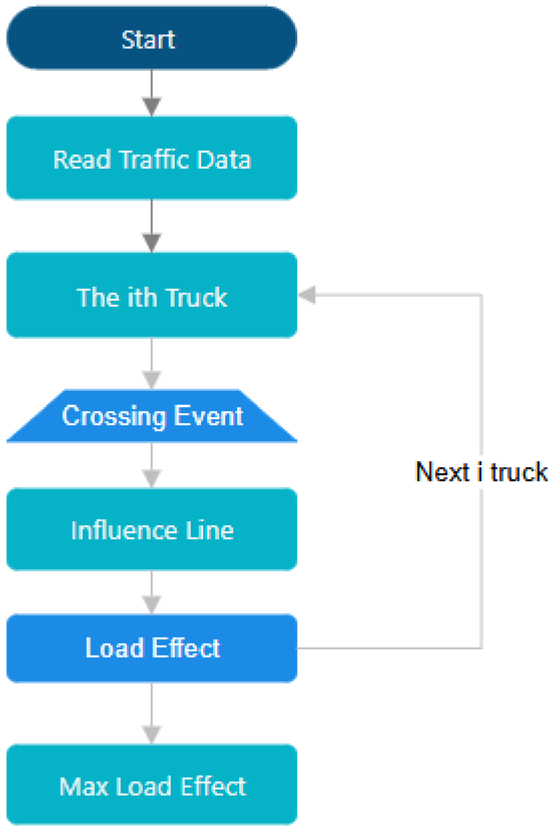

Table 6-2 Flowchart of the Developed Program for Each Overload Truck

When the 23,698 number of recorded overloaded vehicles is large over two years, this can create problems with memory, particularly since memory errors will occur when an output file stream is created; this limitation is addressed regarding RAM usage.

The R program was developed to analyze the overload effects of all 23,698 overload vehicles, which were calculated using the R program over two years to find the maximum value of each overload effect at midspan and both interior and exterior supports.

Over the course of two years, the program processed approximately 4.27 million traffic load combinations. For each scenario, the peak overload effect and the date it occurred were recorded for further evaluation. The associated load configurations were also preserved, resulting in a substantial dataset of critical events. The outcomes generated from this simulation are presented in the tables below.

Table 6-3 Statistical Properties of Actual Truck Bending Moments for each truck configuration

Vehicle Configurations	Bending Moment (kNm)			
	Statistical Properties	**@ mid span-1**	**@ mid span-2**	**@ mid span-3**
3-Axle	**Mean**	1772.28	1868.73	1772.28
	Standard Deviation	306.41	323.08	306.41
	Coefficient of Variation	0.17	0.17	0.17
4-Axle	**Mean**	2036.59	2147.43	2036.59
	Standard Deviation	264.76	279.17	264.76
	Coefficient of Variation	0.13	0.13	0.13
5-Axle	**Mean**	2778.10	2478.62	2778.10
	Standard Deviation	341.10	359.66	341.10
	Coefficient of Variation	0.12	0.12	0.12
6-Axle	**Mean**	3544.08	3736.95	3544.08
	Standard Deviation	354.41	373.70	354.41
	Coefficient of Variation	0.10	0.10	0.10
7-Axle	**Mean**	3761.46	3966.16	3761.46
	Standard Deviation	488.99	515.60	488.99
	Coefficient of Variation	0.13	0.13	0.13

Table 6-4 Statistical Properties of Actual Truck Shear Forces for each truck Configuration

Vehicle Configurations	Shear force (kN)				
	Statistical Properties	**Abutment-A**	**Peir-B**	**Pier-C**	**Abutment-D**
3-Axle	**Mean**	283.44	283.44	283.49	283.44
	Standard Deviation	49.00	49.00	49.01	49.00
	Coefficient of Variation	0.17	0.17	0.17	0.17
4-Axle	**Mean**	325.71	325.71	325.77	325.71
	Standard Deviation	42.34	42.34	42.35	42.34
	Coefficient of Variation	0.13	0.13	0.13	0.13
5-Axle	**Mean**	444.30	444.30	444.38	444.30
	Standard Deviation	54.55	54.55	54.56	54.55
	Coefficient of Variation	0.12	0.12	0.12	0.12
6-Axle	**Mean**	566.81	566.81	566.90	566.81
	Standard Deviation	20.94	20.94	20.94	20.94

Vehicle Configurations	Shear force (kN)				
	Statistical Properties	**Abutment-A**	**Peir-B**	**Pier-C**	**Abutment-D**
	Coefficient of Variation	0.04	0.04	0.04	0.04
7-Axle	**Mean**	601.57	601.57	601.67	601.57
	Standard Deviation	26.18	26.18	26.18	26.18
	Coefficient of Variation	0.04	0.04	0.04	0.04

Table 6-5 Statistical Properties of Actual Truck Bending Moments

	Bending Moment (kNm)			
All Vehicle Configurations	**Statistical Properties**	**Midspan-1**	**Midspan-2**	**Midspan-3**
	Mean	3514.50	3705.76	3514.50
	Standard Deviation	492.03	518.81	492.03
	Coefficient of Variation	0.14	0.14	0.14

Table 6-6 Statistical Properties of Actual Truck Shear Force

	Shear force (kN)				
All Vehicle Configuration	**Statistical Properties**	**Abutment-A**	**Pier-B**	**Pier-C**	**Abutment-D**
	Mean	562.08	562.08	562.17	562.08
	Standard Deviation	44.97	44.97	44.97	44.97
	Coefficient of Variation	0.08	0.08	0.08	0.08

From the statistics of the two years, 455 different days and 23,698 traffic overloads were simulated from January 2023 to December 2024. Different load response values were computed and also obtained when overloaded cars traveled through the simply supported 90 m three-span bridge, but they were not constant. Variation here can be attributed to the differing levels of overloading of the trucks and the mix of truck types.

6.8 Statistical Distributions of the overload effect at the critical location

The main aim of this investigation, based on the data collected from the weighing station, is to assess the impact of overloading on the current bridge superstructure that the bridge may be prone to throughout its lifespan. The evidence herein suggests that theoretical probability distributions can be used to represent the observed data. From the application of the aforementioned mathematical models, it is possible to determine the probability of occurrence of rare-loading instances, such as the representation of a distribution curve of critical location moments and shear force, and the cumulative distribution function (CDF) that corresponds to the aforementioned representation. The CDFs and corresponding distributions related to critical location moments and shear force values can be found in Annex A and B, respectively.

It has been determined that the overload effects on critical points obey various kinds of statistical distributions based on the nature and intensity of the load involved. Some of the statistical distributions include normal and Gumbel distributions. The most primary motivation in using the statistical distribution analysis is to determine the parent distribution of the overload effects from the statistical data. The differences in the statistical distributions lie in the nature of the loads involved.

6.9 Extrapolation using Chow and Silvakumar methods

As explained earlier, in Section 2.8, two known methods, those given by Chow and by Sivakumar, were used to make the extrapolation of the effects of overloading on the critical location. The results were given for a return period of 75 years, based on three possible ways to interpret the given data. In the first, based on Block Maxima, the data interpretation was carried out by month, thus making each month a separate data point, a separate observation period. The second involved the Castillo scheme, a fitting process to the top 2√n, a statistical process whereby only the highest data points are taken into consideration, according to a given function tied to the data sample size. The third involved the Enright fitting to the top 30%, a process whereby the largest amount of data is taken into consideration, specifically referring to the top 30% of the extreme value data. The results generated by the methods given by Chow and by Sivakumar, depending on the given data on the overload effects exploration, are presented in Tables 6-7 and 6-8, and in Figures 6-10 and 6-11.

Table 6-7 Bending Moment Exploration at critical location using Gumbel Distribution

Location	Bending Moment(kNm)					
	Block Maxima		Castillo's top $2\sqrt{n}$		Enright top 30%	
	Chow	Sivakumar	Chow	Sivakumar	Chow	Sivakumar
Midspan-1	4159.112	4184.615	3947.908	4038.511	3020.314	4116.294
Midspan-22	4385.458	4412.349	4162.760	4258.294	3184.685	4393.031
Midspan-3	4159.112	4184.615	3947.908	4038.511	3020.314	4116.294

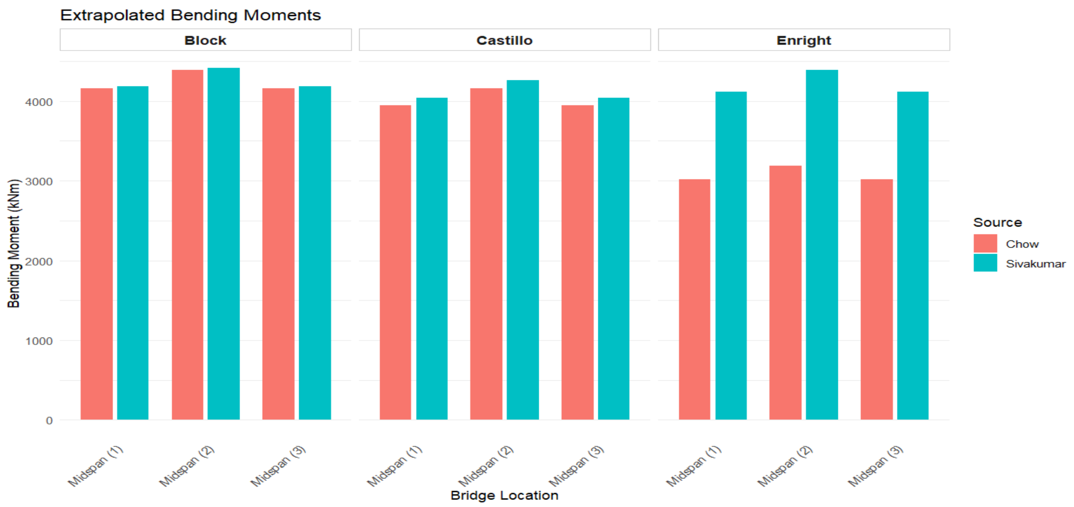

Figure 6-4 Gumbel Distribution Histogram Plot of the extrapolated moment at the critical location

Table 6-8 Shear Force Exploration at a critical location using the Gumbel Distribution

Location	**Shear force(kN)**					
	Block Maxima		**Castillo's top $2\sqrt{n}$**		**Enright top 30%**	
	Chow	**Sivakumar**	**Chow**	**Sivakumar**	**Chow**	**Sivakumar**
Abutment(A)	665.169	669.247	631.391	645.881	483.040	666.317
Pier-1 (B)	665.169	669.247	631.391	645.881	483.040	666.317
Pier-2 (C)	665.278	669.358	631.495	645.987	483.120	666.427
Abutment (D)	665.169	669.247	631.391	645.881	483.040	666.317

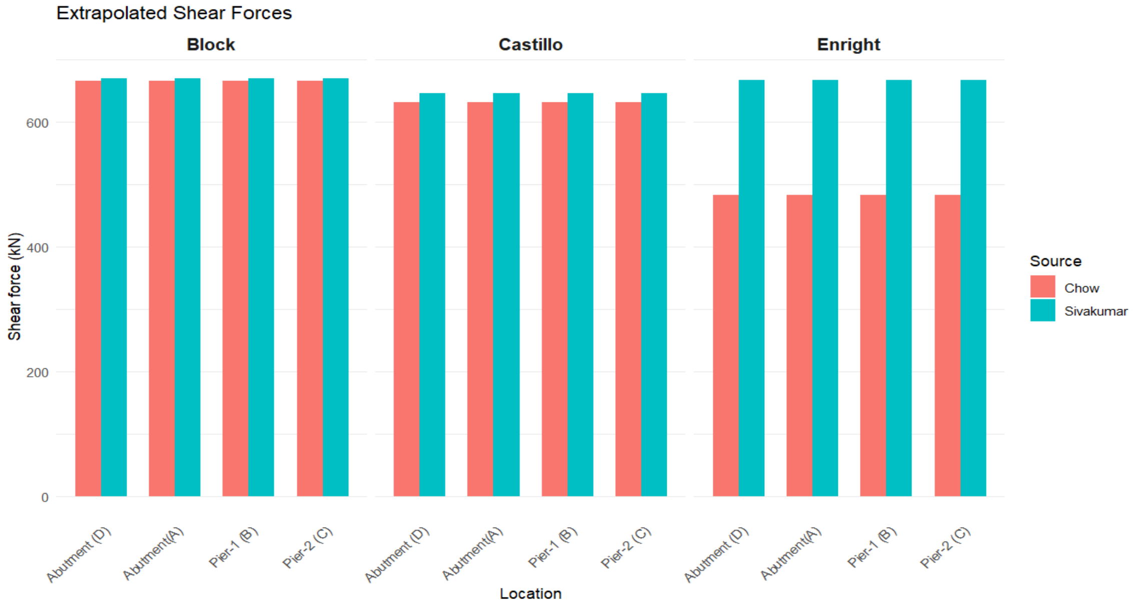

Figure 6-5 Gumbel Distribution Histogram Plot of the extrapolated shear forces at the critical location

On the basis of the earlier findings, a detailed analysis of the overload effects was performed to check the response of the results to the assumed return period of 75 years. By identifying the differences in the extreme event data and checking the effects on the results, the study determined the sensitivity of the results. The extrapolated values helped in comparing the estimation techniques and resulted in some differences in the values. It is pertinent to mention that the block maxima technique using the method developed by Sivakumar resulted in higher estimated values compared to the other models. It can be interpreted that the values of the bending moments and shear forces estimated in the study are dependent to some extent on the actual load in the critical areas. The differences in the results reiterate the significance of the chosen technique in determining the final results.

The method proposed by Chow is an extrapolation method based upon the Gumbel extreme value distribution and also uses the return period in the estimation of the probable maximum value for a given period of time and is applicable for both short and long return periods. Conversely, the Sivakumar method is an approximation of the extreme value based only upon the statistical characteristics of the data sets and is not dependent upon the return period and, therefore, is not specifically applicable for estimating extreme values that are dependent upon different periods of bridge service.

6.10 Structural Reliability Assessment

According to Section 2.12, reliability assessment is one of the methods in the evaluation of a structure's safety under uncertainty. First-order reliability method analysis was made on flexural and shear reliability, failure risk, service life prediction, and deterioration rate, considering the combined load effect of dead load and extrapolated truck overload.

A comprehensive statistical record for Ethiopian bridges is not available; the limit state functions in this study are developed using the random statistical parameters summarized in Tables 5.3 and 5.5. LHS is applied to generate various sets of random variables to assess the box girder bridge's reliability. This technique divides each cumulative distribution function into intervals having equal probabilities and takes a sample from each interval. The required variable combinations are produced using an LHS design function available in the R programming language [19].

Table 6-9 Bending Moments (kNm) at Key Structural Points

Mide Span Location	Service Periods										
	5	10	15	20	25	30	35	40	45	50	55
Midspan (1)	9677.35	9710.78	9724.98	9733.65	9739.75	9744.40	9748.13	9751.22	9753.85	9756.13	9758.14
Midspan (2)	9698.96	9734.21	9749.19	9758.32	9764.76	9769.66	9773.59	9776.85	9779.62	9782.03	9784.14
Midspan (3)	9961.44	9994.87	10009.07	10017.74	10023.84	10028.49	10032.22	10035.31	10037.94	10040.22	10042.23

Table 6-10 Shear Force (kN) at Key Structural Points

Location	Service Periods										
	5	10	15	20	25	30	35	40	45	50	55
Abutment(A)	1449.81	1455.15	1457.43	1458.81	1459.79	1460.53	1461.13	1461.62	1462.04	1462.41	1462.73
Pier-1 (B)	1490.41	1495.76	1498.03	1499.42	1500.39	1501.14	1501.73	1502.23	1502.65	1503.01	1503.33
Pier-1 (C)	1490.52	1495.87	1498.14	1499.52	1500.50	1501.24	1501.84	1502.34	1502.76	1503.12	1503.44
Abutment(D)	1449.81	1455.15	1457.43	1458.81	1459.79	1460.53	1461.13	1461.62	1462.04	1462.41	1462.73

Predicting the remaining service life of the bridge in reliability assessment involves identifying a failure threshold. A reliability index of 2.8 has been used to represent the point at which the structure no longer meets acceptable performance standards for serviceability concerns [19].. Assuming that $\beta = 3.8$ was a design reliability level at construction in 2004, the reliability has gradually degraded with time [50]. The structure has been subjected to 21 years of service-related deterioration. This methodology offers a rationale for an estimate of how many more years the bridge can serve safely before it attains the critical reliability threshold.

Moreover, the index in reliability for the bridge may be determined considering the entire effect on the bridge that is existing and through resistance using a probabilistic approach. This approach would consider the traffic load variability and randomness of variables without using one deterministic value.

A probabilistic approach was used to evaluate the reliability index of this critical location bridge. The calculations are summarized in Table 6.11 and 6.12, and the estimates of the remaining service reliability, consistent with this analysis, are shown in Figure 6.14. By taking the current load effect data as input and assuming projections for future performance due to traffic overloads, the evaluation was made for service periods from 5 to 55 years in increments of 5 years, which helped to understand the behavior of the bridge structure over the different time cycles. In Table 6.11, the result of the evaluations of the reliability indices associated with the respective analyses is given. This table shows how the performance of the structure evolves over cycles. In general, this approach provides a systematic way of analyzing long-term reliability at critical locations in the structural elements.

Table 6-11 Summary of Bending Moment Reliability Index

Location	Remaining Bridge Service Life (year)											
	0	5	10	15	20	25	30	35	40	45	50	55
Midspan-1	3.29	2.84	2.80	2.77	2.75	2.73	2.72	2.71	2.70	2.68	2.67	2.66
Midspan-2	3.10	2.72	2.67	2.65	2.63	2.61	2.60	2.59	2.57	2.56	2.55	2.54
Midspan-3	3.29	2.70	2.70	2.69	2.68	2.68	2.67	2.66	2.65	2.65	2.64	2.63

Table 6-12 Summary of Shear Reliability Index

Location	Remaining Bridge Service Life (year)											
	0	5	10	15	20	25	30	35	40	45	50	55
Abutment-A	5.01	4.28	4.23	4.19	4.16	4.14	4.12	4.10	4.08	4.06	4.04	4.03
Pier -B	4.65	3.92	3.87	3.84	3.81	3.78	3.76	3.74	3.72	3.71	3.69	3.67
Pier-C	4.65	3.92	3.87	3.83	3.81	3.78	3.76	3.74	3.72	3.70	3.69	3.67
Abutment-D	5.01	4.28	4.23	4.19	4.16	4.14	4.12	4.10	4.08	4.06	4.04	4.03

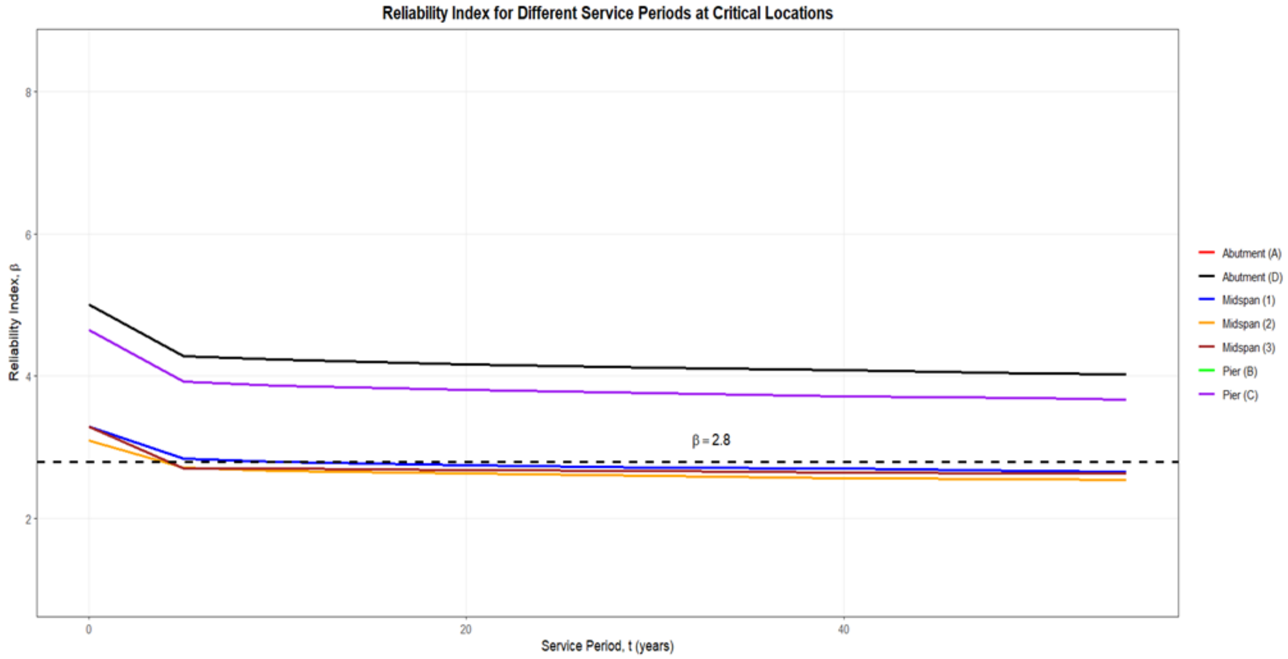

Figure 6-6 Reliability Index for Different Service Periods at Critical Locations

6.11 Discussion of the results

In the research, the impact of extreme traffic loads together with the time-dependent uncertainties of the key bridge parameters was evaluated. In the analysis of the bridge reliability, the study took into account the cumulative effect of heavy traffic, in addition to the material property changes over time. This method was realistic for the anaysis of the bridge performance under working conditions.

In the reliability analysis, the improved values of the resistance parameters were used in order to better capture the actual operating conditions of the bridge. In estimating the average values of the mean flexural resistance, the influences of the time-dependent factors, namely corrosion and creep, as well as the uncertainties associated with the fundamental material properties and other controlling variables, were considered. Due to material degradation over the structure's lifespan, the values of the resistances had been reduced from the original designs because of the reduction of the yield strength from 460 MPa to 400 MPa with the corresponding reduction of the resistance factor from 0.9 to 0.75 [3].

The current results obtained showed that the reliability index of 3.10 at midspan-2 was above the target value of 2.8. Over the life of the bridge of 21 years, the long-term deterioration measured 0.033 β-units per year. The value of the deterioration measured was responsible for the considerable decrease in the flexural strength capacity of the bridge span. Consequently, the value of the reliability index reduced to 2.72 after 5-years' service period. This indicates that the bridge has not been able to support traffic load safely.

The assessment result reveals that all flexural reliability indices for the next five years remain below the desired target values. This indicates that the bridge's ability to resist bending forces is declining steadily with time. This is evident from this decreasing trend in reliability values. The result is fraught with a potential threat to the bridge's serviceability under normal loads. The result highlights that maintenance measures geared towards arresting this deteriorating trend should be taken promptly. Compliance with traffic loads is also paramount to avert faster deterioration.

CHAPTER 7 RECOMMENDATION AND CONCLUSION

7.1 Conclusion

In the course of this research work, a substantial effort was made to assess the structural implications of truck overloading on an existing bridge superstructure. The load effect assessment was based on natural data that was largely sourced from the Samara weighing station, due to its strategic positioning along a major corridor that records volumes of heavy truck traffic at consistently high levels. The selection of this site ensured the data represented natural operational conditions, hence reducing uncertainties commonly associated with the estimation of traffic overload.

This paper is focused on the overloaded truck impact on superstructural capacity according to a typical in-service bridge. The main goal of this study was to reflect realistic conditions by assessing the response of the bridge to the real traffic patterns and to derive conclusive information about how these loads compromise structural resistance over time. This ensuing analysis has highlighted a crucial link between the real-world traffic data and the performance of the infrastructure of bridge when under stress.

A statistical analysis of the measured overloads was also made, by fitting various probability distributions, describing variability and extremity of loading events corresponding to 75-year return periods. It was seen that, depending on the effect being considered, different distributions such as Normal and Gumbel capture the statistical patterns to a varying degree of exactitude. Projections for a 75-year return period were obtained through appropriate extrapolation methods using these distributions to understand the implications of rare load cases but with severe effects.

Among these, the Gumbel distribution turned out to be rather efficient in analyzing the upper extreme of load effects due to overloaded trucks. Its appropriateness in modeling the tail behavior of load data made it a very useful tool for the prediction of rare but critical structural demands. Further analysis was supported by Block Maxima and POT methods with the purpose of isolation of extreme values. Assumptions suggested by Castillo and Enright were tried, which showed that the way extremes are defined is crucial in modeling structural risk.

A specific bridge was selected based on selection criteria and inspection data from the bridge management system in order to perform a focused evaluation. This selection allowed a case study with the integration of statistical modeling and field-based information. The load-bearing elements of the bridge were then analyzed probabilistically with their section resistance to provide a complete picture of structural performance under critical conditions.

The analysis dealt with the interaction between extreme traffic overloads and time-dependent uncertainties in the bridge's critical parameters. The reliability assessment considered the combined effects of the cumulative heavy vehicle loads and the progressive material property changes with time. It was seen from the analysis that the reliability index at midspan-2 had degraded to as low as 2.72, below the target value of 2.8, after five years' service period. The estimated long-term deterioration within the service life of 21 years for the bridge was approximately 0.033 β-units per year. This resulted in a sharp fall in the flexural capacity at the span, degrading the reliability index to 2.8. Such distressing performance indicates increased structural fragility and implies that the bridge will not be able to carry out the proper function of safely carrying traffic without maintenance at regular intervals.

7.2 Recommendation

In this study, the need to use probabilistic methods instead of conventional ones in the evaluation of existing bridges is emphasized. The conventional values used in design may not be sufficient, especially after many years of use. This is especially true in relation to bridge structure assessment.

The study was based on a reliability calculation, where the resistance values of the bridge are updated for in-service conditions. The following activities are recommended:

- Reevaluate Load Presumptions & Control
    - There exists a misalignment between the truck load used in reality and the model assumed by the existing methods of AASHTO and ERA for evaluation.
    - There arises the need to reassess axle load standards in response to modified traffic parameters caused by the growth of the economy and the increased weights of transported loads.
    - Installation of Weigh-in-Motion systems should be carried out to increase the accuracy of traffic data.

- Customers can use
  - Although WIM technology provides automation, a weigh station is always required for health and structural analysis.
  - The extension of these stations along important routes with high traffic volume can increase the accuracy of bridge loads and contribute to the management of overloaded vehicles.
- Conduct Similar Reliability Assessment
  - Though this particular study has emphasized a 90-meter bridge with three spans, its implications stress that other bridges must also be assessed for their structure.
  - The national-level reliability study will help in understanding how well the aging infrastructure copes with rising traffic volumes.
- Implement an active Maintenance Program
  - Perform routine inspections on the infrastructure and pay attention to defects such as cracks, corrosion, and section losses.
  - Update resistance value data periodically on the basis of field data and perform load testing.
- Apply Probabilistic Load Rating Methods
  - To provide a more accurate representation of variability in loading and Time variant material degradation.
  - First Order Reliability Method
- Plan for Short-Term Reassessments
  - based on the trends of deterioration, reassessment should be planned after 12 to 18 months.
  - Certain components of bridges may fall below acceptable levels of reliability if proper action is not taken sooner rather than later, with some components potentially failing the
- Develop a Long-Term Rehabilitation
  - Perform a Life Cycle Cost Analysis to compare the advantages of staged repairs to replacing the facility completely.

REFERENCES

[1] I. M. Metwally, "Bridge Failures: Causes, Analysis & Lessons Learned - S02-032," p. 19, 2023.

[2] AASHTO, "AASHTO LRFD Bridge Design Specifications,8th edition," American Association of State Highway and Transportation Officials (AASHTO), Washington, DC, 2017.

[3] ERA, "Ethiopian Roads Authority Bridge Design Manual Part II," *ERA,* 2013.

[4] E. O'Brien, F. Schmidt and D. Hajializadeh, "A review of probabilistic methods of assessment of load effects in bridges," pp. 45-50, 2015.

[5] Buckland and Peter G., "North American and British Long- Span Bridge Loads," *Journal of Structural Engineering,* 1991.

[6] B. Wesenseged, "Development of Live Load Model for Ethiopian Short to Medium Span Bridges," *Addis Ababa University, Addis Ababa Institute of Technology,* 2020.

[7] X. Y. Zhou, "Statistical analysis of traffic loads and their effects on Bridges," 2013.

[8] J. Zhou, R. Smith and H. Liu, "Load Rating of Bridges: Methods and Considerations," *Journal of Structural Engineering,* 2020.

[9] A. S. &. C. K. R. Nowak, Probability, Statistics, and Reliability for Engineers and Scientists, Boston: McGraw-Hill, 2000.

[10] D. C. M. &. G. C. Runger, Applied Statistics and Probability for Engineers, Third Edition, Hoboken, New Jersey: John Wiley & Sons, Inc., 2003.

[11] E. W. Ronald , H. M. Raymond and L. M. Sharon, Probability & Statistics for Engineers & Scientists,Ninth Edition, Boston: Pearson Education, 2011.

[12] S. Coles, An Introduction to Statistical Modeling of Extreme Values, London:

Springer, 2001.

[13] A. Getachew, "Traffic Load Effects on Bridges: Statistical Analysis of Collected and Monte Carlo Simulated Vehicle Data," *Royal Institute of Technology,Structural Engineering (Doctoral thesis)*, 2003.

[14] . J. O. Eugene, S. Franziska, Z. Xiaoyi and H. Donya , "A Review of Probabilistic Methods of Assessment of Load Effects in Bridges," *Engineering Structures,* pp. 45-50, March 2015.

[15] Fabio Biondini and Dan M, Bridge Maintenance, Safety, Management, Resilience and Sustainability, London: CRC Press, 2018.

[16] AASHTO, "Bridge Element Inspection, 8th Edition.," 2017.

[17] Lauridsen; Jensen; Enevoldsen, "Bridge owner's benefits from probabilistic approaches," *Structure and Infrastructure Engineering,* pp. 281-302, 2007.

[18] C. Hellier, Handbook of Non-destructive Evaluation, New York: McGraw-Hill, 2001.

[19] A. G. Tarekegn, "Time-dependent reliability analysis for deflection of a reinforced concrete box girder bridge," *International Journal of Engineering and Applied Sciences.,* pp. 60-75, 2023.

[20] D. Frangopol, B. Kozy, B. Zhu and S. Sabatino, "Bridge System Reliability based Redundancy Factors," *FHWA-HIF-19-093, US Department of Transportation, Federal Highway Administration*, 2019.

[21] E. G. Y. G. Abrham Gebre, "Probabilistic Assessment and Field Test Verification for Strength Evaluation of Bridge with Defective Girder," *ZEDE Journal ,* vol. 41, pp. 16-28, August 2023.

[22] A. A. Sebhatu, "An analysis of the import trade logistics service through the Ethio–Djibouti corridor," *Master's thesis, World Maritime University.,* 2005.

[23] E. J. &. E. B. O'Brien, "Modeling same-direction two-lane traffic for bridge loading," *Structural Safety,* pp. 296-304, 2011.

[24] L. Gao, Y.-L. Mo, S. Dhonde, D. Saldarriaga, L. Song and A. Senouci, "Synthesis of Service Life Prediction for Bridges in Texas," University of Houston in cooperation with Texas Department of Transportation & Federal Highway Administration, Houston, Texas, March 2019.

[25] P. M. B. J. E. B. Michael E. Kreger, "An Exploratory Study of Shear Fatigue Behavior of Prestressed Concrete Girders," *Precast/Prestressed Concrete Institute,* vol. 34, no. 4, pp. 104-125, August 2007.

[26] ERA, "Ethiopian Roads Authority Bridge Design Manual Part I," *Ethiopian Roads Authority,* 2013.

[27] A. &. O. E. J. Getachew, "Simplified site-specific traffic load models for bridge assessment," *Structure and Infrastructure Engineering,* vol. 3, pp. 303-311, September 2007.

[28] D. S. M. K. M. M. S. Ana Mandić Ivanković, "Performance-Based Ranking of Existing Road Bridges," *Applied Sciences*, 2021.

[29] E. Bernard and J. O. Eugene, "Cleaning Weigh-in-Motion Data: Techniques and Recommendations.," *Transportation Research Record,* p. 42, 2011.

[30] M. G. Balasingam Sivakumar, "Recalibration of LRFR Live Load Factors in the AASHTO Manual for Bridge Evaluation," *National Cooperative Highway Research Program (NCHRP), Transportation Research Board (TRB), Washington, D.C.,* p. 190, 2011.

[31] A. G. Tarekegn, B. Wesenseged, Y. G. Tarekegn and G. S. Tulu, "Live Load Models for Ethiopian Highway Bridges using Truck Weigh in Motion (WIM) Data," *Transportation Research Record,* August 2025.

[32] A. Mehari, "Influence of Overloaded Freight Transportation on Pavement Life,"

Addis Ababa University, Addis Ababa Institution of Technology, p. 104, 2015.

[33] S. Behailu, "Evaluation of Vehicle Overload Control System on Major Road Corridors in Ethiopia," *Addis Ababa University, Addis Ababa Institute of Technology,* p. 79, 2016.

[34] B. T. Beyene, "Implications of axle load limitation in Ethiopia (The case study on axle load management at Holeta and Modjo weighbridge stations)," *Addis Ababa University, Addis Ababa Institution of Technology,* p. 65, January 2015.

[35] European Standard, "Eurocode 2: Design of Concrete Structures," 1992.

[36] A. T. B. Robert E. Melchers, Structural Reliability Analysis and Prediction (3rd edition), Hoboken, New Jersey (NJ), USA.: John Wiley & Sons Ltd., 2018.

[37] T. H. C. A. N. a. D. Shojaeddin Jamali, "Reliability-Based Load Carrying Capacity Assessment of Bridges Using Structural Health Monitoring Analysis," *Structural Health Monitoring,* vol. 18(1), pp. 20-34, 2019.

[38] A. S. Nowak, "Calibration of LRFD Bridge Design Code," National Cooperative Highway Research Program (NCHRP) Report 368, Transportation Research Board, National Research Council, Washington, D.C., 199.

[39] R. Y. H. M. F. H. C. Fatima Hajj Chehade, "Time-Dependent Reliability Analysis of Reinforced-Concrete Bridges Under The Combined Effect of Corrosion, Creep and Shrinkage.," *Safety and Security Engineering* , June 2017.

[40] A. R. Marí, J. M. Bairán, A. Cladera, E. Oller and C. Ribas, "Shear-flexural strength mechanical model for the design and assessment of reinforced concrete beams," *Structure and Infrastructure Engineering,* vol. 11(11), p. 1399–1419, 2015.

[41] A. C. I. C. 209, "Prediction of Creep, Shrinkage, and Temperature Effects in Concrete Structures (ACI 209R-92)," American Concrete Institute (ACI), Farmington Hills, MI: American Concrete Institute, 1997.

[42] E. F. Y. Hamed, "Simplified Creep Analysis for Bridge Assessment," *Journal of Bridge Engineering,* 2010.

[43] Y. Z. W. Zhu, "Time-Dependent Reliability of Concrete Bridges Under Overweight Trucks," *Structural Safety,* 2018.

[44] A. F. R. Ghali, "Simplified Method for Creep Analysis of Concrete Structures," *ACI Structural Journal,* 1982.

[45] C. Y. H. N. Peng Lou, "Live Load Multiple Presence Factors for Design and Evaluation of Short-to-Medium Span Highway Bridges," *Transportation Research Record: Journal of the Transportation Research Board,* p. 204–219, 2023.

[46] . &. H. Yousif, "AASHTO-LRFD Live Load Distribution for Beam-and-Slab Bridges: Limitations and Applicability.," *Journal of Bridge Engineering,* pp. 765-773, 2007.

[47] W. M. I. P. J. &. K. J. Choi, "Development of Live Load Distribution Factor Equation for Concrete Multicell Box-Girder Bridges under Vehicle Loading," *International Journal of Concrete Structures and Materials,* 2019.

[48] A. &. G. A. Rafizadeh, "Evaluation of Load Distribution Factors on AASHTO LRFD Design Parameters of the Bridge Deck by Harmonic Analysis.," *KSCE Journal of Civil Engineering,* p. 2550–2560, 2019.

[49] AASHTO, AASHTO LRFD Bridge Design Specifications,8th edition, Washington, DC: American Association of State Highway and Transportation Officials (AASHTO), 2017.

[50] E. C. f. S. (CEN), "Eurocode – Basis of Structural Design (EN 1990)," *European Standard, CEN,* p. Annex B for reliability indices, 2007.

[51] ASCE-ACI Committee 445, "Recent Approaches to Shear Design of Structural Concrete," *American Society of Civil Engineers,* December 1998.

[52] ASTM, The American Society for Testing and Materials, Conshohocken, Pennsylvania.: American Society for Testing and Materials (ASTM), 2004.

[53] G. Janusz , S. Ryszard and B. Piotr, "Designing the Calibration Process of Weigh-In-Motion Systems," *Transportation Research Record,* 2021.

[54] T. K. Nathabandu and R. Renzo, Applied Statistics for Civil and Environmental Engineers, Second Edition, Oxford: Blackwell Publishing Ltd, 2008.

[55] B. d. Finetti, Theory of Probability, Chichester,United Kingdom: John Wiley & Sons Ltd, 2017.

[56] Zhang, L., Wang, Y. and Zhao, X, "Finite Element Modeling: A Key Tool in Structural Engineering," *Journal of Civil Engineering.,* 2020.

[57] Li, H., & Wang, S., "Advanced Applications of Finite Element Modeling in Bridge Analysis," *International Journal of Engineering Research.,* 2019.

[58] R. Smith and T. Johnson, "Evaluating Bridge Load Capacity through Finite Element Analysis.," *Journal of Bridge Engineering.,* 2022.

[59] Y. Chen, X. Zhang and J. Liu, "Integration of FEM and Probabilistic Methods in Structural Engineering.," *Journal of Structural Engineering.,* 2021.

[60] G. W. &. C. W. G. Snedecor, Statistical Methods, Ames, Iowa: Iowa State University Press, 1989, p. 524.

[61] A. S. A. M. A. U. I. Abdulmumin Shuaibu, "Probabilistic Assessment of a Typical Reinforced Concrete Girder Under Critical Loading," *Arid Zone Journal of Engineering, Technology & Environment,* pp. 341-354, June 2023.

[62] M. Bimrew, "Performance Evaluation of Reinforced concrete Bridges: A case study on the assessment of Koka Bridge," *Addis Ababa University, Addis Ababa Institute of Technology,* p. 83, June 2019.

[63] E. J. M. B. &. E. B. O’Brien, "Probabilistic assessment of bridge load effects from

weigh-in-motion data," *Journal of Bridge Engineering,* pp. 803-812, 2011.

[64] F. H. Administration, "TRaffic Monitoring Guide," Federal Highway Administration, Washington, D.C., 2022.

[65] D. J. H. a. A. G. Davenport, "A Statistical Approach to Traffic Loading on Highway Bridges," Canadian Journal of Civil Engineering (NRC Research Press), Ottawa, Canada, 1979.

[66] E. J. O. Barry Enright, "Monte Carlo simulation of extreme traffic loading on short and medium span bridges," *Structural Safety,* pp. 23-33, 2013.

[67] X. R. J. R. C. M. Z. Xuejing Wang, "Probabilistic model of traffic scenarios for extreme load effects in long-span bridges," *Structural Safety,* vol. Volume 106, 2024.

ANNEX

Annex A Statistical Distribution of Truck Overload Effect

Statistical Distributions of Midspan-1 Moment

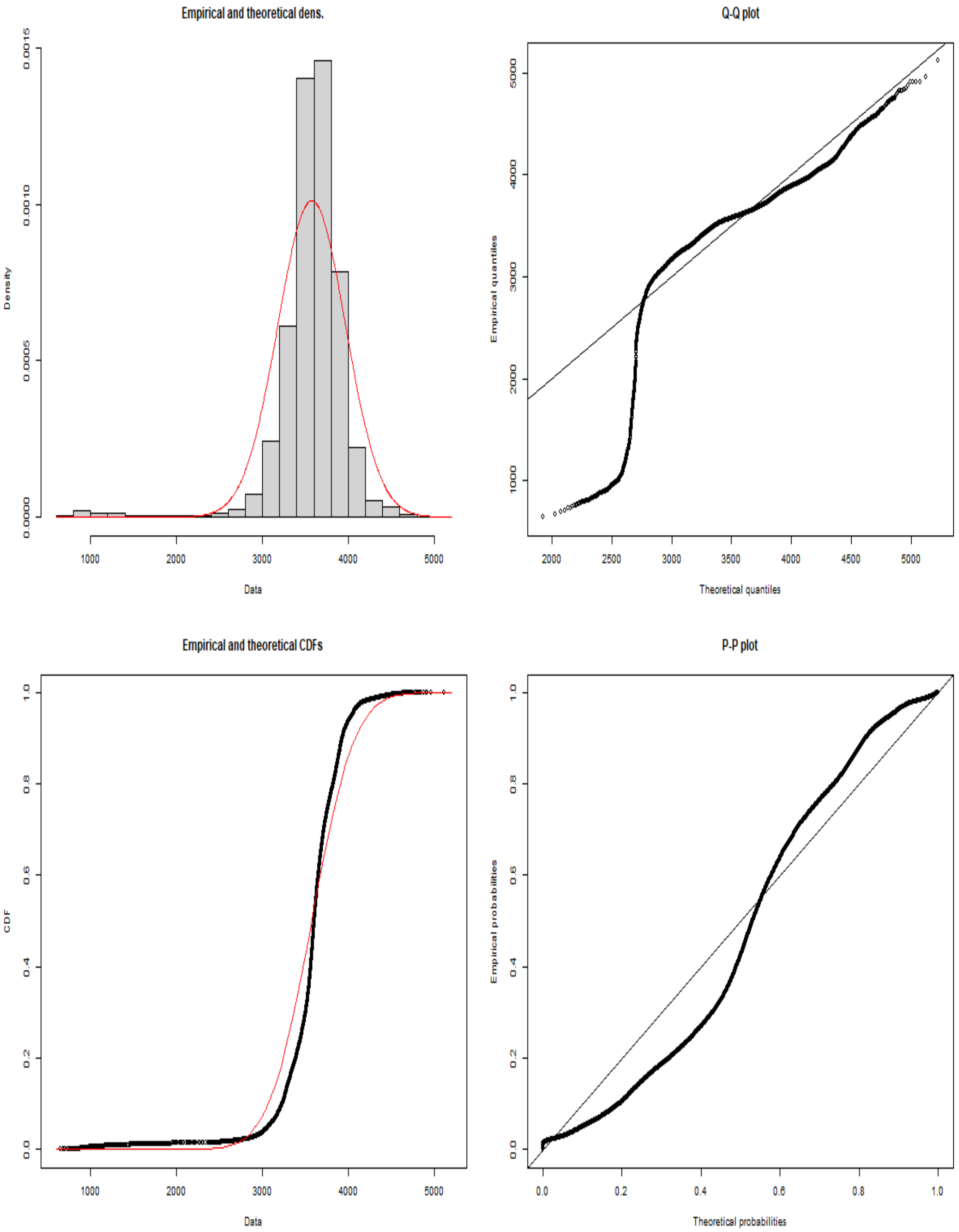

Statistical Distributions of Midspan-2 Moment

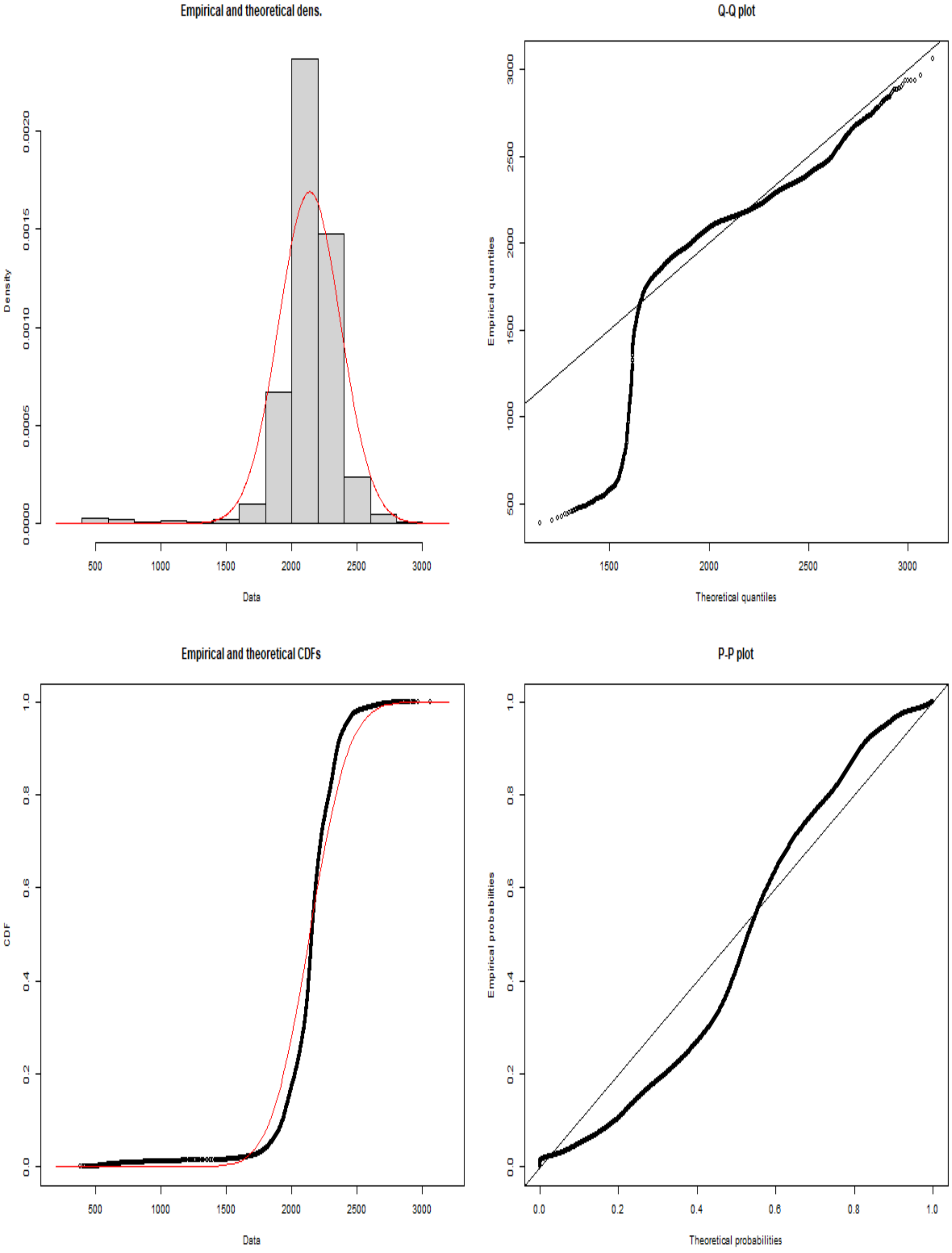

Statistical Distributions of Midspan-3 Moment

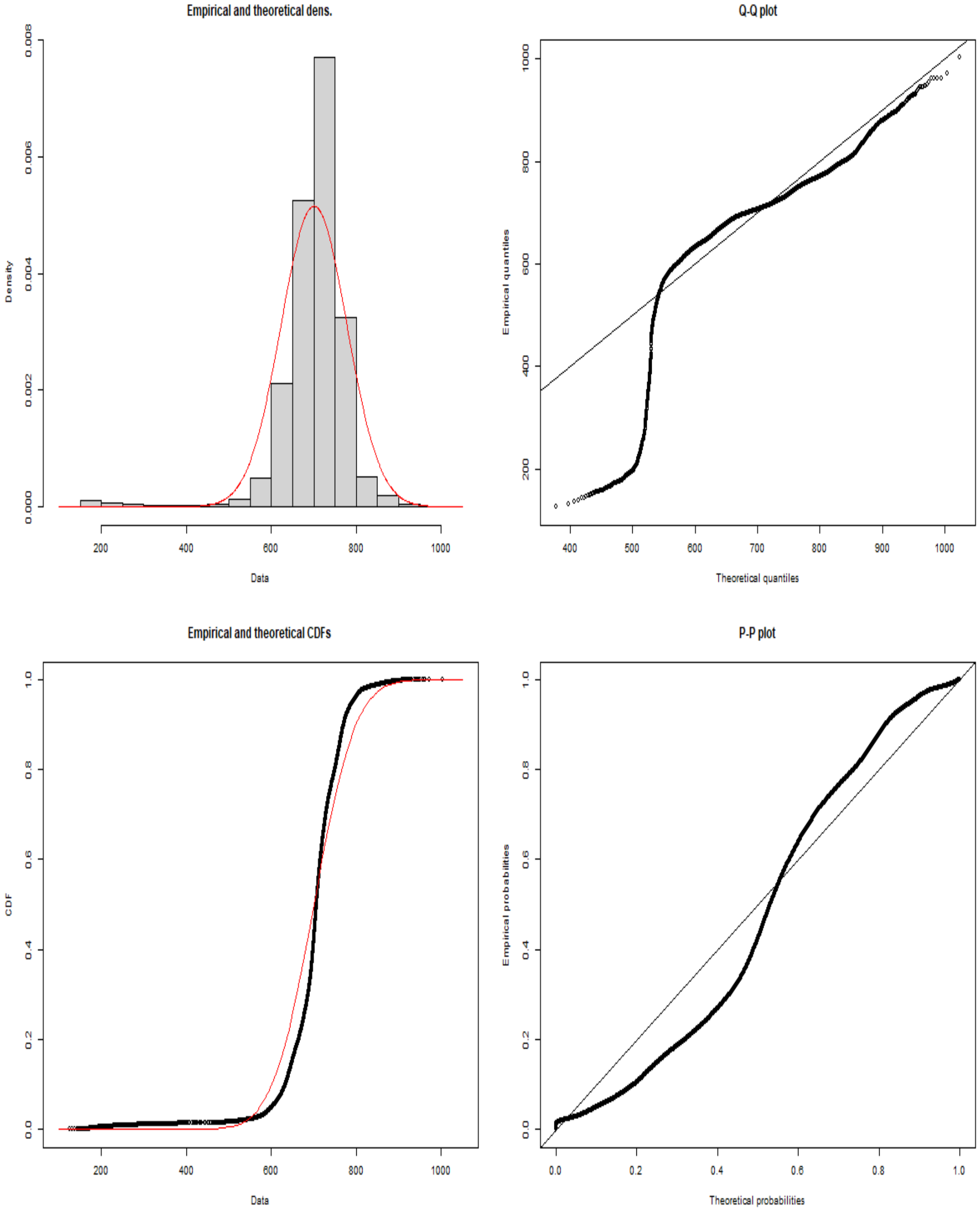

Statistical Distributions of Shear Forces for Abutment

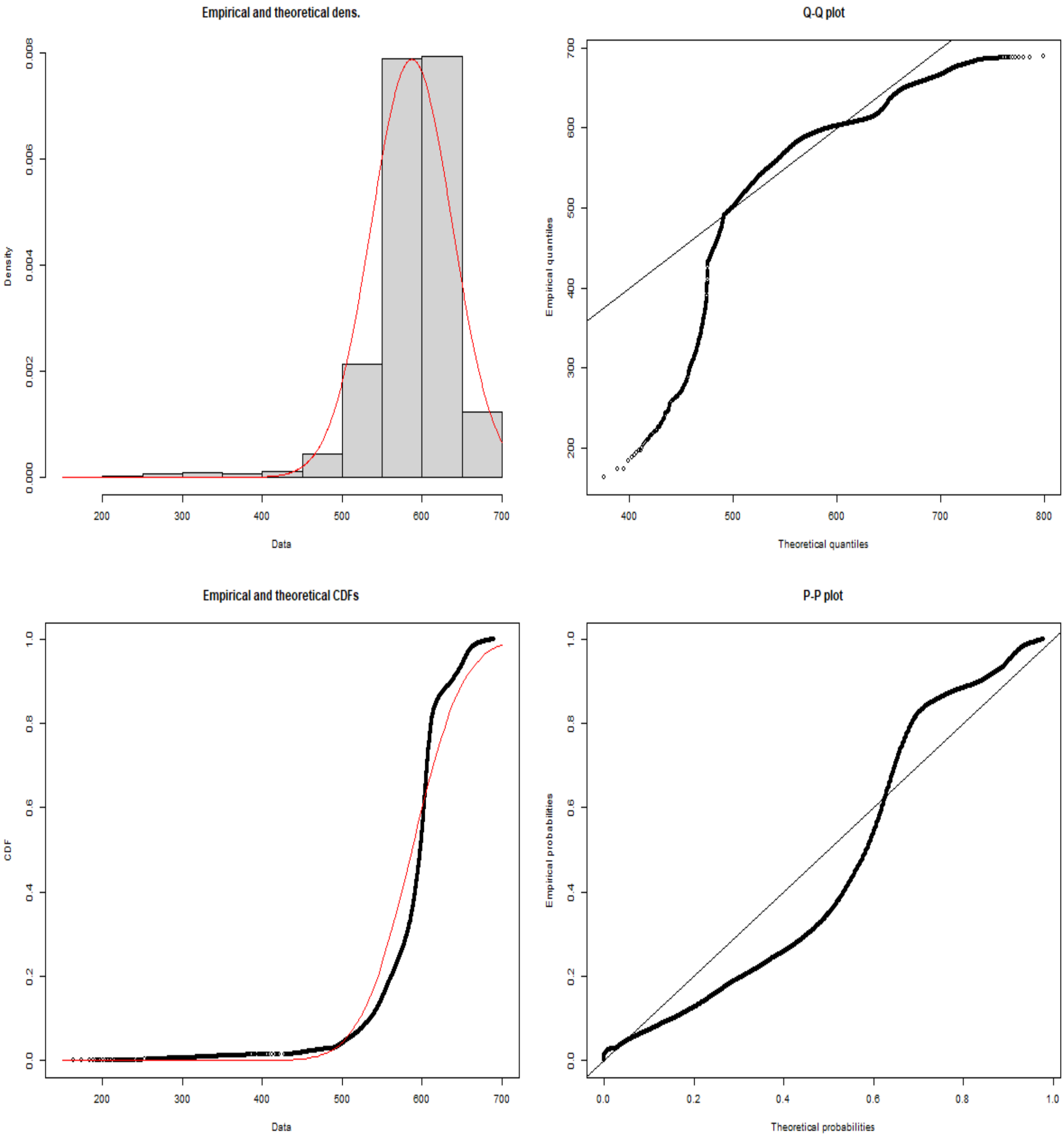

Statistical Distributions of Shear Forces for Pier B and C

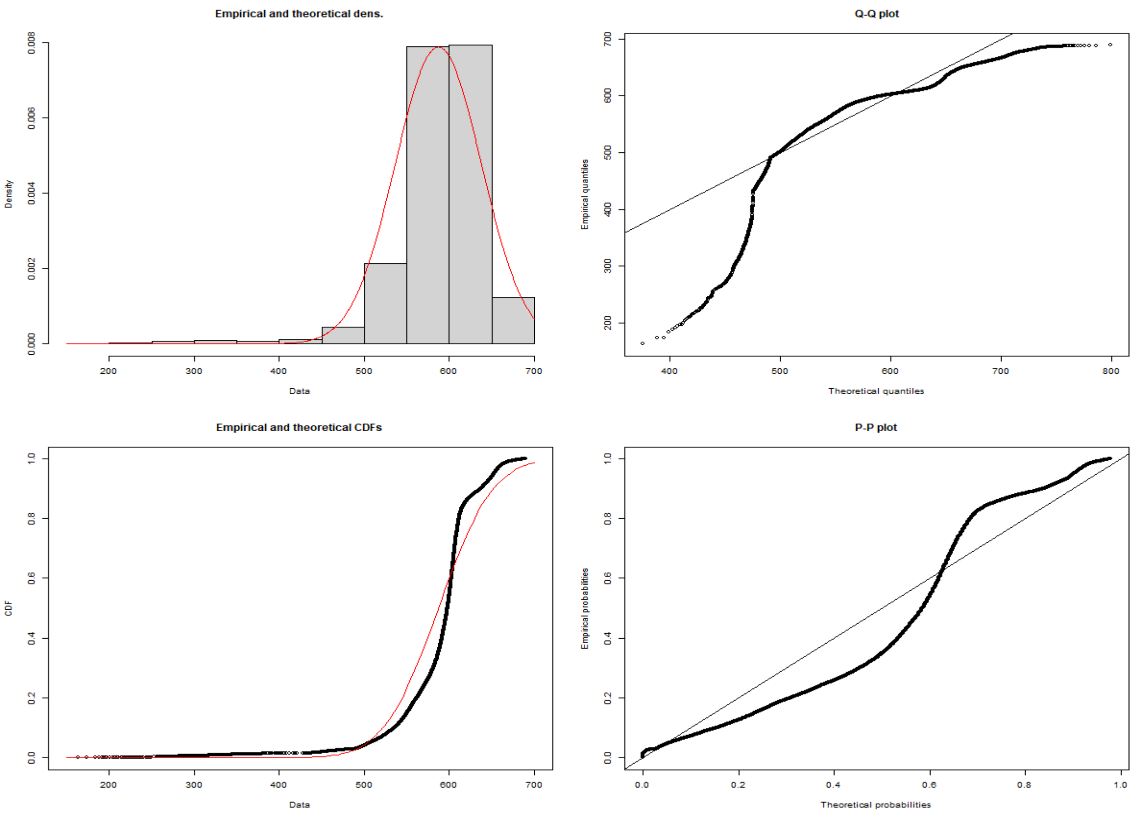
Empirical and theoretical dens.
Density
Data
Q-Q plot
Empirical quantiles
Theoretical quantiles
Empirical and theoretical CDFs
CDF
Data
P-P plot
Empirical probabilities
Theoretical probabilities

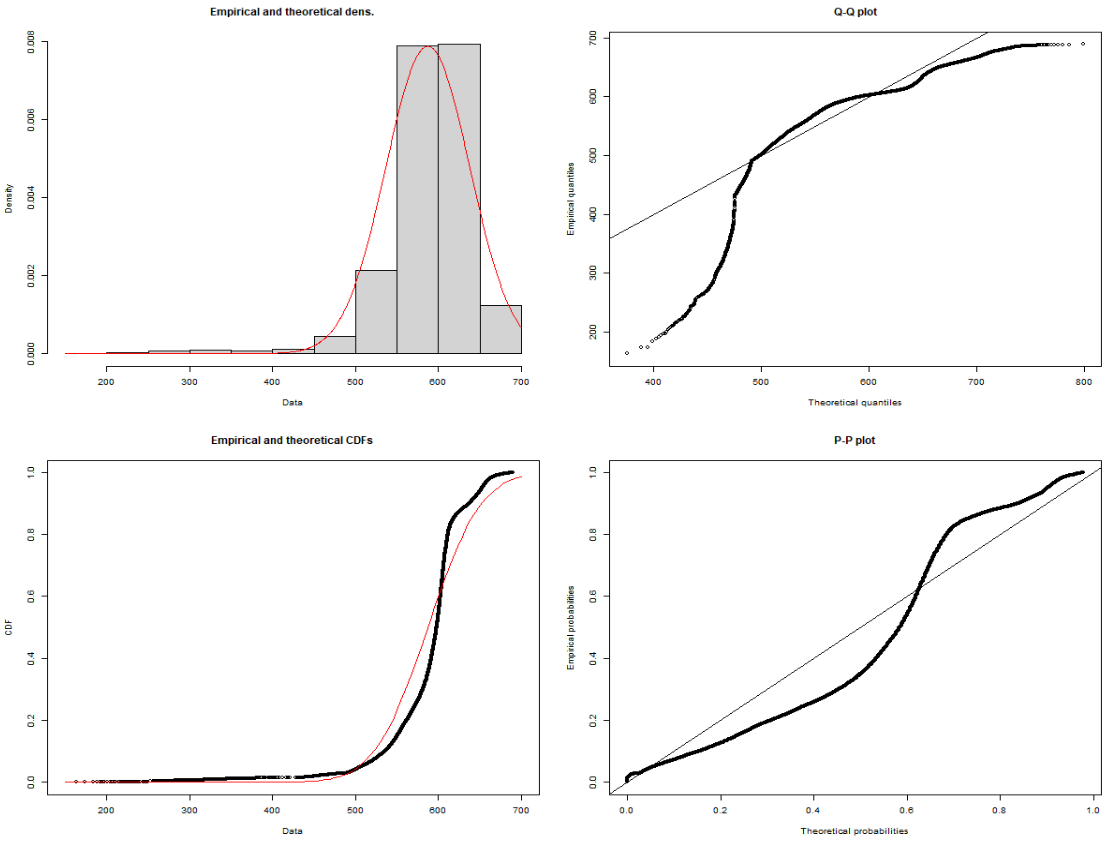
Empirical and theoretical dens.
Density
Data
Q-Q plot
Empirical quantiles
Theoretical quantiles
Empirical and theoretical CDFs
CDF
Data
P-P plot
Empirical probabilities
Theoretical probabilities

Annex B The Collected Bridge from Mile-1 to Galafi

Bridge Name	Bridge Type	Bridge Length (m)	Construction Year
Galaetoli-1	RC Slab Bridge	6.8	2000
Gelatoli	RC Slab Bridge	8.1	2000
Beguda	Masonry Arch	24	1935
Awsunom-l	RC Slab Bridge	5	2000
Kede Absinum	RC Slab Bridge	8	2000
Unda Absinum	Masonry Arch	24	1935
Mille No1	RC Slab Bridge	5	1940
Mille No2	RC Slab Bridge	5	1945
Mille No-3	RC Box Girder	90	2004
Un-named	RC Slab Bridge	6.6	2000
Gedita	Masonry Arch	28.5	1935
Bekel Dera-1	Masonry Arch	32	1935
Bekel Dera-2	Masonry Arch	10.5	1945
Gudiaytu-1	RC Deck Girder	31	2017
Un-named	Masonry Arch	32	1945
Gudiaytu-2	Masonry Arch	5	1935
Un-named	Masonry Arch	5	1935
Defura-1	Masonry Arch	14.9	1935
Defura-2	Masonry Arch	9.1	1935
Defura-3	Masonry Arch	27	1935
Antimegyta	RC Slab Bridge	11	2000
Eraso	RC Deck Girder	23	2017
Un-named	RC Slab Bridge	5	2001
Seraytu	RC Deck Girder	25	2017
Gitta	Masonry Arch	14.8	1935
Alea-1	RC Slab Bridge	5	2000
Alia	Masonry Arch	24.6	1935
Amestegna	Masonry Arch	9	1945
Dehara	Masonry Arch	25	1935
Arsis No.1	Masonry Arch	8.8	1935
Arsis No.2	Masonry Arch	65.5	1935
Mesgid-dar	RC Slab Bridge	4	1945
Un-named	RC Slab Bridge	4	1945
Weya neta	Masonry Arch	30.7	1935
Adedira-2	RC Box Culvert	6	2001
Adedira-3	Masonry Arch	10	1935
Wea	Masonry Arch	72.6	1935
Rudaytu	RC Slab Bridge	7	2001
Oru daitu	RC Slab Bridge	8	2003
Un-named	Masonry Arch	5	1935
Un-named	RC Slab Bridge	4.6	2000
Un-named	RC Slab Bridge	4.5	2000
Kurubmeda	Masonry Arch	9.5	1940
Asasileabera	RC Slab Bridge	7.3	2001
Serdo	Masonry Arch	31.4	1935

Bridge Name	Bridge Type	Bridge Length (m)	Construction Year
Serdo-2	Masonry Arch	9	1935
Dere Alie	RC Slab Bridge	10	2016
Un-named	RC Slab Bridge	5	2003
Serdo-2	RC Slab Bridge	5	1996
Un-named	RC Slab Bridge	4	1996
Un-named	RC Slab Bridge	4	1996
Kerbis-2	RC Slab Bridge	6	1996
Finini-1	RC Slab Bridge	5	1996
Finini-2	RC Slab Bridge	6	1996
Un-named	RC Slab Bridge	4	1996
Un-named	RC Slab Bridge	4	1996
Un-named	RC Slab Bridge	4	1996
Finini-3	RC Slab Bridge	6	1996
Un-named	RC Slab Bridge	4	1996
Buldugum	RC Slab Bridge	6	1997
Un-named	RC Slab Bridge	4	1997
Kurseli	RC Slab Bridge	4	1997
Gebelu-1	RC Slab Bridge	6	1996
Gebelu-2	RC Slab Bridge	6	1996
Gebelu-3	RC Slab Bridge	6	1996
Gebelu-4	RC Slab Bridge	7.2	1995
Gebelu-5	RC Slab Bridge	6	1998
Gebelu-6	RC Slab Bridge	5	1998
Gelebu-7	RC Slab Bridge	6	1998
Un-named	RC Slab Bridge	4	1998
Wednan	RC Slab Bridge	5	1998
Gemeri	RC Deck Girder	36.5	1997
Uper Dichoto	Masonry Arch	11.5	1935
Un-named	RC Slab Bridge	4.8	1998
Un-named	RC Slab Bridge	4	1998
Un-named	RC Slab Bridge	4	1998
Un-named	RC Slab Bridge	4	1998
Geleba	RC Box Girder	111.9	2001
Gela-af-1	RC Slab Bridge	9.8	2001
Gela-af-2	RC Slab Bridge	4.5	2001
Robe	RC Deck Girder	16	2001
Hanaf	RC Deck Girder	14	2001
Un-named	RC Slab Bridge	6	2001
Un-named	RC Slab Bridge	4.3	2001
Un-named	RC Box Culvert	4	2010
Un-named	RC Box Culvert	4	2010
Buhuli	RC Box Culvert	15	2010
Amayad	Masonry Arch	9.6	1935
Melkalemi	Masonry Arch	25	1945
Dobi	RC Slab Bridge	42	1970
Ambedom	RC Slab Bridge	8	2018
Lumma	Masonry Arch	7.7	1945

Bridge Name	Bridge Type	Bridge Length (m)	Construction Year
Un-named	Masonry Arch	9.3	1945
Un-named	RC Slab Bridge	4	1970
Un-named	RC Slab Bridge	5.8	1970
Guma	Masonry Arch	30	1935
Alakel	Masonry Arch	7.6	1945
Leadn	Masonry Arch	7.5	1940
Lieadu-1	RC Slab Bridge	6	2000
Liadu-3	RC Slab Bridge	6.2	1970
Solis	RC Slab Bridge	9	1945
Asomudo	RC Slab Bridge	3.1	1970
Esisilae	RC Slab Bridge	6	1970
Un-named	RC Slab Bridge	4	1970
Elideare	Masonry Arch	55.75	1935
Lefeflae-1	RC Slab Bridge	5	1995
Lefeflae-2	Masonry Arch	10.6	1945
Beli-Etu-1	Masonry Arch	7.6	1945
Burka	RC Slab Bridge	8	1995
Un-named	RC Slab Bridge	8.5	1995
Gewaha-1	Masonry Arch	9.4	1945
Gewaha-2	Masonry Arch	8.3	1945
Gewaha-3	RC Slab Bridge	4.5	1995
Un-named	RC Slab Bridge	4	1995
Gewaha-4	RC Slab Bridge	6	1995
Gewaha-5	Masonry Arch	9.1	1937
Un-named	RC Slab Bridge	4	1995
Un-named	RC Slab Bridge	4	1995
Sola	Masonry Arch	27.6	1935
Gurobehri-1	RC Slab Bridge	4.5	1995
Gurobehri-2	RC Slab Bridge	4.5	1995
Regidneba-1	Masonry Arch	12.4	1945
Regidneba-2	Masonry Arch	5	1945
Su-oulidaba-1	RC Slab Bridge	9	1938
Su-oulidaba-2	Masonry Arch	10.6	1945
Su-oulidaba-3	RC Slab Bridge	9	1945
Su-oulidaba-4	Masonry Arch	9.1	1945
Su-oulidaba-5	RC Slab Bridge	4.5	1995
Bodo	RC Slab Bridge	11.7	1995
Goraybalu	RC Slab Bridge	4	1995
Dola	RC Slab Bridge	4.5	1995
Ginilea-1	RC Slab Bridge	6	1995
Ginilea-2	RC Slab Bridge	9	1995
Ganga Kaylea	RC Slab Bridge	9	1995
Kaylea-1	RC Slab Bridge	4.5	1995
Kaylea-2	Masonry Arch	9	1945
Gede-elea	RC Slab Bridge	4.5	1995
Kaylea-3	Masonry Arch	10.65	1945
Hakera-1	RC Slab Bridge	4.5	1995

Bridge Name	Bridge Type	Bridge Length (m)	Construction Year
Hakera-2	RC Slab Bridge	4	1995
Diweyta	Masonry Arch	8.2	1945
Un-named	Masonry Arch	5	1945
Un-named	RC Slab Bridge	4	1995
Hiraytu	RC Slab Bridge	5	1995
Un-named	RC Slab Bridge	4	1995
Harsa-1	RC Slab Bridge	4.5	1995
Harsa-2	RC Slab Bridge	4.5	1995
Harsa-3	RC Slab Bridge	4.5	1995
Harsa-4	RC Slab Bridge	4.5	1995
Harsa-5	RC Slab Bridge	4.5	1995
Gebulea	RC Slab Bridge	4.5	1995
Lemeou	RC Slab Bridge	4.5	1995
Bododa	RC Slab Bridge	4	1995
Dog-eyyo	Masonry Arch	9	1945
Hiraygefur-l	Masonry Arch	9	1938
Wekreoulla-l	RC Slab Bridge	4.5	1995
Wekreoulla-2	Masonry Arch	9	1945
dear Bure	Masonry Arch	29.2	1935
Hiraygefur-2	Masonry Arch	9	1939
Hiraygefur-3	RC Slab Bridge	7.5	1995
Hudude-1	RC Slab Bridge	6	1995
Hudude-2	RC Slab Bridge	6	1995
Hudude-3	RC Slab Bridge	6	1995
Hudude-4	RC Slab Bridge	4.5	1995
Aunda Burrie-1	RC Slab Bridge	4.5	1995
Aunda Burrie-2	RC Slab Bridge	4.5	1995
Aunda Burrie-3	RC Slab Bridge	5.4	1995
Un-named	RC Slab Bridge	4	1995
Un-named	RC Slab Bridge	4.5	1995
Un-named	RC Slab Bridge	4.5	1995

Annex C: R Code for Statistical modeling of Truck overload and Remaining Service Life Load Exploration

```r
# MSc Thesis
# Thesis Title: Probabilistic Impact Assessment of Traffic Overload on Bridge Structural Capacity: A Case Study Approach
# Thesis Advisor: Dr. Abrham Gebre
# Prpared By : Gebyaw Amare
# For Maximum effect analysis

library(readxl)
library(writexl)
library(dplyr)
library(tidyr)
library(ggplot2)

# ----------------------------
# Load Axle Load and Spacing Data
# ----------------------------
load_path <- "C:/Users/user/Desktop/1. November/4. Axle Load/3. 4-axle data.xlsx"
spacing_path <- "C:/Users/user/Desktop/1. November/2. Generated Axle Spacing/2. Axle_Four_ Spacing.xlsx"

axle_loads <- read_excel(load_path)
axle_spacings <- read_excel(spacing_path)

n_trucks <- nrow(axle_loads)
n_spacings <- nrow(axle_spacings)

# ----------------------------
# Bridge Geometry
# ----------------------------
Lspans <- c(29.5, 31.0, 29.5)
nodes <- c(0, cumsum(Lspans))
totalL <- sum(Lspans)
dx <- 0.1
x_global <- seq(0, totalL, by = dx)

which_span <- function(xg, nodes, Lspans) {
  for (i in seq_along(Lspans)) {
    if (xg >= nodes[i] && xg <= nodes[i+1]) {
      return(list(span = i, x_local = xg - nodes[i]))
    }
  }
  return(list(span = NA, x_local = NA))
}

# ----------------------------
# Influence Line Functions
# ----------------------------
V_IL <- function(L, a, x) ifelse(x < a, -x/L, (L-x)/L)
M_IL <- function(L, a, x) ifelse(x <= a, x*(L-a)/L, a*(L-x)/L)

# ----------------------------
# Key Sections
# ----------------------------
shear_sections <- c(
  0, Lspans[1]/2, Lspans[1],
  Lspans[1] + Lspans[2]/2, Lspans[1] + Lspans[2], totalL
)

moment_sections <- c(
  Lspans[1]/2, Lspans[1] + Lspans[2]/2, totalL - Lspans[3]/2
)

# ----------------------------
# Generate Influence Lines
# ----------------------------
IL_shear <- list()
for(sec in shear_sections){
  span_info <- which_span(sec, nodes, Lspans)
  span_idx <- span_info$span
  a_local <- span_info$x_local
  Vvals <- numeric(length(x_global))

  for(i in seq_along(x_global)){
    xg <- x_global[i]
    span_x <- which_span(xg, nodes, Lspans)
    if(!is.na(span_x$span) && span_x$span == span_idx){
      Vvals[i] <- V_IL(Lspans[span_idx], a_local, span_x$x_local)
    } else {
      Vvals[i] <- 0
    }
  }
  IL_shear[[paste0("V_", round(sec,2))]] <- Vvals
}

IL_moment <- list()
for(sec in moment_sections){
  span_info <- which_span(sec, nodes, Lspans)
  span_idx <- span_info$span
  a_local <- span_info$x_local
  Mvals <- numeric(length(x_global))

  for(i in seq_along(x_global)){
    xg <- x_global[i]
    span_x <- which_span(xg, nodes, Lspans)
    if(!is.na(span_x$span) && span_x$span == span_idx){
      Mvals[i] <- M_IL(Lspans[span_idx], a_local, span_x$x_local)
    } else {
      Mvals[i] <- 0
    }
  }
  IL_moment[[paste0("M_", round(sec,2))]] <- Mvals
}
```

```
# -----------------------------
# Compute Load Effects for One Truck
# -----------------------------
compute_effects <- function(weights, spacings){

  valid_axles <- !is.na(weights)
  weights <- weights[valid_axles]

  if(length(weights) > 1){
    spacings <- spacings[valid_axles[-1]]
    spacings[is.na(spacings)] <- 0
  } else {
    spacings <- numeric(0)
  }

  axle_positions <- cumsum(c(0, spacings))
  axle_positions[is.na(axle_positions)] <- 0

  # Shear
  effects_shear <- sapply(IL_shear, function(IL){
    sum(sapply(1:length(weights), function(i){
      xi <- axle_positions[i]
      if(is.na(xi) || xi < 0 || xi > totalL) return(0)
      approx(x_global, IL, xout = xi, rule = 2)$y * weights[i]
    }))
  })

  # Moment
  effects_moment <- sapply(IL_moment, function(IL){
    sum(sapply(1:length(weights), function(i){
      xi <- axle_positions[i]
      if(is.na(xi) || xi < 0 || xi > totalL) return(0)
      approx(x_global, IL, xout = xi, rule = 2)$y * weights[i]
    }))
  })

  c(effects_shear, effects_moment)
}

# -----------------------------
# Iterate over all generated spacings
# -----------------------------
all_results <- list()

for(s_idx in 1:n_spacings){

  current_spacing <- axle_spacings[s_idx, ] %>% slice(rep(1, n_trucks))

  truck_data_current <- bind_cols(axle_loads, current_spacing)

  results <- truck_data_current %>%
    rowwise() %>%
    mutate(
      Effects = list(compute_effects(
        c_across(starts_with("A")),
        c_across(starts_with("S"))
      ))
    ) %>%
    unnest_wider(Effects)

  # Rename effect columns
  colnames(results)[(ncol(axle_loads) + ncol(current_spacing) + 1):ncol(results)] <- c(
    "V_SupportA",
    "V_Midspan1",
    "V_SupportB",
    "V_Midspan2",
    "V_SupportC",
    "V_SupportD",
    "M_Midspan1",
    "M_Midspan2",
    "M_Midspan3"
  )

  results$Spacing_ID <- s_idx

  all_results[[s_idx]] <- results
  cat("Processed spacing:", s_idx, "\n")
}

final_results <- bind_rows(all_results)

# -----------------------------
# SPLIT INTO CHUNKS OF 200,000 ROWS
# -----------------------------
chunk_size <- 200000
n_chunks <- ceiling(nrow(final_results) / chunk_size)

for(i in 1:n_chunks){
  start <- (i - 1) * chunk_size + 1
  end <- min(i * chunk_size, nrow(final_results))

  chunk_data <- final_results[start:end, ]

  out_path <- paste0("C:/Users/user/Desktop/4_axle_results_part_", i, ".xlsx")

  write_xlsx(chunk_data, out_path)
  cat("Saved:", out_path, " (rows ", start, "-", end, ")\n")
}
```

```
# MSc Thesis
# Thesis Title: Probabilistic Impact Assessment of Traffic Overload on Bridge Structural Capacity: A Case Study Approach
# Thesis Advisor: Dr. Abrham Gebre
# Prpared By : Gebyaw Amare
# For overload Exploration

# Load required libraries
# ============================
required_packages <- c("readxl", "dplyr", "lubridate", "extRemes", "writexl")
new_packages <- required_packages[!(required_packages %in% installed.packages()[, "Package"])]
if(length(new_packages)) install.packages(new_packages)

library(readxl)
library(dplyr)
library(lubridate)
library(extRemes)
library(writexl)

# ============================
# Define file paths & Desktop
# ============================
file_paths <- c(
  "C:/Users/user/Desktop/Thesis August/1. Load Exploration/1. Three_axle_Trucks_LoadEffects.xlsx",
  "C:/Users/user/Desktop/Thesis August/1. Load Exploration/1. Four_axle_Trucks_LoadEffects.xlsx",
  "C:/Users/user/Desktop/Thesis August/1. Load Exploration/Five_Axle_Results.xlsx",
  "C:/Users/user/Desktop/Thesis August/1. Load Exploration/1. Six_axle_Trucks_LoadEffects sectiion-1.xlsx",
  "C:/Users/user/Desktop/Thesis August/1. Load Exploration/2. Six_axle_Trucks_LoadEffects section-2.xlsx",
  "C:/Users/user/Desktop/Thesis August/1. Load Exploration/3. Six_axle_Trucks_LoadEffects section-3.xlsx",
  "C:/Users/user/Desktop/Thesis August/1. Load Exploration/Seven_Axle_Results.xlsx"
)

desktop_path <- "C:/Users/user/Desktop"

# ============================
# Columns to extract
# ============================
cols_needed <- c("Date", "M_Midspan1", "M_Midspan2", "M_Midspan3",
                 "V_SupportA", "V_SupportB", "V_SupportC", "V_SupportD")

moment_cols <- c("M_Midspan1", "M_Midspan2", "M_Midspan3")
shear_cols  <- c("V_SupportA", "V_SupportB", "V_SupportC", "V_SupportD")
all_cols    <- c(moment_cols, shear_cols)

# ============================
# Block maxima functions
# ============================
block_maxima <- function(vec, method = c("castillo", "enright")) {
  method <- match.arg(method)
  n <- length(vec)
  k <- if (method == "castillo") round(2 * sqrt(n)) else 30
  b <- floor(n / k)
  k <- floor(n / b)
  maxima <- sapply(1:k, function(i) {
    start <- (i - 1) * b + 1
    end <- min(start + b - 1, n)
    max(vec[start:end], na.rm = TRUE)
  })
  return(maxima)
}

monthly_maxima <- function(vec, date_vec) {
  data.frame(Date = date_vec, Value = vec) %>%
    mutate(year_month = format(Date, "%Y-%m")) %>%
    group_by(year_month) %>%
    summarise(Max = max(Value, na.rm = TRUE), .groups = "drop") %>%
    pull(Max)
}

return_level_75yr <- function(fit) {
  tryCatch(
    as.numeric(return.level(fit, return.period = 75)),
    error = function(e) NA
  )
}

# ============================
# Safe extractor for GEV results
# ============================
extract_gev_results <- function(fit) {
  s <- tryCatch(summary(fit), error = function(e) NULL)
  if (is.null(s)) return(data.frame())

  # Parameter estimates
  par_df <- as.data.frame(t(s$par))

  # Add AIC and BIC if possible
  par_df$AIC <- tryCatch(AIC(fit), error = function(e) NA)
  par_df$BIC <- tryCatch(BIC(fit), error = function(e) NA)

  return(par_df)
}

# ============================
# Collect results for ALL files
# ============================
all_results <- list()

for (file_path in file_paths) {

  if (!file.exists(file_path)) {
```

```
      warning(paste("File not found:", file_path))
      next
    }

    fname <- tools::file_path_sans_ext(basename(file_path))
    cat("Processing file:", fname, "\n")

    # Read data
    df <- read_excel(file_path)
    df <- df %>% select(any_of(cols_needed)) %>% filter(!is.na(Date))

    # Convert Excel Date safely
    if (is.numeric(df$Date)) {
      df$Date <- as.Date(df$Date, origin = "1899-12-30")
    } else {
      df$Date <- as.Date(df$Date)
    }

    df <- df %>% arrange(Date)

    # Containers
    results_list <- list()
    return_levels <- data.frame()

    # Analyze each variable
    for (col in all_cols) {
      vec <- df[[col]]

      if (all(is.na(vec))) {
        warning(paste("Column", col, "has all NA values in file", fname))
        next
      }

      max_castillo <- block_maxima(vec, "castillo")
      max_enright  <- block_maxima(vec, "enright")
      max_monthly  <- monthly_maxima(vec, df$Date)

      # Fit models safely
      fit_c <- tryCatch(fevd(max_castillo, type = "GEV"), error = function(e) NULL)
      fit_e <- tryCatch(fevd(max_enright,  type = "GEV"), error = function(e) NULL)
      fit_m <- tryCatch(fevd(max_monthly,  type = "GEV"), error = function(e) NULL)

      # Return levels
      rl_c <- if (!is.null(fit_c)) return_level_75yr(fit_c) else NA
      rl_e <- if (!is.null(fit_e)) return_level_75yr(fit_e) else NA
      rl_m <- if (!is.null(fit_m)) return_level_75yr(fit_m) else NA

      return_levels <- bind_rows(return_levels, data.frame(
        Variable = col,
        Method = c("Castillo", "Enright", "Monthly"),
        Return_Level_75yr = c(rl_c, rl_e, rl_m)
      ))

      # Store results
      results_list[[paste0(col, "_Castillo_Maxima")]] <- data.frame(Maxima = max_castillo)
      results_list[[paste0(col, "_Enright_Maxima")]]  <- data.frame(Maxima = max_enright)
      results_list[[paste0(col, "_Monthly_Maxima")]]  <- data.frame(Maxima = max_monthly)

      if (!is.null(fit_c)) results_list[[paste0(col, "_GEV_Castillo")]] <- extract_gev_results(fit_c)
      if (!is.null(fit_e)) results_list[[paste0(col, "_GEV_Enright")]]  <- extract_gev_results(fit_e)
      if (!is.null(fit_m)) results_list[[paste0(col, "_GEV_Monthly")]]  <- extract_gev_results(fit_m)
    }

    results_list[["Return_Level_75yr"]] <- return_levels

    # Add this file's results into all_results (sheet name = file name)
    all_results[[fname]] <- return_levels
  }

# ==============================
# Save ONE Excel file with sheets
# ==============================
output_file <- file.path(desktop_path, "All_Truck_GEV_Results_75yr.xlsx")
write_xlsx(all_results, output_file)

cat("✅ All results saved to:\n", output_file, "\n")
```